Climate Change, Water Resources, and Sustainability in the Pacific Basin: Emphasis on O'ahu, Hawai'i and Majuro Atoll, Republic of the Marshall Islands

Michael W. Guidry and Fred T. Mackenzie
School of Ocean and Earth Science and Technology
Department of Oceanography
University of Hawai'i at Mānoa
Honolulu, HI 96822

Climate Change, Water Resources, and Sustainability in the Pacific Basin:

Emphasis on Oʻahu, Hawaiʻi and Majuro Atoll, Republic of the Marshall Islands

Michael W. Guidry and Fred T. Mackenzie
School of Ocean and Earth Science and Technology
Department of Oceanography
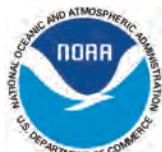University of Hawaiʻi at Mānoa
Honolulu, HI 96822

TABLE OF CONTENTS

PREFACE - Climate Change and Small Pacific Island States

Importance of Climate Change to Small Pacific Island States

Looking at the Earth from space, the world's oceans occupy 71% of the planet's surface area and land occupies 29%. There are three primary oceans – Pacific, Atlantic, and Indian – that comprise 89% of the world's ocean surface area with the aerial extent of the Pacific Ocean about as large as the Indian and Atlantic oceans combined. The Pacific Ocean occupies about 46% of the total world ocean area and is home to a wide variety of islands and people that call them home. Small island states and Pacific Islanders are susceptible to variations in climate. They share climate-linked vulnerabilities such as:

- susceptibility to storm systems, tidal variation, and long-term sea level rise;
- impacts to local hydrology;
- pressures imposed by population density;
- impacts to local species density, distribution, biodiversity; and
- limited natural resources.

This is not to say that each Pacific Island and its inhabitants are impacted in the same manner and degree by climate change. Island to island variations in:

- island geology (i.e., island bedrock of volcanic origin versus that of sedimentary origin);
- relative size and large scale structure of the island (e.g., from relatively high islands such as Hawai'i to low-lying atolls such as Majuro);
- extent of reef formation; and
- size of groundwater resources;

all regulate how future climate variation will impact Pacific Islands and their inhabitants.

Future Climate Change Impacts for Small Pacific Island States

From recent modeling projections of Pacific region climate change for this century (some of which are discussed in this case study), there are several common themes:

- surface air temperatures will increase;
- increased precipitation will occur in some areas with decreased precipitation in others;
- changes will occur in large scale natural climatic variability, such as El Niño, that can impact long-term rainfall and tropical storm frequency;
- ocean surface temperatures will increase; and
- a long-term rise in sea level will take place.

The future well-being and way-of-life of Pacific Islanders are both intimately tied to future climate change.

CASE STUDY OVERVIEW

To investigate how future climate change will impact Pacific Island nations and their water resources, this case study focuses on the Island of Oʻahu, Hawaiʻi, and Majuro Atoll, Republic of the Marshall Islands. While both islands are in the Pacific, there are numerous differences between the two entities and this is why they were chosen for this case study.

The island of Oʻahu is part of the Hawaiian Archipelago consisting of 132 islands stretching more than 2451 kilometers (1,523 miles) from Kure Atoll to the Island of Hawaiʻi (also named the "Big Island of Hawaiʻi"). The Hawaiian Islands are one of the most isolated island systems on Earth being some 3,862 kilometers (2,400 miles) from the nearest continental land mass, North America, and the islands of Polynesia in the South Pacific. Due to this isolation, the Hawaiian Islands were one of the last places discovered and colonized by humans. The total population of the Hawaiian Island chain is a little over 1.2 million with the Island of Oʻahu the epicenter of population with around 876,000 residents. Honolulu, located on Oʻahu, is the state's largest city and also serves as the political and commercial capital. The peak elevation (Mt. Kaʻala) of Oʻahu is slightly over 1200 meters (4,000 feet).

The island of Majuro is one of 34 atolls and islands that comprise the Republic of the Marshall Islands. The Republic of the Marshall Islands lies halfway between Australia and Hawaiʻi and consists of a series of low-lying mid-ocean reef platforms with a total surface area of 181 square kilometers (70 square miles), which is roughly the size of Washington, D.C. The total population of the Republic of Marshall Islands is around 58,000 with about 27,000 residing on Majuro. The peak elevation of Majuro is about 2.5 meters (8 feet).

This case study investigates how changes in future climate patterns will impact the water resources of Oʻahu and Majuro. The case study is structured in the following manner:

1) Development of the necessary scientific background for understanding climate change and the greenhouse effect;

2) Discussion of how recent trends and projected change in climate have led to international legislation (e.g., The Kyoto Protocol) to mitigate the impacts of climate change;

3) Overview of projected changes in climate for the Pacific Basin; and

4) Consequences of projected climate change for water resources on (a) Oʻahu, Hawaiʻi and (b) Majuro atoll, Republic of Marshall Islands.

An effort was made to provide the reader with a scientific background to understand impacts of climate change on water resources. Material in grey text boxes provide detailed descriptions about the science behind the predictions and phenomenon discussed. This case study leans heavily on information from two sources for its foundation. Preparing for a Changing Climate: The Potential Consequences of Climate Variability and Change (Shea et al., 2001) provided (1) an overview of the Pacific Island Region and the impacts and consequences (economic, social, and environmental) of climate variability, and (2) an overview of predicted (i.e., computer modeled) climate change over the next 100 years for the Pacific Basin. Review of climate systems, greenhouse effect, and the science behind global climate change was derived largely from Our Changing Planet 3rd edition (Mackenzie, 2003).

FIGURES

TABLES

BOXES

BOX FIGURES

I   Introduction – Overview of Climate Change

Climate has profoundly impacted and shaped human existence and in turn humans via their activities have impacted local and regional and now even global climate. Beginning around 10,000 years ago, the Agricultural Revolution and resultant growth in population altered the local and regional climate of many regions around the world including islands. For example, as huge tracks of forest were felled to make way for agriculture to support growing populations, the pre-Agricultural Revolution Mediterranean hydrological cycle and thus climate was altered from a wet to the present relatively dry climate.

In the past half-century, humans have increased their monitoring of various aspects or indicators of climate change to understand further how climate not only changes, but also to predict what impact these changes might have on the world around them. One area of monitoring focus has been on greenhouse gases. Atmospheric levels of gases, such as carbon dioxide (CO_2), methane (CH_4), nitrous oxide (N_2O), chlorofluorocarbons (CFCs), and sulfate (SO_4) aerosols have all been sampled and concentrations recorded for the past half-century or longer. The measured increases in atmospheric concentrations of these gases and aerosols along with historical comparisons from proxy records have led the world's community – on local, regional, national, and international levels – to consider the potential climatic implications of past, current, and future increases in greenhouse gases.

One of the more notable global efforts has been through the United Nations and the Intergovernmental Panel on Climate Change. The United Nations Environment Programme (UNEP) and the World Meteorological Organization established the Intergovernmental Panel on Climate Change (comprised of approximately 2,500 scientists from around the world) at the 1988 Toronto Conference on the Changing Atmosphere. The Intergovernmental Panel on Climate Change released its "First Assessment Report" in 1990, which led to a general agreement (the Framework Convention on Climate Change) among countries at the 1992 Rio de Janeiro United Nation's Conference on Environment and Development that an international treaty or convention was needed and in turn laid the groundwork for the 1997 Kyoto Protocol. The Kyoto Protocol is a legally binding international agreement that commits industrialized countries to reducing emissions of the following six greenhouse gases: carbon dioxide, methane, nitrous oxide, hydrofluorocarbons (HFCs), perfluorocarbons (PFCs), and sulfur hexafluoride (SF_6). In addition to the Intergovernmental Panel on Climate Change reports, reports such as the 2001 "Preparing for a Changing Climate: Pacific Islands"

(Shea et al., 2001) completed for the U.S. Global Change Research Program have been published to investigate local and regional impacts of climate change. One other global effort worth mentioning is the 1987 Montreal Protocol, which focused on the reduction and phase out of chlorofluorocarbons and other halocarbons, potent greenhouse gases and the culprits in stratospheric ozone depletion.

The purpose of this case study is to investigate: (1) the science of greenhouse gas forcing on climate; (2) the evidence of human influence on greenhouse gas concentrations; (3) the global response to mitigating future climatic impacts due to human forcings on greenhouse gas concentrations; and (4) the regional and global impacts of projected human-induced climate change on water resources and water resource sustainability.

II Climate System and Greenhouse Effect Overview

There are many factors influencing climate variability and climate change. As an introduction to how future climate change will impact the Pacific Region and island states, we will briefly survey these factors.

A. Climate System Forcings

There is a wealth of data on past climates. Deep sea sediments and ice cores provide proxies (chemical and other indicators) for long-term temperature records. By examining these, the composition and chemical changes in atmospheric gases as well as temperatures of the planet can be determined during Pleistocene (past 1.2 million years) and Holocene (past 10,000 years) time. Cores of sediments and sedimentary rocks contain fossils that provide insights in past climate. Analyses of tree rings provide records of precipitation, temperature, and soil moisture for the last several thousand years. It is from these records along with our current understanding of atmospheric and oceanic science that we obtain our climate projections. This section discusses the major factors that influence global climate change and global climate variability.

At this point, it is necessary to discuss the difference between climate change and climate variability as often these terms are used interchangeably, which can confuse the discussion about future climate. Climate variability refers to relatively short-term variations in the natural climate system, such as the El Niño Southern Oscillation Cycle. Variability implies shifts about some mean point. Climate change (as used in the Intergovernmental Panel on Climate Change volumes) refers to long-term changes from decades to centuries that are associated with increasing concentrations of greenhouse gases. These changes are often viewed as unidirectional -- at least over relatively long time scales. Global climatic change involves unidirectional changes in climatic features over the entire globe and may either be amplified or lessened by climate variability.

1. Fluctuations in Solar Energy

The amount of energy radiated by the sun fluctuates. For 500 years, astronomers have observed visible changes on the sun's surface such as sunspot activity. This record indicates that there is an approximately 11-year cycle in the number of sunspots visible on the sun's surface. Furthermore, when sunspots are in abundance, an increase in solar emis-

sions from the darker sunspots and the sun's polar regions is observed. When sunspot activity is minimal, these solar emissions are less intense. This correlation between changes in sunspot activity and solar emissions has been confirmed by satellite observations over two complete sunspot cycles. Solar radiation incident at the top of the Earth's atmosphere has been measured to vary by 2.5 watts over the 11-year sunspot cycle. Such a change in incoming solar radiation could result in a variation of Earth's temperature by 0.1° C in response to the 11-year variation in the intensity of the sun's radiation. The linkages between sunspot variation, the sun's strength, and Earth climate are uncertain at a decadal to century time scale. It is interesting to note that there exists a significant correlation between the northern hemisphere land temperature record for the last 100 years and the length of sunspot cycle (Figure 1).

2. Orbital Parameters

The amount of radiation received from the sun and its distribution on the Earth's surface varies with the relative position between the sun and the Earth. These natural variations in the orbit impact the planet's climate and appear to set the conditions for the cooler and warmer periods of glacial-interglacial stages. Figure 2 depicts the three parameters that
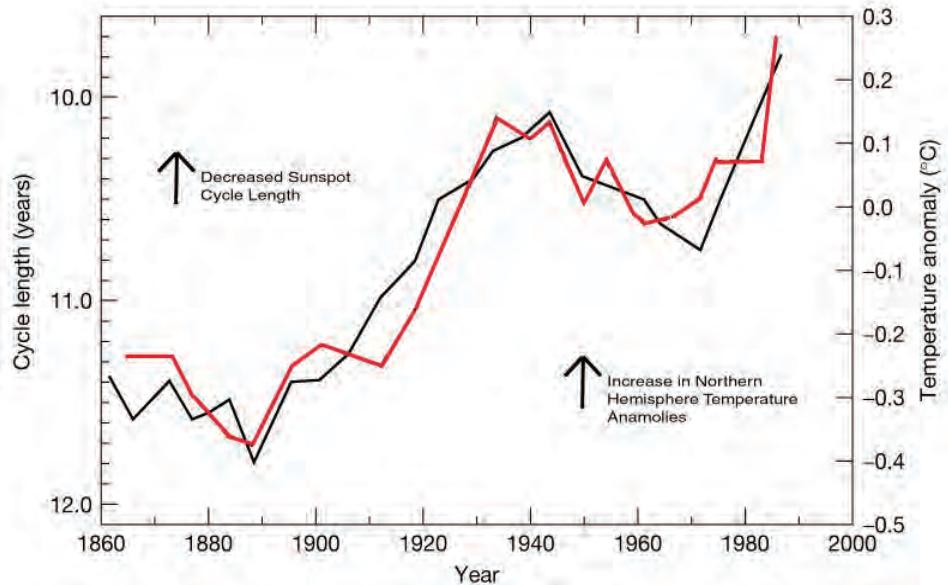
Figure 1. Correlation between the variation of the sunspot cycle length (solid dark line, left hand scale) and Northern Hemisphere land temperatures anomalies (red line, right hand scale) from 1861 to 1989. The temperature anomalies are the deviations in temperatures relative to the period of 1951 to 1980. (After Friis-Christensen and Lassen, 1991).

15
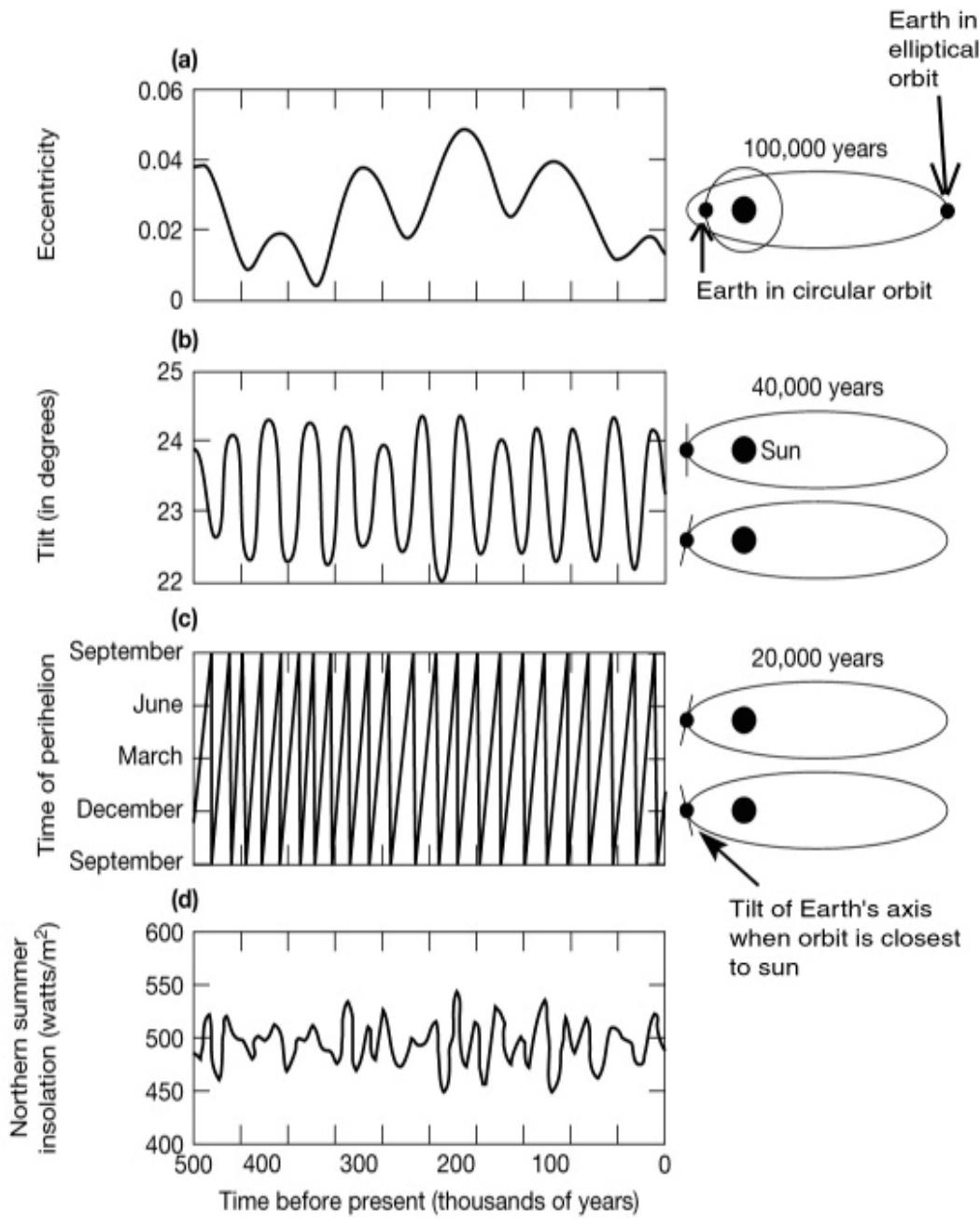
Figure 2. The Milankovitch theory of climate change during the Pleistocene. The onset of ice ages is due to variations in three orbital parameters of Earth. (a) The eccentricity is the degree to which Earth's orbit departs from a circle. Times of maximum eccentricity are separated by roughly 100,000 years. (b) The tilt angle is the angle between Earth's axis and a line perpendicular to the plane of the orbit of the planet. (c) The time of perihelion involves the tilt of Earth's axis at its closest approach to the sun. The cycles of tilt and time of perihelion are roughly 40,000 and 20,000 years, respectively. (d) The calculated amount of sunlight received at 60° to 70° north latitude during the summer (summer insolation, July), based on the cycles of variation of Earth's orbital parameters. (After Covey, 1984).

(3) time of perihelion (precession). In 1920, Milutin Milankovitch proposed a theory that changes in climate cycles of glacial-interglacial periods were initiated by both the amount and the distribution of radiation received from the sun. Every 100,000 years or so, these orbital parameters vary in such a way so as to reduce the amount of energy received at mid-latitudes in the northern hemisphere. This reduction in energy is therefore thought to lead to the onset of an ice age.

3.   Planetary Albedo

The albedo or reflectivity of Earth affects the heat budget and thus climate of the planet. Things such as, but not limited to, aerosols, clouds, ice, snow, water, land, plant surfaces, asphalt, and concrete all contribute to the Earth's albedo. Aerosols are small micrometer-sized airborne particles that can be derived from natural environmental sources – e.g., volcanoes, wildfires, windblown soil dust, land and ocean emissions of biologically produced gases, and sea-salt spray – or they can be emitted from human sources – e.g., spray cans, industry, fossil fuel combustion, etc.

The size and distribution of the aerosols determine whether the surface temperature of Earth increases or decreases. Generally, the larger the number of aerosol particles, the greater the aerosol cooling effect due to the increased amount of heat radiated or reflected back to space. Aerosols will be discussed in more depth in *II. Climate System and Greenhouse Effect. B. Greenhouse Effect – Natural and Anthropogenic. 6. Aerosols*.

Ice and snow surfaces have a very high albedo. When sunlight strikes ice or snow, most of the light and heat energy is reflected. Assuming other factors influencing climate are held constant, the greater the area of Earth's surface covered by ice, snow, glaciers, sea ice, etc. the more energy is reflected back to space and the cooler the planet. Deserts and other non-vegetated areas have albedos less than that of ice and reflect only half of the radiation they receive. Liquid water in oceans and lakes has a very low albedo and absorbs most of the radiation received and is warmed in the process. Land and aquatic plants absorb almost all incoming radiation. An increase of vegetation coverage with all other climate factors held constant would lead to an increase in the temperature of the planet.

The global atmosphere extends 500 kilometers (310 miles) above the Earth's surface from the lower troposphere to the upper exosphere (Figure 3). The atmosphere has evolved ever since the Earth was formed and along with the ocean is responsible for heat being distributed throughout the globe and thus is a principal driver of climate and weather. Climate and weather have much in common, but are not the same. Weather is an everyday experience representing the sum total of atmospheric variables in a particular region for a short duration. Climate is a long-term composite of day-to-day weather conditions and atmospheric variables in a region. The atmospheric variables that drive climate and weather are solar energy, humidity, precipitation, atmospheric pressure, and wind currents.

The sun primarily provides the energy that drives the Earth's climate and weather by influencing atmospheric and surface processes (see Box 1). The temperature of the surface of the sun is approximately 5480° C and the light energy

Figure 3. Layer structure of the Earth's atmosphere. (After Mackenzie, 2003).

that radiates from the sun travels through space and impacts the Earth's atmosphere. This energy is primarily in the form of visible, short wave (ultraviolet), and long wave (infrared) radiation. Some of the sun's energy is reflected back to space by the outer atmosphere, but the remainder of energy incident at the space-atmosphere boundary passes through.

Box 1:   The Electromagnetic Spectrum (adapted from Mackenzie, 2003)

The major source of energy for the Earth's surface is radiant energy from the sun. The sun's radiation travels through space as electromagnetic radiation. One way to characterize this radiation is by its wavelength. A wavelength (Figure 1.1) is defined as the distance between two consecutive wave crests (e.g. peaks) or troughs. The amount of energy in radiation is dependent upon its wavelength.
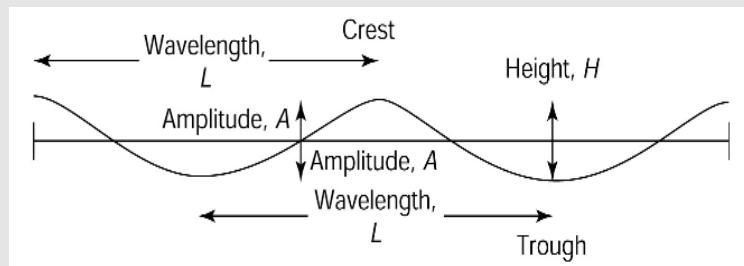
Figure 1.1. Wave description. (After Mackenzie, 2003)

The shorter the wavelength is the stronger the radiation. Hot bodies, like the sun, emit shorter wavelength radiation while cooler bodies emit longer, less intense, radiation. The surface temperature of the sun is 5,480° C. Objects in this temperature range emit radiation with wavelengths in the 0.2 to 3.0 micrometer range, which is in the ultraviolet, visible, and infrared range (Figure 1.2). The sun emits 95% of its radiation in this wavelength range. The sun gives off a smaller amount of gamma, radio, and x-ray radiation. Both gamma and x-ray radiation are very powerful, can penetrate most objects, and are very harmful to life. Gas molecules in the outer atmosphere absorb both of these types of radiation. Ultraviolet radiation is also dangerous to life. UV radiation is mostly absorbed in the stratosphere with just a small percentage reaching the Earth's surface. Visible light reaches the Earth and human eyes are sensitive to this wavelength region.
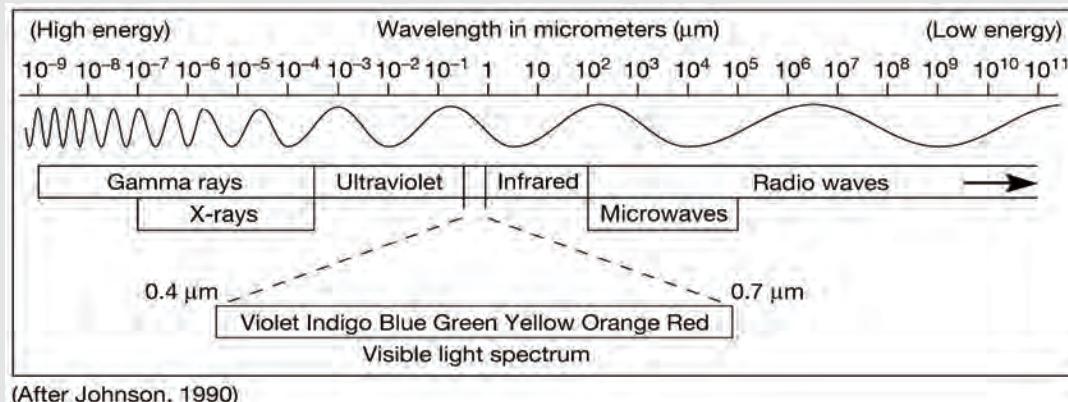
Figure 1.2. Electromagnetic spectrum. (After Mackenzie, 2003)

The atoms and molecules that make up the atmosphere absorb the various types of radiation (visible, ultraviolet, and infrared) to varying degrees (Figure 4). Oxygen, in the form of O_2 (diatomic oxygen) and O_3 (triatomic oxygen, ozone), is the most important absorber of incoming solar radiation in the atmosphere. High in the atmosphere, diatomic oxygen (O_2) absorbs radiation with wavelength less than 240 nanometers (240×10^{-9} meters)

Figure 4. Illustration of relationship between radiation intensity and incoming solar radiation at the top of Earth's atmosphere and outgoing Earth radiation. (Note: Much of the incoming shortwave UV solar radiation is absorbed by oxygen (O_2 and O_3) in the upper atmosphere. The outgoing long wavelength radiation emitted by the Earth is partially (hatched area) to totally absorbed (grey area) by the greenhouse gases of water vapor (H_2O), carbon dioxide (CO_2), methane (CH_4), nitrous oxide (N_2O), and tropospheric ozone (O_3). (After Streete, 1991).

and at lower altitude ozone (O_3) absorbs radiation within the globally encircling stratospheric ozone layer with wavelengths mainly between 200 to 300 nanometers (200 to 300 $\times 10^{-9}$ meters). This incoming solar radiation is actually strong enough to break bonds holding the diatomic oxygen (O_2) and ozone (O_3) molecules together causing the molecule to split:

$$O_2 + \text{solar radiation} = O + O \quad (1)$$
$$\text{and}$$
$$O_3 + \text{solar radiation} = O_2 + O \quad (2).$$

Most atmospheric ozone in the atmosphere occurs in the stratosphere. The absorption of solar radiation by ozone in the stratosphere is the source for heat in the stratosphere and mesosphere (see Figure 3). The ozone also absorbs and blocks most ultraviolet radiation below 300 nanometers. As solar radiation continues to penetrate the atmosphere and gets closer to the Earth's surface, it is scattered, reflected, and absorbed by air molecules, clouds, and various types of particles. Of the incoming solar radiation, about 30% is reflected back to space by clouds and the Earth's surface, 25% is absorbed by the atmosphere and reradiated back to space, and 45% is absorbed by the surface of land and ocean (Figure 5). The temperature of the Earth's surface and lower atmosphere is higher than would be expected for a planet the distance of the Earth from the sun,

a result of the insulating qualities of the greenhouse gases. When short wavelength radiation from the sun is not intercepted by the outer atmosphere or the ozone layer, it penetrates to the surface of the planet, and it is reradiated back as energy of a longer wavelength (infrared radiation) because the Earth is much cooler than the sun. Water vapor, carbon dioxide and other greenhouse gases absorb and trap this longer wavelength radiation leading to a natural warming of Earth's surface and the lower atmosphere (see Figure 6).
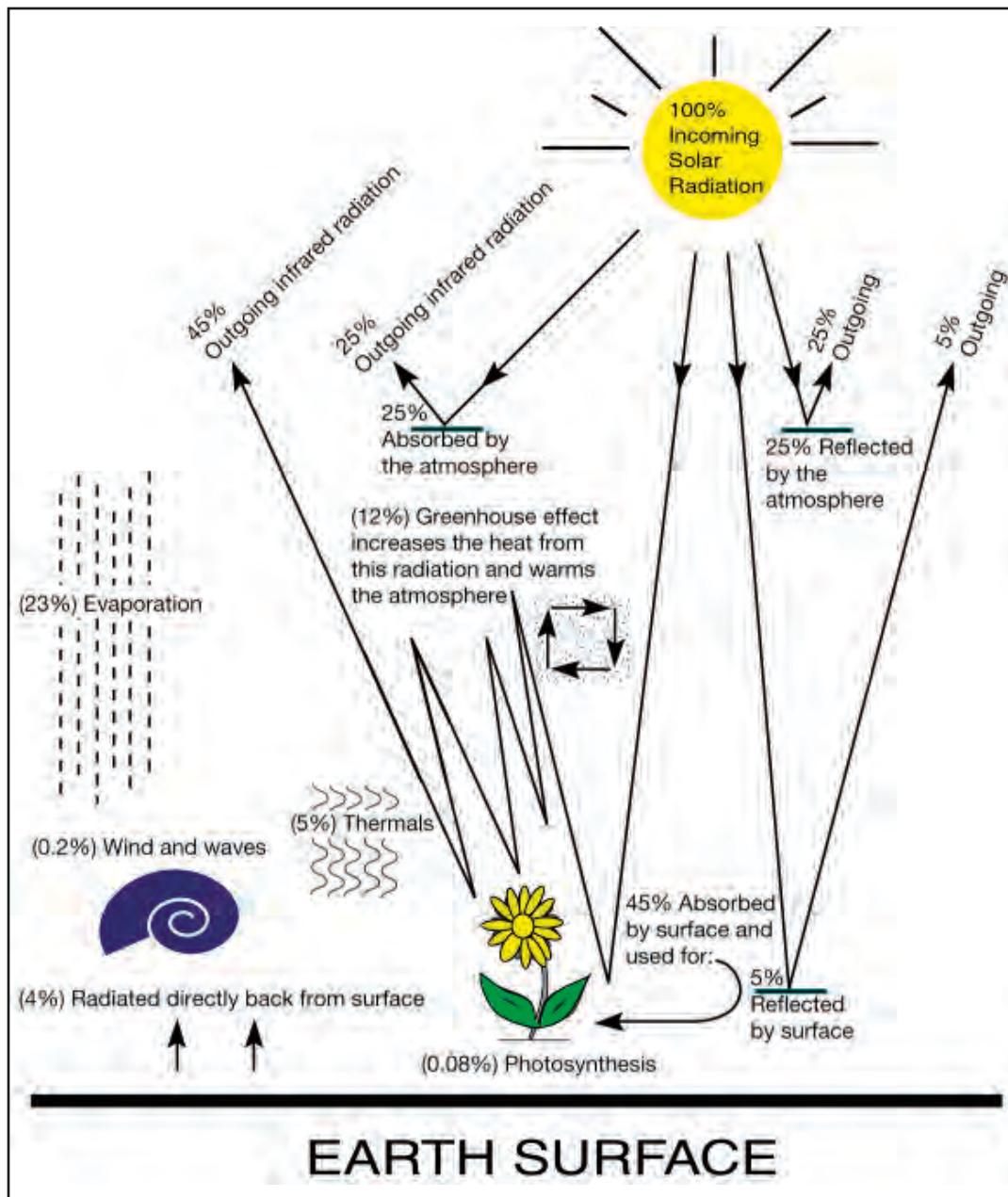
Figure 5. Earth's radiation budget. Incoming solar radiation is shortwave, ultraviolet, and visible radiation; outgoing Earth radiation is long wave infrared radiation. (After Mackenzie, 2003).

The quantity of carbon dioxide residing in the atmosphere affects the amount of heat retained in the atmosphere and in turn affects climate. The more carbon dioxide (CO_2) in the atmosphere, everything else being equal, the warmer the climate will be. Nitrous oxide (N_2O), water vapor (H_2O, the most important greenhouse gas), methane (CH_4) and other gases have effects similar to those of carbon dioxide in controlling the amount of heat retained by the atmosphere. This overall process is the natural greenhouse effect. Without greenhouse gases in the Earth's atmosphere, the planetary surface temperature would be −18° C. This is 33° C cooler than its present average of 15° C (see Box 2: Solar and Earth Radiation and the Greenhouse Effect).

1. Carbon Dioxide - CO_2

The natural carbon cycle involves the cycling of carbon through the reservoirs of the lithosphere, hydrosphere, atmosphere, and biosphere over a wide range of time and space scales. This cycling has gone on throughout most of the history of the planet and variations in fluxes in the cycle are responsible for changes in atmospheric carbon dioxide. Figure 6 shows the processes that involve the transfers of carbon at the Earth's surface.

On short times scales – years to thousands of years – volcanoes, plants, animals, natural forest and grass fires, and decaying organic matter contribute carbon dioxide to the atmosphere. Photosynthesis takes carbon dioxide out of the atmosphere and stores it as carbon in the tissues of plants. Atmospheric carbon dioxide concentration has varied from about 200 parts per million by volume in recent glacial periods to 300 parts per million by volume during interglacial periods. The warm Eemian-Sangamon interglacial of 125,000 years ago had an atmospheric carbon dioxide content of 280 parts per million by volume while the Wisconsin ice age 18,000 years ago had an atmospheric carbon dioxide content of 180 parts per million by volume.

Fossil fuel burning is the major source of anthropogenic carbon dioxide to the atmosphere. The world's use and reliance on this energy source will impact the composition of the atmosphere far into the twenty-first century. Carbon dioxide is also released to the atmosphere by land use practices such as deforestation, which has been occurring for the past 10,000 years. During the 1990s, an estimated 1 to 2 billion tons of carbon per year were vented to the atmosphere from land use practices. The carbon system is currently difficult to balance in terms of inputs and outputs (see "Missing" in Figure 6). The issue is to determine where all the carbon is going that is emitted from human activities. Of the 7.9 billion tons of carbon per year emitted by human activities in the 1990s, 3.3 billion tons remained in the

Box 2: Solar and Earth Radiation and the Greenhouse Effect (adapted from Mackenzie, 2003)

The principal source of energy at the Earth's surface is from the sun in the form of ultraviolet, visible, infrared and other forms of electromagnetic radiation. Only small amounts of energy come from the Earth's interior. Radiation has been described both in terms of particles (photons) and waves. A basic relationship between the two is

$$E = hc/\lambda = h\upsilon$$

where E is the energy of the photon, λ is the radiation wavelength, h is Plank's constant with a value of 6.626×10^{-34} joule-second, υ is the frequency of the radiation, and c is the velocity of light (2.998×10^8 m/sec). It can be seen from the preceding equation that photons with shorter wavelengths have higher energies than photons with shorter wavelengths. The quantity of radiation emitted by a radiating body can be described by Planck's law

$$\Psi = a\lambda^{-5}\, e^{(-b/\lambda T)}$$

where Ψ is the energy flux at a given wavelength of radiation λ, a and b are constants, and T is the temperature in Kelvin (K). From the preceding relationship, Wein's displacement law can be obtained as

$$\lambda = 2898/T$$

where λ is the wavelength of the radiation in micrometers, and T is the temperature in K. This law holds true for blackbodies, which are objects that emit or absorb electromagnetic radiation with 100% efficiency at all wavelengths. The radiation emitted by a blackbody is called blackbody radiation. For the sun with an effective surface temperature of 5780 K, the maximum in its radiated energy is at 0.5 micrometers or 500 nanometers in the middle of the visible electromagnetic spectrum (see Box 1). For Earth with an effective surface temperature of 288 K, its peak emission in radiation is at 10 micrometers, well into the infrared region of electromagnetic radiation (Box 1 and Figure 6). The term effective radiating temperature is the temperature that a true blackbody would need to have to radiate the same amount of energy as an object radiates.

It also can be shown from Planck's law that the energy flux emitted by a blackbody is related to the fourth power of the body's absolute temperature in K

$$F = \alpha T^4$$

where F is the flux, T is temperature in K, and α is a constant with a numerical value of 5.67×10^{-8} watts per square meter per K^4 ($W/m^2/K^4$). This relationship is known at the Stefan-Boltzmann law. Our sun with a surface temperature of 5780 K has an energy flux per unit area of 6.3×10^7 W/m^2. If we treat Earth as a blackbody with an effective radiating temperature of T_E, the total energy emitted by Earth is

$$\alpha T_E^4 \times 4\pi R_E^2 \text{ (the surface area of the Earth)}$$

where T_E is the effective radiating temperature of Earth, $\pi = 3.1416$, and R_E is the radius of Earth. The total energy absorbed by Earth is

$$\pi R_E^2 \times S \times (1-A)$$

where S is the solar flux of energy, and A is the albedo (percentage of incoming solar radiation reflected back to space) of Earth. The planetary energy balance to a first approximation implies that the energy emitted by Earth is equal to the energy absorbed by Earth or

$$\alpha T_E^4 = S/4(1-A).$$

By solving for T_E in the preceding equation, we obtain

$$T_E = S/4\alpha \times (1-A).$$

This is the effective radiating temperature of Earth. Using the known values of S of 1370 W/m^2, A of 30% or 0.30, and an α of 5.67×10^{-8} $W/m^2/K^4$, the Earth's effective radiating temperature is calculated to be very cold, -18° C (255K). The actual surface temperature is 15° C (288K). The difference between the two temperatures is due the greenhouse effect of the atmosphere. The naturally occurring greenhouse gases of water vapor, carbon dioxide, nitrous oxide, methane, and tropospheric ozone absorb part of the infrared Earth radiation radiated upward from Earth's surface and reemit it in all directions. It is anticipated that increasing greenhouse gas concentrations in the atmosphere would eventually lead to warming of the Earth's surface and decreasing concentrations would lead to cooling.

CARBON DIOXIDE
(Fluxes = MTC/yr)

To terrestrial realm
2300

"Missing"
4600

To ocean
2300

Climate sensitivity
2.5°C/doubling CO₂
67% greenhouse

CO_2
783000 MTC
375 ppmv
R.T. = ~7 years
Accumulation:
3300 MTC/yr
1.5 ppmv/yr

Late diagenesis -
metamorphism

60

Land use
1600

Fossil fuel burning
6300

Respiration - decay
61,440

Net primary production
63,000

Weathering
216

Oxidation

Fossil CH_2O
36

Volcanic
60

Precipitation
168

$CaCO_3$

Respiration - decay
45,252

Net primary production
45,000

Land

Ocean

Figure 6. Global biogeochemical cycle of carbon as carbon dioxide (CO₂). Fluxes (denoted by arrows) between land, ocean, and atmosphere reservoirs are in millions of metric tons of carbon (MTC) per year. The reservoir size of carbon dioxide is in millions of tons of carbon. The "Missing" is the amount of global CO₂ emissions taken up by the ocean and terrestrial realms. The relative amount of "Missing" uptake by ocean and terrestrial realm, split evenly in this representation, is still debated although it appears now that the terrestrial realm is a slightly bigger sink for the excess CO₂. Sixty-seven percent of the possible enhanced greenhouse effect over the past 100 years is due to CO₂. A doubling of atmospheric CO₂ concentration could lead to a 2.5° C increase in temperature. R.T. is the residence time of CO₂ in the atmosphere. (After Mackenzie, 2003).

atmosphere leaving 4.6 billions tons per year unaccounted. Scientists have now determined that the oceans and land biomass each take up roughly half of the 4.6 billion tons (Sabine et al., 2004; Mackenzie et al., 2001).

Charles Keeling of Scripps Institution of Oceanography in 1958 began a continuous sampling of atmospheric carbon dioxide at the Mauna Loa Observatory on the island of Hawai'i (Figure 7). The trend in atmospheric carbon dioxide, corroborated by other like measurements around the world, demonstrates without question that in the past 50 years atmospheric carbon dioxide concentration has increased by more than 15%. Atmospheric
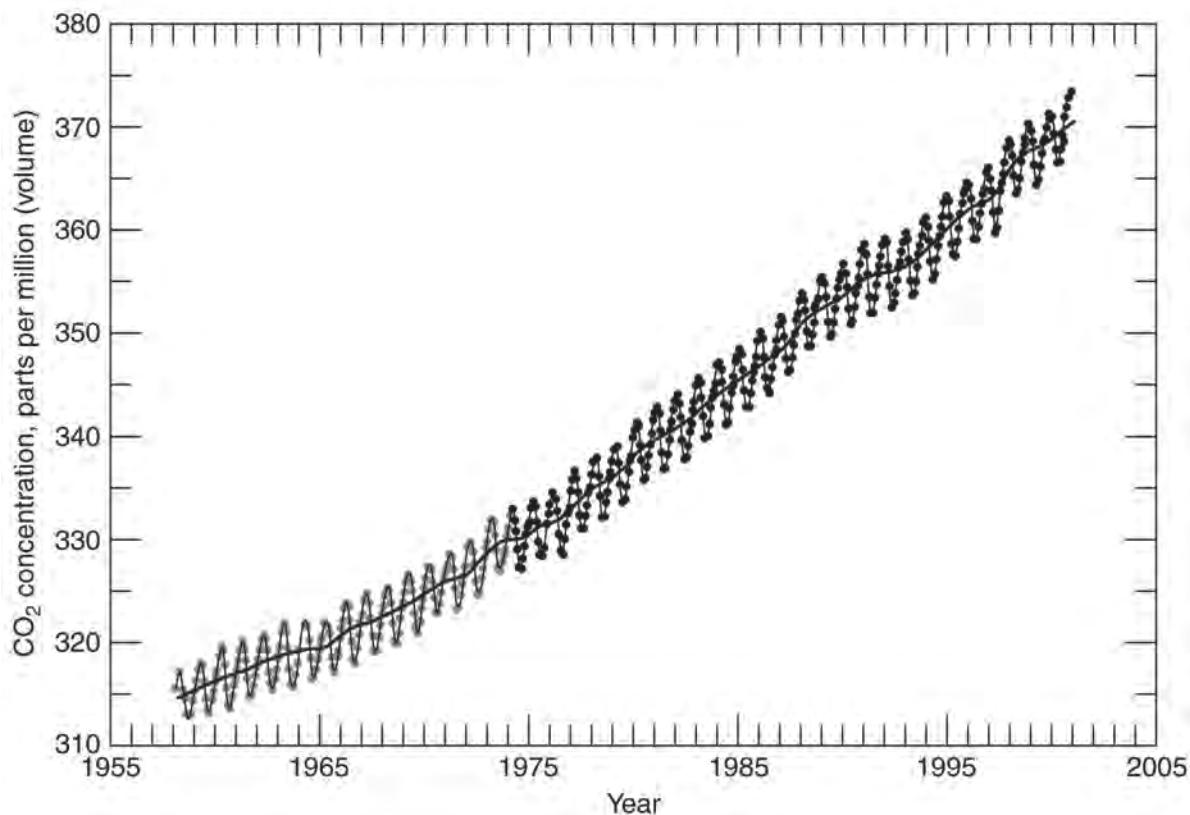
Figure 7. Mauna Loa CO_2 curve. Note the saw-toothed pattern caused by "breathing" of the northern hemisphere land biosphere. In summer, CO_2 levels drop because of photosynthesis and in winter they rise because of respiration. (http://cdiac.esd.ornl.gov/trends/co2/sio-mlo.htm).

carbon dioxide measurements (primarily from measurements of atmospheric gas composition taken from air bubbles trapped in ice cores) demonstrate that atmospheric carbon dioxide levels have increased by 32% since pre-industrial time.

2. Methane - CH_4

Methane (CH_4) is a very effective greenhouse gas. While its atmospheric concentration is much less than that of carbon dioxide, methane is 20 times more effective at trapping infrared radiation. The atmospheric residence time of methane is approximately 8 years. The methane biogeochemical cycle is shown in Figure 8. The global fluxes of methane are difficult to measure and thus the atmospheric sources and sinks are difficult to balance. It is estimated that up to 60% of the current methane flux to the atmosphere is from activities that are related to human society. Some of these activities include emissions from fermenta-

25
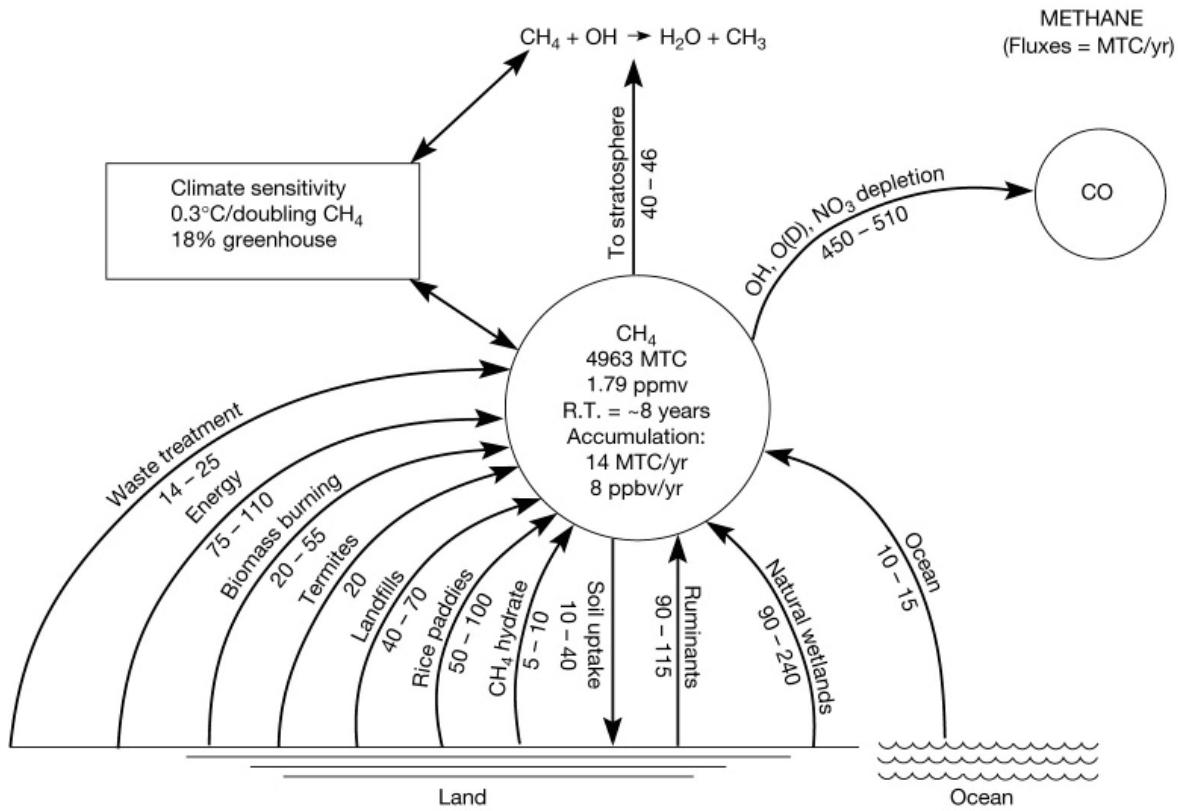
Figure 8. The biogeochemical cycle of methane (CH$_4$). Fluxes are in millions of tons of carbon per year, and the reservoir size of methane is in millions of tons of carbon. Eighteen percent of the possible enhanced greenhouse effect within the last 100 years is due to CH$_4$. A doubling of atmospheric CH$_4$ concentration could lead to a 0.3° C increase in temperature. R.T. is the residence time of CH$_4$ in the atmosphere. (After Mackenzie, 1995, 1999).

tion processes associated with livestock, from cultivated rice paddies, from fossil fuel and biomass burning, and from landfills. Methane concentrations have been increasing steadily for the past 200 years, although the rate of increase is declining, and over this time atmospheric methane concentrations have more than doubled (Figure 9).

Of future concern to the issue of global warming is the methane stored in cold environments such as peat bogs in tundra biomes and methane hydrates (frozen methane-ice compounds) found in permafrost regions and in sediments beneath the sea of continental margins. If the climate were to significantly warm, the methane tied up in these areas could be released resulting in a positive feedback (a positive feedback is a process or mechanism that amplifies a change in a system) to global warming.
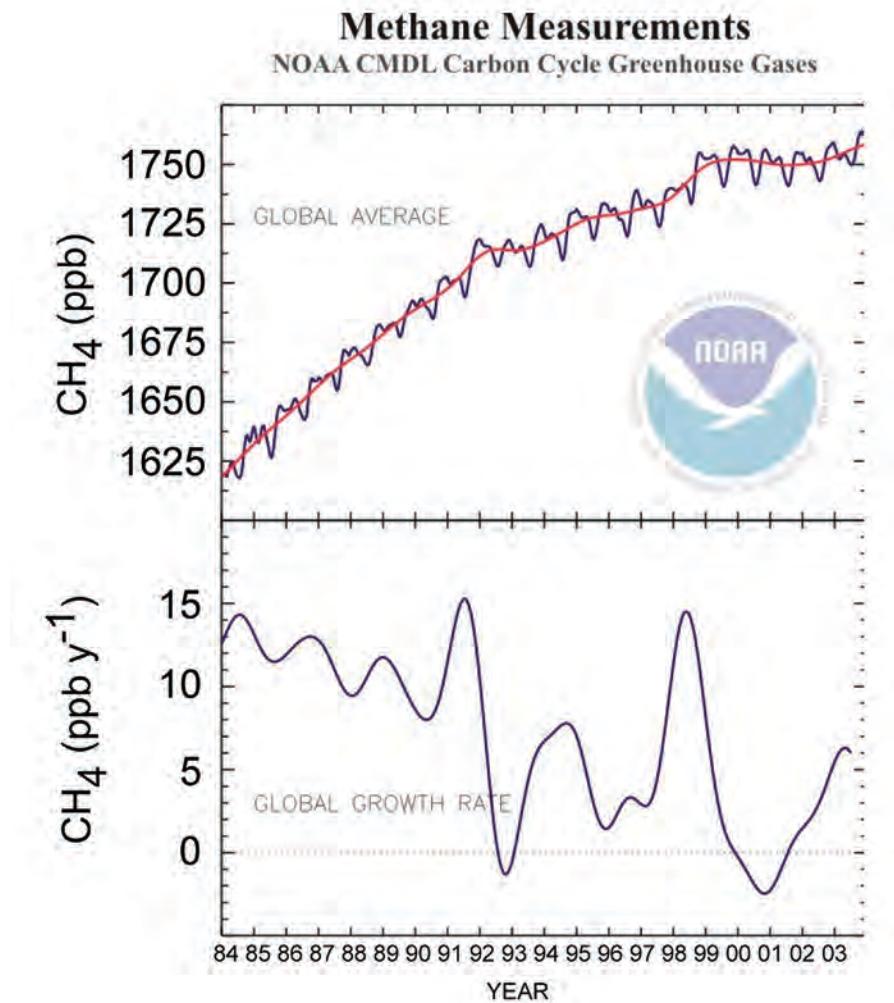
Figure 9. (Top) Global average atmospheric methane concentrations. (Bottom) Methane growth rate. (NOAA Climate Monitoring and Diagnostic Laboratory. http://www.cmdl.noaa.gov/gallery/ccgg_figures).

3. Nitrous Oxide - N_2O

Nitrous oxide (N_2O) gas should not be confused with nitric oxide (NO) or nitrogen dioxide (NO_2). Neither nitric oxide nor nitrogen dioxide are greenhouse gases, although they are important in the process of creation of tropospheric ozone which is a greenhouse gas. There are several sources of nitrous oxide, both natural and anthropogenic, for the atmosphere with many of these sources difficult to measure. Because of this, there is general agreement that the atmospheric sources and sinks of nitrous oxide are difficult to bring into balance. Figure 10 shows the global biogeochemical of nitrous oxide involving transfers between Earth's surface and atmosphere.

27

NITROUS OXIDE
(Fluxes = MTN/yr)

Climate sensitivity
0.4°C/doubling N_2O
5.9% greenhouse

N_2O
1530 MTN
319 ppbv
R.T. = ~120 years
Accumulation:
3.6 MTN/yr
0.8 ppbv/yr

Natural soils ~ 7
Cattle and feedlots 2
Industrial sources 1.3
Biomass burning 0.5
Agricultural soils 4
Ocean 3

Land

Ocean
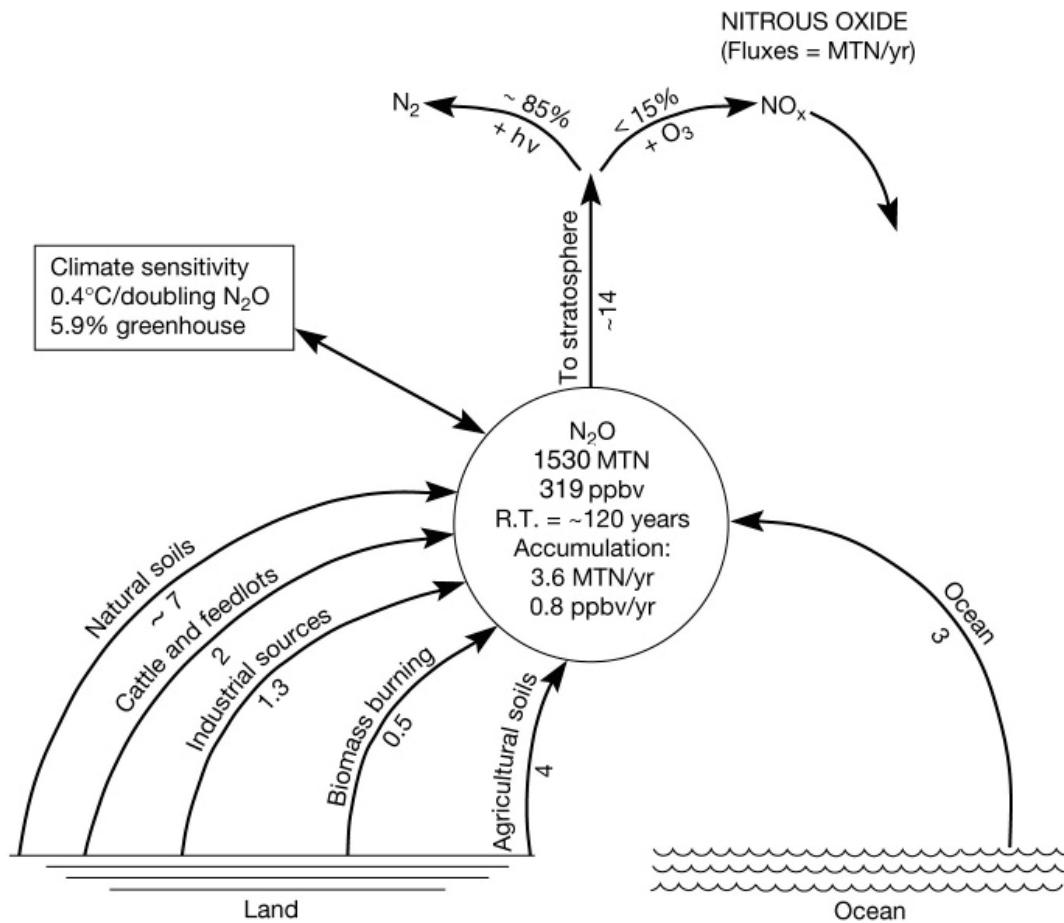
Figure 10. The global biogeochemical cycle of nitrous oxide (N_2O). The major processes and fluxes involve transfer of nitrogen as N_2O between the atmosphere and the surface of the Earth. Fluxes are millions of tons of nitrogen (MTN) per year, and the reservoir size of N_2O is in millions of tons of nitrogen. Five point nine percent of the possible enhanced greenhouse effect over the past 100 years is due to N_2O. A doubling of atmospheric N_2O concentration could lead to a 0.4° C increase in temperature. R.T. is the residence time of N_2O in the atmosphere (After Mackenzie, 2003).

Natural production of nitrous oxide is from microbial activity in soils and in the ocean and after production the gas is vented to the atmosphere. Anthropogenic production of nitrous oxide is primarily due to combustion of fossil fuels, biomass burning, industrial production of nitric acid, and application of fertilizers to agricultural crops. Nitrous oxide enhances the greenhouse effect just as carbon dioxide does by capturing reradiated infrared radiation from the Earth's surface and subsequently warming the troposphere (lower atmosphere). It is chemically inert in the troposphere and stays in the troposphere for about 120 years before moving into the stratosphere (upper atmosphere) where it ultimately leads to
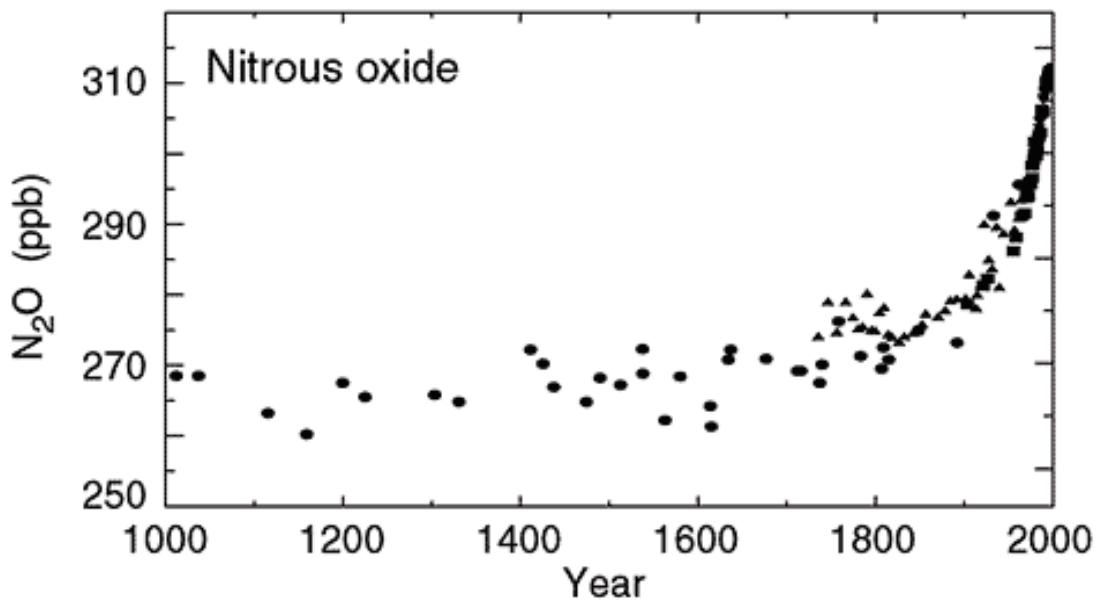
Figure 11. Atmospheric nitrous oxide concentrations. (Intergovernmental Panel on Climate Change: http://www.grida.no/climate/ipcc_tar/wg1/fig4-2.htm).

destruction of stratospheric ozone. The atmospheric nitrous oxide concentration has been growing due to human activities (Figure 11).

4.   Chlorofluorocarbons - CFCs

Halocarbons are the carbon-based compounds that contain chlorine, fluorine, bromine, or iodine. The compounds that only contain carbon, chlorine, and fluorine are called chlorofluorocarbons (CFCs). Chlorofluorocarbons are exclusively of industrial origin and have only been around for the past 60 years. Chlorofluorocarbons are exceptionally strong greenhouse gases and are also responsible for the destruction of stratospheric ozone. The most publicized of these compounds are those used as coolants in refrigeration and air conditioners, as propellants in spray cans and similar products, and as solvents for industrial purposes. Chlorofluorocarbons are far less abundant than carbon dioxide in the atmosphere, but they are 10,000 times more powerful as greenhouse gases and can remain in the atmosphere for more than 45-100 years. Figure 12 shows the atmospheric concentrations of chlorofluorocarbons. Chlorofluorocarbons are regulated under the 1987 Montreal Protocol and are therefore not addressed in the 1997 Kyoto Protocol.
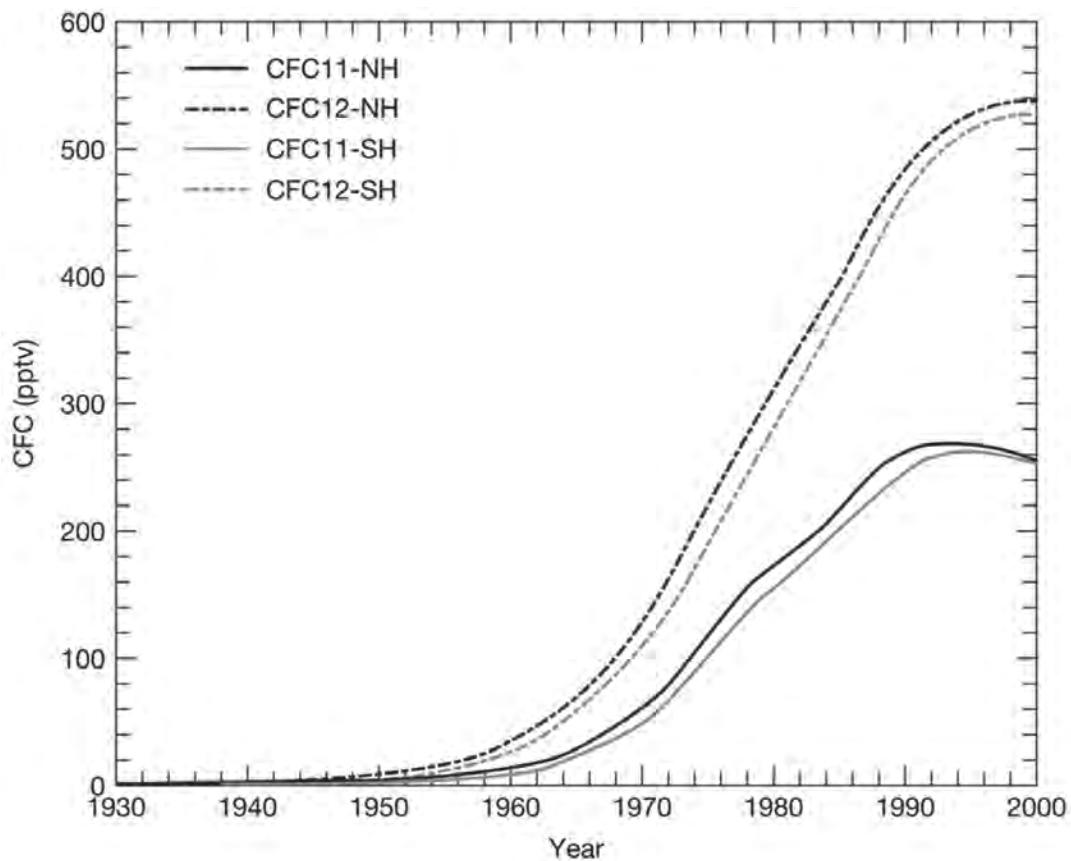
Figure 12. Concentrations (pptv = part per trillion by volume) of chlorofluorocarbon-11 and chlorofluorocarbon-12 in the atmosphere from 1940 to 2000. Notice the higher concentrations in the Northern Hemisphere (NH), the source of major emissions of CFCs to the atmosphere from human activities before the Montreal Protocol, relative to the Southern Hemisphere (SH) and the decrease in the rate of growth of the two gases in the atmosphere since the late 1980s. (After National Oceanic and Atmospheric Administration [NOAA] Climate Monitoring and Diagnostics Laboratory [CMDL], Carbon Cycle Greenhouse Gases, www.cmdl.noaa.gov/ccgg/figures/figures.html.)

5. Hydrofluorocarbons - HFCs, Perfluorocarbons - PFCs, Sulfur Hexafluoride - SF_6

    Hydrofluorocarbons (composed of hydrogen, fluorine, and carbon) and perfluoro-carbons (composed of fluorine and carbon) have been created for industrial applications and been adopted as ozone safe replacements for chlorofluorocarbons and thus are growing in atmospheric concentration (Figure 13). Even though hydrofluorocarbons and perfluoro-carbons are emitted in relatively small quantities, they have a disproportionate effect on the greenhouse effect. As greenhouse gases, the most potent hydrofluorocarbons and perfluoro-carbons are 11,700 times and 7000 to 9000 times per molecule more effective as greenhouse

gases than a molecule of carbon dioxide, respectively. Also, perfluorocarbons have relatively long atmospheric lifetimes (up to 50,000 years). Rated as the most powerful greenhouse gas ever released to the atmosphere, sulfur hexafluoride is used as an electric insulator, heat conductor, and a freezing agent. In comparison to one molecule of carbon dioxide, the global warming potential of one sulfur hexafluoride molecule is approximately 24,000 times greater. Sulfur hexafluoride has now been banned from use due to its global warming potential.

Figure 13. Hydrofluorocarbons (HFCs) and hydrochlorofluoro-carbons (HCFCs) atmospheric concentrations (ppt = part per trillion). (Intergovernmental Panel on Climate Change: http://www.grida.no/climate/ipcc_tar/wg1/137.htm).

6. Aerosols

Aerosols are very small micrometer-sized airborne particles, either liquid or solid, that can be produced naturally from volcanoes, wildfires, windblown dust of soils, land and ocean emissions of biologically produced gases, and sea-salt spray. The size and distribution of the aerosols are critical to their influence on climate and there is great spatial and temporal variability in aerosol concentrations. In addition, aerosols overall have short atmospheric lifetimes (times spent in the atmosphere), which suggests that they should not be considered or relied upon to act in such a way as to offset long-term greenhouse warming. Generally speaking, the larger the number of aerosol particles, the greater the amount of heat radiated back to space and thus aerosols most likely produce a cooling effect on climate. Aerosols can cool by (1) reflecting incoming radiation back to space, and (2) serving as cloud condensation nuclei for certain cloud types that reflect radiation back to space.

An example of the global cooling effect that aerosols can have on climate is the 1815 eruption of Tambora volcano in Indonesia. The dust and aerosol produced by the eruption entered the stratosphere and reduced the solar radiation reaching the planet. In 1816, because of late snows and continuous rains, Europe experienced a year without a summer. The cool conditions continued in Europe for three years after the eruption resulting in massive crop failures, subsequent starvation, and near collapse of society in Europe.

Biological emissions of sulfur gases from the land and ocean surface also can lead to creation of aerosols in the atmosphere and hence affect climate. These emissions are dominated by dimethylsulfide (DMS), hydrogen sulfide (H_2S), and carbonyl sulfide (OCS). The biogenic gases can be oxidized to sulfur dioxide gas in the atmosphere and then to sulfate aerosol.

The major source of cloud condensation nuclei in the remote atmosphere above the ocean is dimethylsulfide gas escaping the sea surface. The magnitude of the dimethylsulfide flux is related to phytoplankton (primary) production and bacterial degradation of the organic products derived from primary production. One hypothesis put forth related to the feedback between dimethylsulfide emissions and climate is that if the Earth warms, then phytoplankton production will increase. This increase would lead to an increased flux of dimethylsulfide to the atmosphere, which in turn would result in more formation of sulfate aerosols and thus cloud condensation nuclei. The increased production of cloud condensation nuclei and therefore degree of cloudiness would lead to reflection of solar radiation and hence to cooling of the atmosphere (specifically the troposphere). This is a negative feedback (a negative feedback is a process or mechanism that diminishes a change in a system) to global warming. The acronym for this hypothesis, CLAW, is from the first letters of the authors of the hypothesis – Charlson, Lovelock, Andreae, and Warren.

Industry, biomass and fossil fuel burning and the resultant emission of sulfur dioxide can lead to formation of sulfate aerosols that contribute to tropospheric sulfate aerosol (Figure 14). These aerosols potentially could have a cooling effect on climate. It has been argued that the enhanced anthropogenic emissions of sulfur dioxide to the atmosphere, especially in the northern hemisphere, have helped cool the planet during the twentieth century. If this is true, the cooling effect may have offset part of the expected temperature increase owing to anthropogenic emissions of greenhouse gases to the atmosphere, especially over industrialized areas (Figure 15).

32
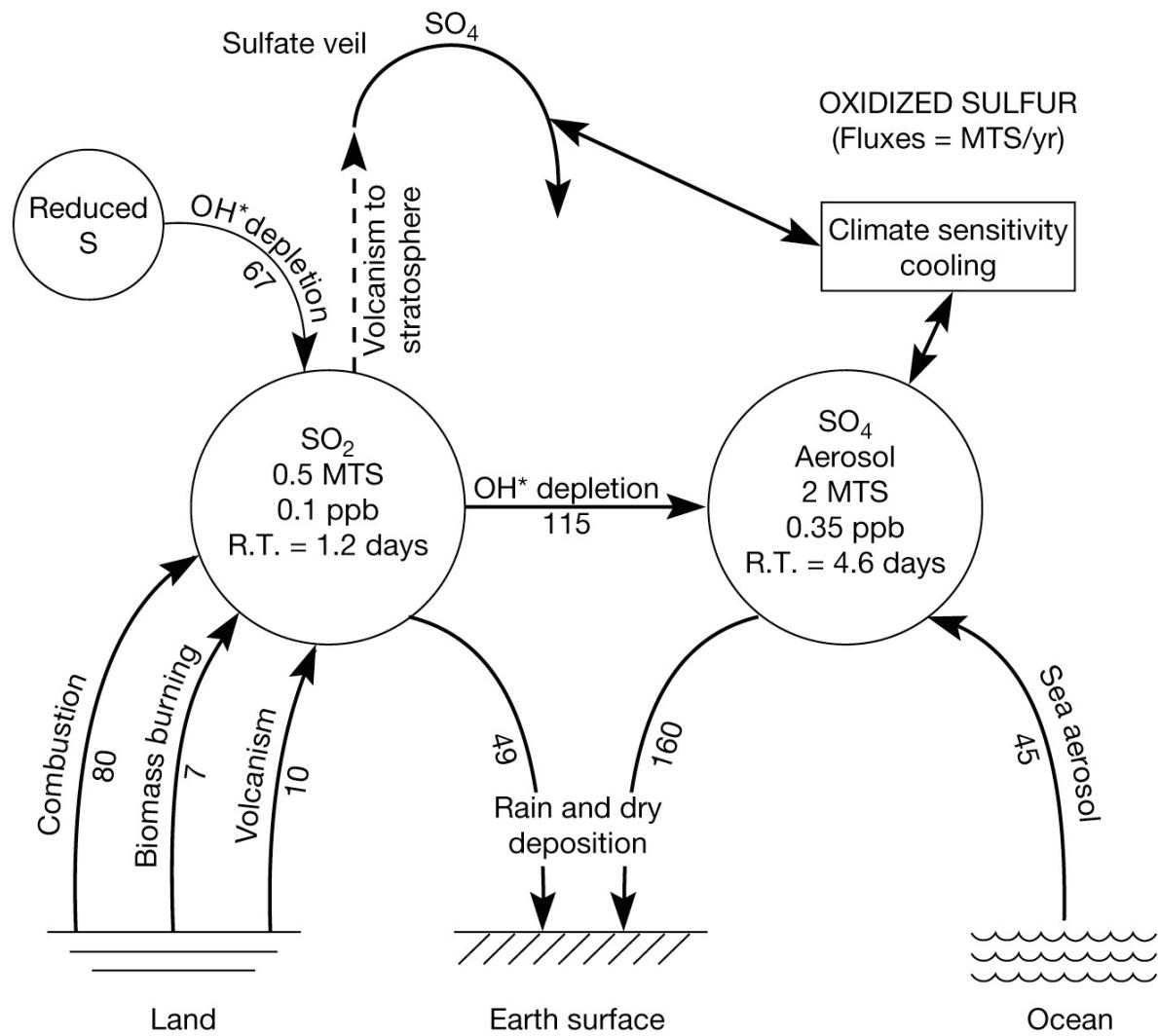
Figure 14. Earth surface-atmosphere global biogeochemical cycle of oxidized sulfur species. Sulfur dioxide (SO_2) released from the land surface to the atmosphere reacts with hydroxyl radical (OH) to form sulfate (SO_4) aerosol. Sulfate aerosol, directly or indirectly, potentially exerts a cooling influence on the climate. Flux values are in units of million tons of sulfur per year. R.T. is the residence time of SO_2 and SO_4 in the atmosphere. (After Mackenzie, 2003).*
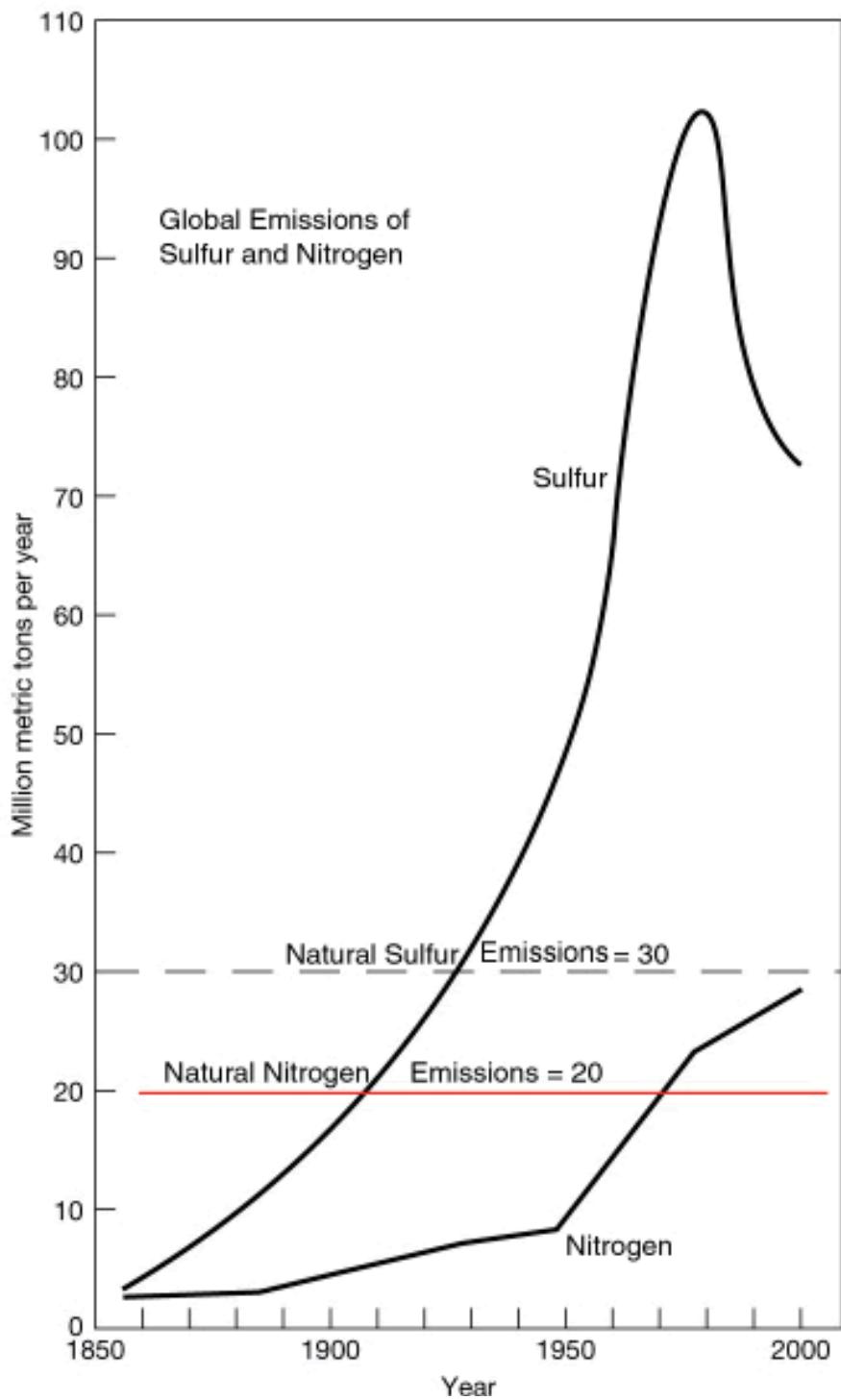
Figure 15. Annual anthropogenic global emissions of sulfur and nitrogen as SO$_x$ and NO$_x$ to the atmosphere from the burning of fossil fuels, and for sulfur from the smelting of sulfide ores from 1860 to 2000. An estimate of the natural biological sulfur flux (dashed line) and natural nitrogen flux (red line) to the atmosphere is given for comparison. (After Dignon and Hameed, 1989; Hameed and Dignon, 1992; Smil, 1997).

7. Summary

The current concern about the greenhouse effect and climate stems from the amounts of greenhouse gases that are being released into the atmosphere from the burning of fossil fuels, deforestation, agricultural and industrial practices, release of synthetic chlorofluoro-carbons, and other humankind activities. Accumulation of these heat-absorbing greenhouse gases in the atmosphere can result in an enhanced greenhouse effect and consequent global warming induced by human activities. The concern is that an enhanced greenhouse effect may elevate global temperatures above levels that have not occurred for hundreds of thousands of years. The degree to which the accelerating rate of increase of greenhouse gases in the atmosphere will impact our climate is a topic of much debate and uncertainty because of the many variables that are involved in the climate system and their feedbacks.

In an effort to determine what effects these human-induced changes to greenhouse gas concentrations could have on climate, sophisticated computer models have been developed by the scientific community and are continually refined. In 1990, 1995, and 2001 the Intergovernmental Panel on Climate Change released three reports intended to provide information not only how climate has changed over human times, but also how it might change in the future, and given the range of projected future change, what would be the resultant impacts– e.g., environmental, economic, social, political, etc. – for the world's population. The climate forecasts in these reports are based upon the projections from large-scale computationally intensive global climate models. The first two Intergovernmental Panel on Climate Change reports, and their climate forecasts, led to the 1997 Kyoto Protocol.

III. Kyoto Protocol: Global Policy Response to Climate Change

In an effort to mitigate the myriad of problems associated with human-induced amplification of the greenhouse effect and climate change, including the impacts on island nations and states, the United Nations Framework Convention on Climate Change (UNFCCC) was adopted and opened for signing in 1992 at the Rio Earth Summit. The convention called for signatory countries to strive to return their individual CO_2 emissions back to 1990 levels by the year 2000 and also established the Conference of Parties (COP). The United States refused to make the terms of the agreement legally binding. In 1994, it was decided that the Convention would enter into force 90 days after the receipt of the 50th ratification. In 1995, the first Convention of Parties (COP-1) took place in Berlin with delegates agreeing that the United Nations Framework Convention on Climate Change proposed greenhouse reductions commitments are inadequate, but no agreement was reached over new emission targets. The Intergovernmental Panel on Climate Change climate scientists released their Second Assessment Report in 1995 and these findings become a major impetus for negotiations that eventually resulted in the 1997 Kyoto Protocol.

The 1997 Kyoto Protocol is a legally binding international agreement that commits signatory countries to reducing their global emissions of greenhouse gases. The Kyoto Protocol becomes legally binding when ratified by 55 nations and in addition that these nations represent 55% of the 1990 carbon dioxide emissions by the 39 industrialized countries. As of mid-2004, 122 countries representing 44% of the total 1990 carbon dioxide emissions had signed the protocol. There were thus more than enough countries that had ratified the agreement for it to go into effect, but these nations did not represent 55% of the 1990 carbon dioxide emissions. At that time, both the United States and Russia had not ratified the Kyoto Protocol, but one of the two nations needed to ratify it before the 55% of the 1990 carbon dioxide emission goal could be met and the Kyoto Protocol would become a globally binding agreement. This is because of these nations' relative contributions to the 1990 carbon dioxide emissions (United States – 36%; Russia – 17%). In 2001, the United States stated it would not sign the agreement – even though the U.S. government accepts climate change as a fact – because of the restrictions it felt the protocol placed on industry and world economic growth. The U.S. instead is promoting policies meant to support new and emerging energy and climate protection technologies. Russia initially indicated it would sign the agreement, retracted that promise, and then sent mixed signals about its intentions. It too, as the U.S., took the stance that if the Kyoto Protocol was enacted, it would retard

future economic growth. In a turn of events though, Russia announced in late 2004 that they were going to ratify the agreement and on November 18, 2004 the 90 day countdown to the Kyoto Protocol's entry into force was triggered by the receipt of the Russian Federation's instrument of ratification by the United Nations Secretary-General. The Protocol became legally binding on its then 128 Parties on February 16, 2005. The developing countries are not included within the protocol, despite the fact that greenhouse gas emissions from these countries will exceed those of the developed, industrialized world by 2010. The Kyoto Protocol requires that the 39 industrialized nations involved in the protocol reduce their greenhouse gas emissions by a specified annual percentage of their 1990 emissions by 2008-2012. The average overall reduction is targeted to be approximately 5%, but the percentages vary from country to country – e.g., U.S. is 7%, European Union is 8%, New Zealand is no change. Because of their relatively low emissions, Australia and New Zealand are allowed to increase their emissions by 8 and 10%, respectively. The emissions of the following six gases are included in the protocol: carbon dioxide, nitrous oxide, methane, hydrofluorocarbons (HFCs), perfluorocarbons (PFCs), and sulfur hexafluoride. Each country's emission limit is based on a radiation-weighted sum of the six gases, which takes into account the relative impact and abundance that each of the six gases has on global warming. Sinks for gases are also included in the protocol. An example is that if a country demonstrates that carbon is being stored in its forests because of planting trees, this carbon storage will be entered as a negative value into the country's net emissions counting as a reduction and credit against emissions. Because the protocol will influence most major sectors of the world economy, it is considered to be the most far-reaching agreement on environment and sustainable development ever adopted.

The Kyoto Protocol, based on the 1990 and 1995 Intergovernmental Panel on Climate Change reports, is necessarily global in scope. The regional effects of a future enhanced greenhouse effect on climate variables of temperature, precipitation, storm variability, and on sea level rise, etc. are difficult to resolve with global models due to their course resolution. In 2001, The Pacific Islands Regional Assessment Group (PIRAG) on behalf of the U.S. Global Change Research Program (USGCRP) published the report *Preparing for a changing climate: The potential consequences of climate variability and change* (Shea et al., 2001). The Pacific Islands Regional Assessment Group focused on the consequences of climate variability and change on the American Flag Pacific Islands including Hawai'i, Guam, American Samoa and the Commonwealth of the Northern Mariana Islands (CNMI), and the U.S.-affiliated Pacific Islands, which include the Federated States of Micronesia (FSM: Yap, Pohnpei, Kosrae and Chuuk), the Republic of the Marshall Islands (RMI), and the Republic of Palau (Figure 16).

37
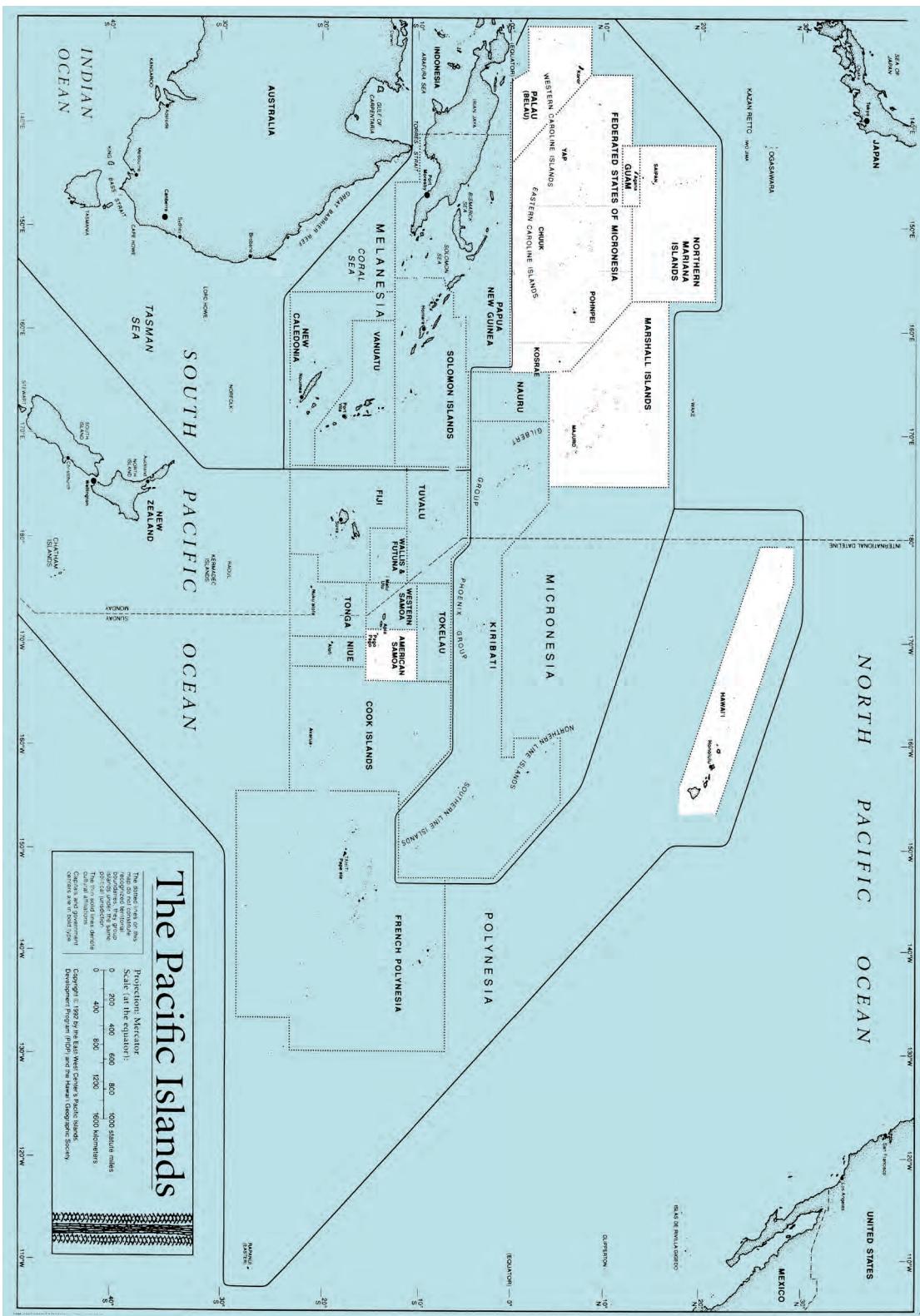
Figure 16. The Pacific Island region studied in the report Preparing for a changing climate: The potential consequences of climate variability and change. (Shea et al., 2001).

In the Pacific Islands Regional Assessment Group report, the effects of changing climate on sea-surface temperatures, precipitation, and sea level in the Pacific region were modeled using two models: the Canadian Center for Climate Modeling and Analysis (CGCM1) and a similar general circulation model used by the United Kingdom's Hadley Centre for Climate Prediction and Research (HADCM2). The CGCM1 and HADCM2 results were compared to two model results (A2 and B2) generated by the Intergovernmental Panel on Climate Change *Special Report on Emission Scenarios* (SRES).

IV. Overview of CGCM1 and HADCM2 Model-based Scenarios of Future Climate Conditions for the Pacific Islands

The Pacific Islands Regional Assessment Group report discussed the results of the two regional coupled ocean-atmosphere models that spanned approximately 75 years using the core greenhouse-gas emissions scenario for the first United States National Assessment of the Consequences of Climate Variability and Change (USGCRP, 2001), which is equivalent to a 1% rate of annual increase in carbon dioxide, and commensurate changes in sulfate aerosols. The rate of carbon dioxide increase is based on rates of observed increases modified by estimates of how the current sources of emissions are likely to change in the future; as such, it is deemed plausible as a "business as usual" case with little policy intervention anticipated in the future.

Carbon dioxide increases in these two models cause warming by limiting outgoing long-wave radiation from the Earth's surface in the absence of a simultaneous reduction of incoming solar radiation. Increases in sulfate aerosol concentrations produce a net cooling over regions where sulfur emissions are greatest, generally corresponding to industrial regions in the midlatitudes of the northern hemisphere. The effect of the SO_4 aerosols, which is the reflection of solar radiation back away from the Earth's surface, is taken into account in these two models. The radiative forcing (radiative forcing is the change in the balance between radiation coming into the atmosphere and radiation going out) of sulfate aerosols resulting in cooling is less than the forcing of carbon dioxide and thus warming of the globe is projected for the future.

Since the results from both models were generally consistent, only the Hadley HADCM2 results were discussed in the Pacific Islands Regional Assessment Group report. The HADCM2 results were also compared to the two model runs (A2 and B2) described in the Intergovernmental Panel on Climate Change *Special Report on Emission Scenarios*. These Intergovernmental Panel on Climate Change models represent an average of nine "state-of-the-science" global, coupled climate models from groups in the U.S., Canada, Germany, Australia, U.K., and Japan.

Two time periods (2025-2034 and 2090-2099) were projected using the HADCM2 model to study future changes in temperature, rainfall, storminess, and sea level for the Pacific region. The 2025-2034 results are termed "short-lead" and the 2090-2099 results are termed "long-lead". The long-lead results are more speculative than the short-lead results. During these two time periods, there were two seasons analyzed [December-January-February (DJF) and June-July-August (JJA)]. These months were chosen because they represent two seasonal extremes.

A. HADCM2 Sea Surface Skin Temperature Results

Gradual warming of the sea-surface temperature (SST) and the near-surface air temperature is projected to occur for both the short and long-lead results (Figure 17). The
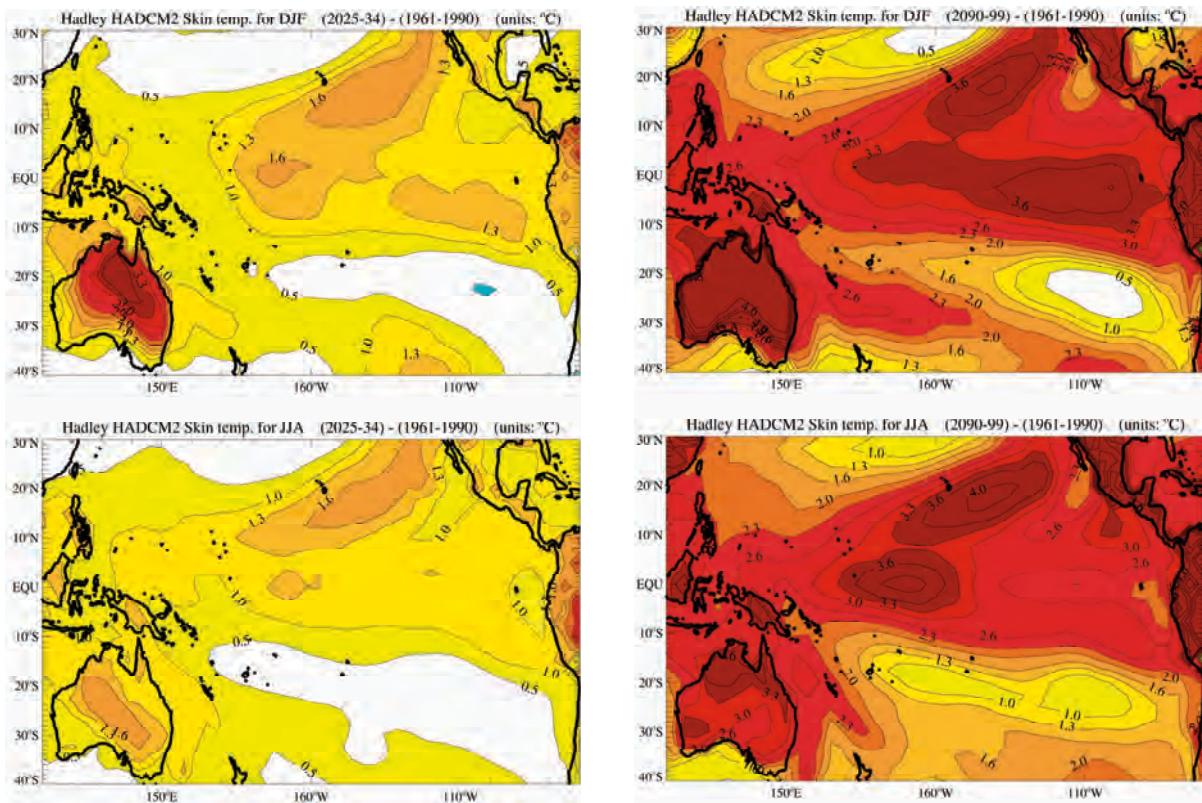
Figure 17. Projected changes in skin temperature (SST over ocean and surface –air temperature over land) difference for the short-lead results (the model's 2025-2034 average minus the 1961-1990 base period average) and the long-lead results (2090-2099 average minus the 1961-1990 base period) for the seasons DJF and JJA, in ° C. (Shea et al., 2001).

41

projected increase is about 1° C (1.8° F) per 20 to 45 years. Looking at the projections, warming will be greatest in the following Pacific regions: (I) along and slightly south of the equator extending from the international dateline on the west to the South American coast on the east and (II) east-northeastward from the equatorial Central Pacific to the United States-Mexico border and the southwest coast of the United States. Note the warming in the equatorial East Pacific, which is projected to be greater during the peak El Niño season of DJF.

B. Rainfall

With the projected increase in temperature comes increased precipitation due to the fact that warmer water produces more moisture and the atmosphere above a warmer ocean surface can absorb and hold more moisture. The equator around the dateline is the most likely candidate for increased precipitation since the sea-surface temperature is warm enough to support convection (Box 3) and thus cumulus cloud growth and precipitation. Increased sea-surface temperature in these areas would result in more convection and rainfall.

Overall, the projections (Figure 18) suggest that variation in the rainfall pattern will be seasonal with the biggest change coming in the boreal (northern hemisphere) summer months of June,

Box 3: Convection

Convection refers to the process of cloud formation and precipitation associated with areas where warm tropical air rises through the atmosphere and, as it expands and cools, leads to the formation of clouds. As a result, weather patterns tend to be disturbed in these areas. In the tropics, warm air rises to the top of the troposphere and moves off toward the poles. Areas where colder air tends to move downward through the atmosphere and then toward the equator complement these areas of rising air movement. As a general rule, weather in areas of sinking air tends to be dry and relatively calm.

July, and August. During the boreal summer months, increased rainfall is projected to occur along a line from the equator to the Hawaiian Islands. Less change in rainfall is projected in winter because ocean temperatures are cooler and thus less apt to support convection. Model projections for 2025-2034 JJA indicate that areas of increased rainfall extend to 10° S. The projections for the period 2090-2099 show this area extending farther south to between 15 and 20° S with the largest increases in precipitation along a line extending from Republic of the Marshall Islands in the north to Tahiti in the south. The regions near 10° N and to the

Figure 18. Projected changes in total precipitation change for 2025-2034 and 2090-2099 in units of millimeters per day*10 (centimeters per day). (Shea et al., 2001).

west of the dateline (180°) would also receive substantially greater precipitation in the long-lead results compared to the short-lead results.

During the austral (southern hemisphere) summer months of December, January, and February, the increased rainfall is analogous to an intensification of the South Pacific Convergence Zone, an area of the ocean (Western Pacific warm pool) that provides one of the principal sources of heat to the atmosphere. Model projections for 2025-2034 indicate some large areas of enhanced rainfall. The primary area is along a broad band extending from 10° N and 160° E through the equatorial dateline and southeast to near 10° S and 130° W. This already considerable region of enhanced precipitation is further enlarged in the projection for 2090-2099 with increased rainfall extending farther east along the equator and accompanied by large increases in the proximity of the Marquesas Island. This area of increased precipitation also extends westward to the most western of the islands of Micronesia.

Decreased precipitation could be experienced in all seasons in areas near the equator east of about 140° W. Rising, warm, moist air must ultimately come down and therefore areas of rising air that usually produce clouds and rainfall alternate with neighboring areas of sinking air that tend to be relatively dry. Due to this phenomenon, areas of decreased precipitation could also spread poleward of the most rapidly warming equatorial regions (e.g., north of the Hawaiian Islands) negatively affecting many of the islands west of Hawai'i, and tropical South Pacific Islands farthest off the equator but west of French Polynesia.

The projected rainfall scenarios are more tenuous than the temperature projections and as such should be carefully considered. The exact location of borders between adjacent regions of projected enhanced or suppressed rainfall is uncertain and will be further addressed below when the regional model results are compared with results from the multimodel ensemble experiments. Some of the areas near the regional boundaries made alternately wetter and drier by El Niño also bound the areas of the rainfall effects of climate change; examples of such locations are Apia in Samoa and Niualakita in southern Tuvalu.

C. *Natural Variability and El Niño Southern Oscillation*

In the short- and long-lead models, the pattern of increased sea-surface temperatures along the equatorial Central and Eastern Pacific suggests a greater tendency for El Niño-like conditions with sea-surface temperatures steadily warming in the Central and Eastern equatorial Pacific Ocean. Increased precipitation in the aforementioned region is indicative of both the short- and long-lead DJF warming patterns seen in the model results.

Anomalies of sea-surface temperatures in the Niño-3 region (defined as 5° N to 5° S and 150° W to 90° W) are useful in measuring the strength of El Niños and La Niñas (see 2. El Niño Southern Oscillation). The time-series of the Niño-3 sea-surface temperature anomaly index from the Hadley model (Figure 19) shows a general warming trend through 2099. Over this interval and in this region, the average sea-surface temperature increases by roughly 3° C (5.4° F). It should be remembered that the characteristics or behavior of the El Niño Southern Oscillation could change with the overall warming of the atmosphere and ocean. If so, this would complicate and create uncertainty about the details of future climate conditions in the Pacific.
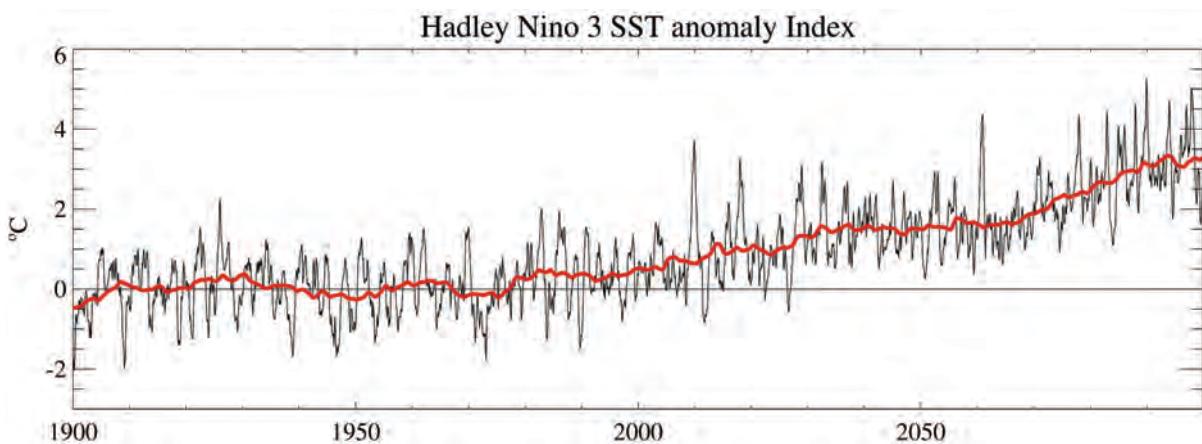
Figure 19. Monthly SST anomaly time series for the period 1900-2099. The El Niño 3 region is defined as 5° N to 5° S and 150° W to 90° W, with the base years for the climatology defined as 1950-1979. The thick red line is the 10-year running average. Units are in ° C. (Shea et al., 2001).

Regarding the short- and long-lead model results in terms of the natural Pacific climate variability and El Niño Southern Oscillation, it is useful to discuss how coupled atmosphere-ocean processes impact climate. Both the Intertropical Convergence Zone and the El Niño Southern Oscillation are consequences of the coupled atmosphere-ocean system, play a role in climate variability, and thus may be impacted by climate change.

1.   Intertropical Convergence Zone

Air-sea interactions are important to the transfer of energy and mass between the oceans and atmosphere. Both atmospheric and ocean circulation are driven by low-latitude heating and high-latitude cooling. Heat is absorbed by the planetary surface at low latitudes and is transferred poleward in both the northern and southern hemispheres. The equatorial region is a barrier to the exchange of materials between the atmosphere of the northern and southern hemispheres. It is also a barrier to water, salt, and heat exchange at the ocean's surface. The large solar input to the tropics leads mainly to heating of the ocean surface. In turn, the air above the surface ocean is heated, expands, and becomes less dense. This reduction in density causes the air to rise owing to convection. A region of low pressure develops because the mass of the overlying atmosphere in the tropics is reduced. The "void" left by the rising, warm, and moist air is replaced by air that moves toward the equator. This region is called the Intertropical Convergence Zone. It is the zone along which the trade wind systems of the northern and southern hemispheres meet (Figure 20).
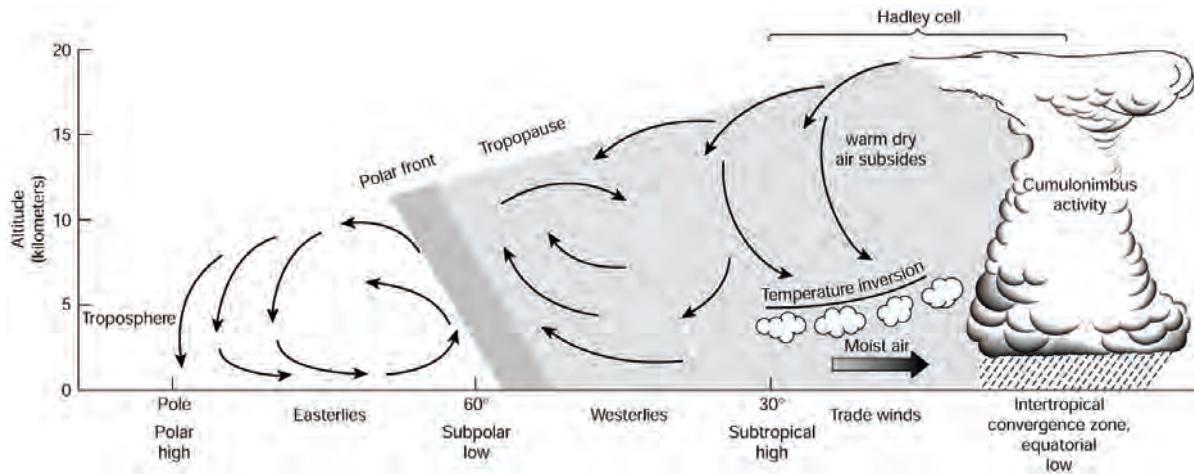
Figure 20. Longitudinal cross section through the lower 20 kilometers of Earth's atmosphere from the polar region to the equator showing general vertical air circulation patterns. (After Open University, 1989).

Heating of the tropical ocean surface causes evaporation of water. The water vapor rises and cools at higher elevations in the atmosphere, leading to the formation of clouds. Thus, the region of the Intertropical Convergence Zone is characterized by cloudiness and heavy precipitation. The zone of the Intertropical Convergence Zone is particularly intensely developed in the western Pacific. Here a warm water pool of surface water (Western Pacific warm pool) is found with mean ocean surface temperatures of about 31° C. On average, this is also a region of intense atmospheric convection and the wettest part of the tropics. This surface ocean warm pool and the associated zone of heavy rainfall are important to the dynamics of El Niño-Southern Oscillation events.

The Intertropical Convergence Zone shifts seasonally. During the northern hemisphere summer, the ITCZ shifts northward as the Asian continent is warmed more than the adjacent ocean (Figure 21a). The warm continental air rises, and air is drawn from the ocean toward the land. The zone of heavy rainfall expands northwestward from Indonesian into India and Southeast Asia. Southerly winds blowing from the oceans toward India and Southeast Asia are dominant at this time (Figure 21a). This is the time of the Southwest Monsoon (May to September). During the northern hemisphere winter, the reverse is true when the air above the Asian continent becomes very cold (Figure 21b). An intense high-pressure region develops in the atmosphere above continental Asia. The flow of air is from the continent toward the ocean. This is the time of the Northeast Monsoon (November to March).
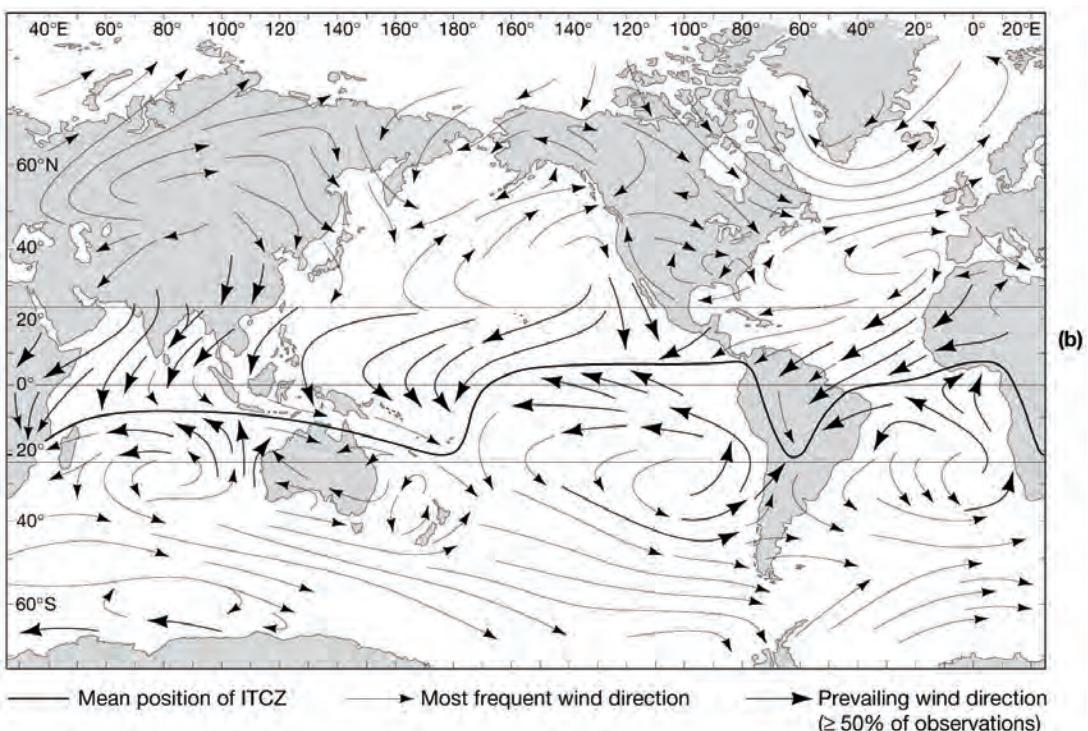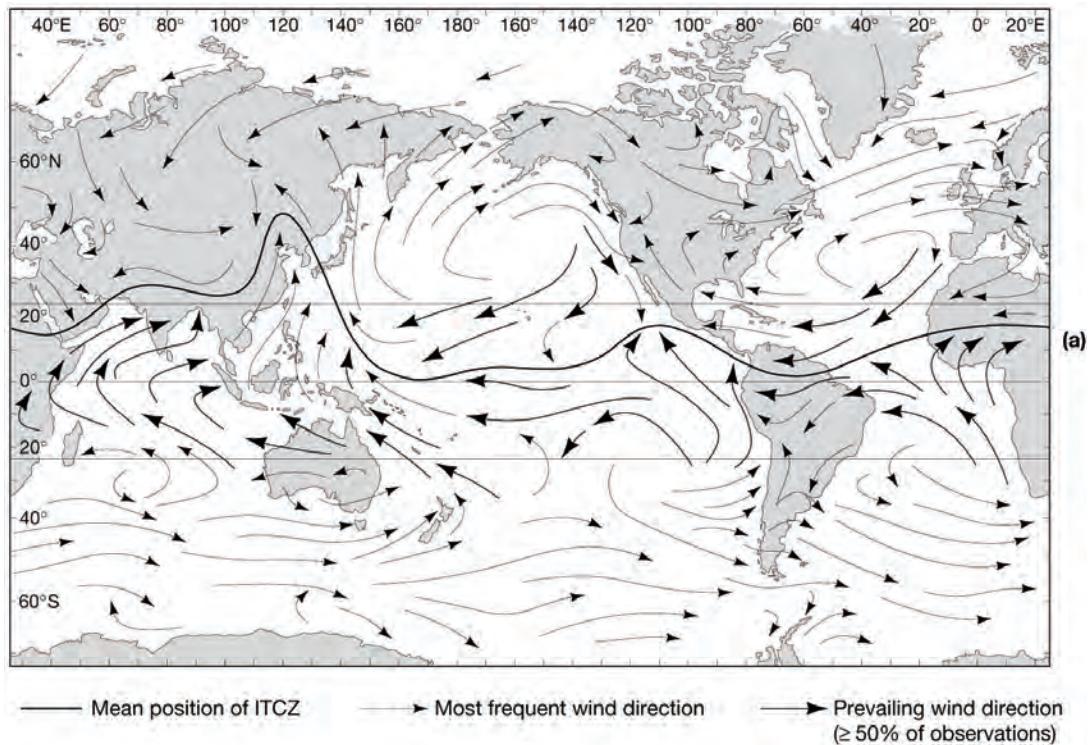
Figure 21. The average prevailing wind directions at Earth's surface during the Northern hemispheric summer (a, July) and winter (b, January). The solid black line shows the Intertropical Convergence Zone (ITCZ) position and its change with season. (After Open University, 1989).

47

2. El Niño Southern Oscillation

     The El Niño Southern Oscillation phenomenon in the Pacific Ocean has regional (Pacific Basin) and global ecological and climatic impacts. The El Niño Southern Oscillation cycle is comprised, among other things, of a range of surface water temperature conditions: (1) extreme warm conditions (El Niño), (2) normal or average surface conditions, and (3) extreme cold conditions (La Niña). During non-El Niño conditions – e.g., La Niña or normal surface water conditions – cool currents flow north along the coastline of Peru and Chile termed the Peru Oceanic and Coastal Currents (Figure 22). The Peru Oceanic Current extends to a depth of 700 meters (2296 feet) and can be as wide as 600 kilometers (1969 feet) and the Peru Coastal Current runs close to the coastline and is 200 meters (656 feet) deep and 200 kilometers (124 miles) wide. Beneath these two currents lies the southward flowing Peru Undercurrent and to the north is the Peru Countercurrent. The prevailing southeast trade winds usually blow approximately parallel to the Peruvian coastline, which results in the deflection and movement of surface currents offshore to the west. This westward movement of the surface waters leads to its replacement by vertical water movement (termed upwelling) from a depth of 40 to 80 meters (131 to 262 feet) at a speed of 1 to 3 meters (3.3 to
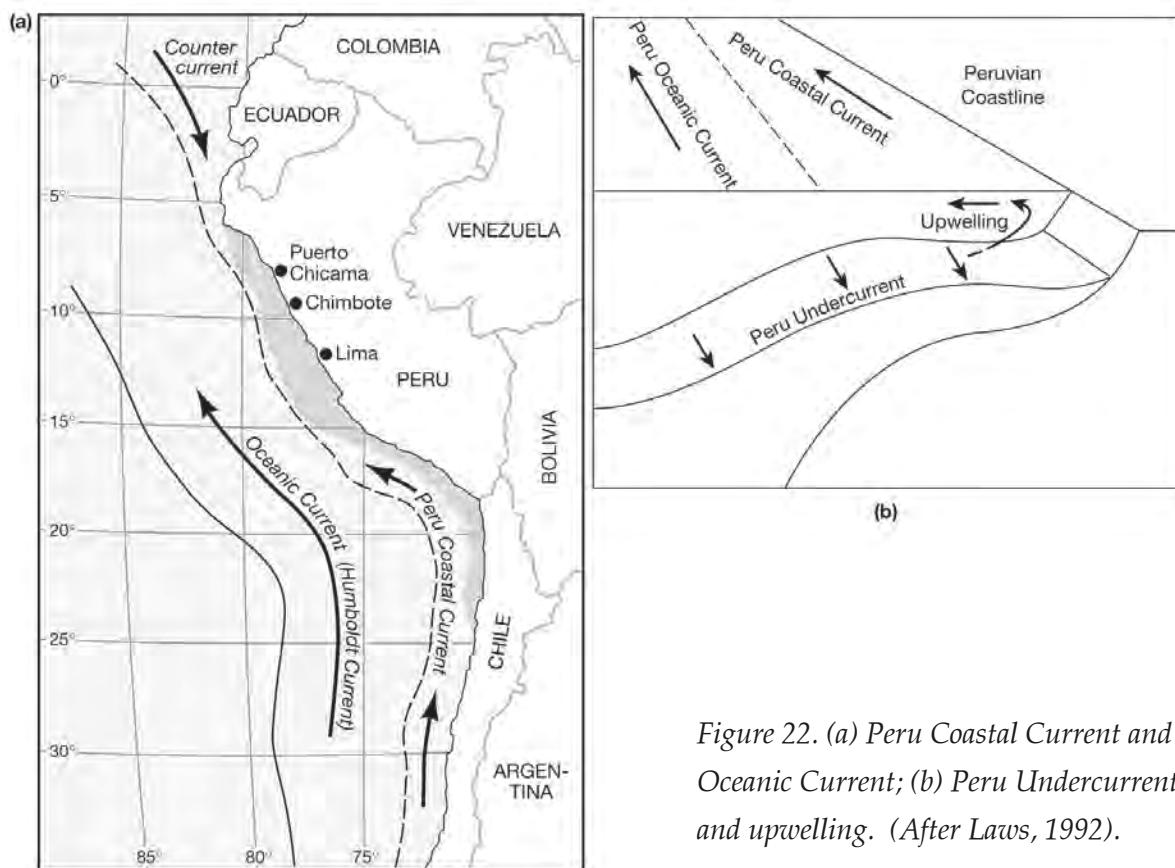
Figure 22. (a) Peru Coastal Current and Oceanic Current; (b) Peru Undercurrent and upwelling. (After Laws, 1992).

48

9.8 feet) per day. This upwelling water is rich in nutrients and stimulates biological production in surface waters. The upwelled nutrient-rich water comes from below the nutricline. The nutricline is the water depth below which nutrients are abundant and have not been consumed by primary production in the layer of surface water.

About every 3 to 7 years, an El Niño occurs that usually lasts 1 to 2 years or sometimes longer. El Niño means "the Christ Child" and is so named because the phenomenon usually begins around Christmas. El Niño is a time when the warm low salinity waters of the Pacific extend far to the east and bathe the coast of central South America in warm (up to 10° C warmer), nutrient-poor water. This western Pacific water is transported to the Peruvian coast by the Peru Countercurrent, which overrides the Peru Coastal Current because it is less dense (being warm and of low salinity) than the water of the coastal current. This nutrient-poor layer of water on the order of 30 meters (98 feet) thick comes to reside along the Peru coast. Due to the layer's thickness, upwelling water no longer comes from below the nutricline but from within the nutrient-poor water layer. So during an El Niño if upwelling occurs, the upwelled water is low in nutrients and biological production is suppressed. Concurrently, trade wind intensity may decrease substantially, perhaps completely causing upwelling to cease. In addition to changes in ocean upwelling and circulation, El Niño can impact rainfall and temperature patterns around the world (see Figure 23). El Niño events are usually responsible for warm, dry winters in the northern United States and wet winters in the southern United States, torrential rains and flooding in coastal South America and parts of Asia, droughts in Africa, Australia, and the Hawaiian Islands, unusual tropical cyclone activity, and failure of the monsoon in Asia.

When the more usual situation of the cool currents offshore Peru return (normal conditions or La Niña conditions), upwelling returns, biological productivity increases, the anchovies return, the birds feed, the fish and bird stocks increase. There has been considerably less research done on the cold extreme (La Niña) of the El Niño Southern Oscillation and its climatic implications compared to El Niño. The impacts of cold events on meteorological conditions throughout the world depend on the intensity of the La Niña event, but are less well known than the impacts of El Niño events. There are geologic records of El Niño events attesting to the fact that these expressions of air-sea interactions have been around for about 5000 years. The record suggests that prior to this time there was a warm background climate without El Niño episodes. Since then the cooler background climate of the past 5000 years has been conducive to the spawning of El Niño events. A question that is of concern to scientists studying the current environmental issue of global climatic change
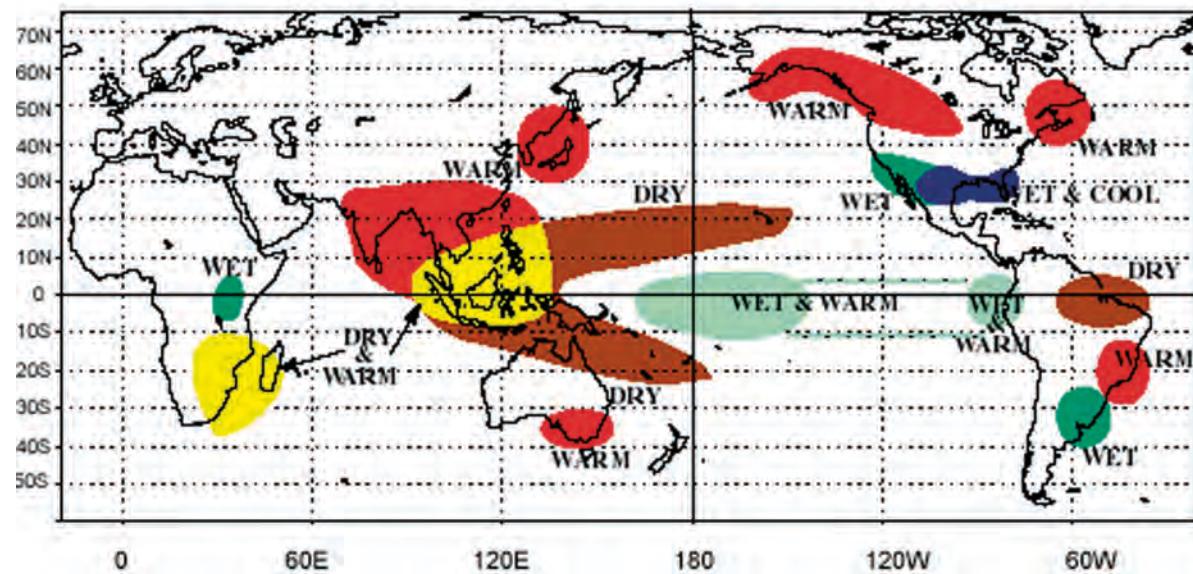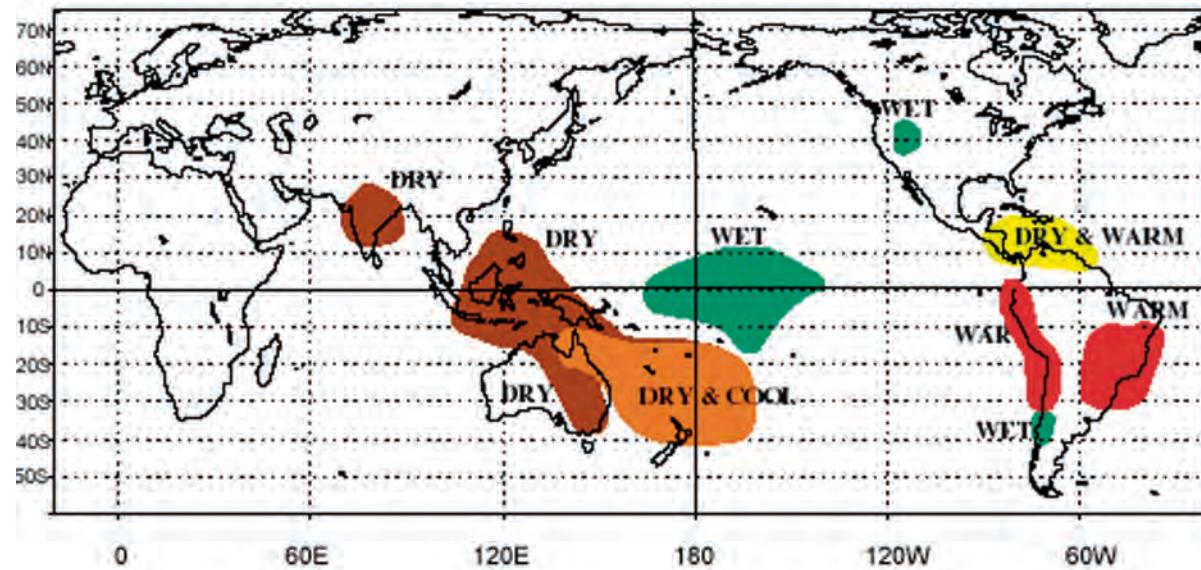
Figure 23. El Niño rainfall and temperature patterns. (National Ocean and Atmospheric Administration: http://www.cpc.ncep.noaa.gov/products/analysis_monitoring/impacts/warm_impacts.html).

is: What might happen to the El Niño – La Niña phenomenon if there is a global warming induced by the accumulation of greenhouse gases in the atmosphere from industrial, transportation, and other sources related to human activities? There is some evidence that global warming might lead to conditions in the Pacific region like that of an extended El Niño event.

In Hawaiʻi, El Niño tends to bring dry winters. Drought is more likely during El Niño years, especially during the October-March period which is traditionally the wettest time of the year. This association is well known in the Hawaiian Islands. In general, in all these regions, La Niña climate effects are approximately, but not exactly, opposite to El Niño climate effects. During the 1997-1998 El Niño, water rationing was implemented on the islands of Maui and Hawaiʻi. Wildfires on Maui and the island of Hawaiʻi were also prevalent problems due to the drought. For the Republic of the Marshall Islands and its island Majuro, El Niño tends to bring dry winters and drought conditions. During the 1997-1998 El Niño, Majuro was under a severe drought. The drought was so severe that measures such as water rationing, installation of a desalination plant, and emergency aid were required to sustain the population. El Niño conditions also tend to bring an enhanced threat of tropical cyclone activity to the Republic of the Marshall Islands. During the 1992-1993 El Niño, severe coral bleaching (bleaching is a result of a coral losing its symbiotic algae – zooxanthellae – that impart color to the coral and provide nutrition to the coral without which the coral will ultimately die) was observed in the lagoon around Majuro killing up to half of many coral colonies. Table 1 summarizes the predicted precipitation impacts of El Niño and La Niña on the islands of Majuro and Oʻahu.

Table 1. Predicted ENSO Precipitation Impacts to Oʻahu, Hawaiʻi and Majuro Atoll, Republic of the Marshall Islands

	Winter (Dec. – Feb.)		Summer (June – Aug.)	
	Majuro	Oʻahu	Majuro	Oʻahu
El Niño	Dryer	Dryer	Normal	Normal
La Niña	Wetter	Wetter	Normal	Normal

D. Tropical Cyclones

The ocean water temperature that is generally required to generate tropical cyclones (see Box 4) is 28° C (82.4° F). Tropical cyclone activity in the eastern Pacific generated off the western coast of Central America and Mexico has been limited over the past 30 years with most of the activity and source for cyclones in the western tropical Pacific. The western

Box 4: Hurricanes and Cyclones

Cyclones, typhoons, or hurricanes (all terms that describe the same phenomena) form when the sea surface temperature exceeds 28° C, which is primarily during the period of midsummer to early fall in the northern hemisphere. In the western part of the North Pacific Ocean, the water can be warm enough to spawn typhoons in winter. The warm tropical ocean supplies abundant moisture to the storm system. The release of large amounts of latent heat from the condensation of atmospheric water vapor into rain warms the atmosphere. Because warm air weighs less than cold air, the air pressure drops, and an initial low-pressure disturbance may intensify. As the low develops, the convergence of air leads to the rise of more warm air and increased release of latent heat sometimes to the point that a hurricane forms.

As of October 19th, 2005 (the hurricane season starts June 1 and ends Nov. 30th), the year 2005 was tied with 1933 for the busiest Atlantic storm season (21) since record keeping started in 1851. Hurricane Wilma was the 21st storm and hit the Yucatan Peninsula on October 21 as a Category 4 hurricane with maximum sustained winds of 145 mph. Wilma had briefly strengthened to Category 5 before the Yucatan landfall and became the most intense hurricane recorded in the Atlantic Ocean with 882 millibars of pressure, breaking the record low of 888 set by Hurricane Gilbert in 1988. Hurricane Rita – the 17th named storm of the 2005 Atlantic hurricane season – made landfall as a category 3 hurricane near the Louisiana-Texas border late September 23. Early estimates are that Rita caused over 8 billion dollars worth of damage and 121 hurricane-related deaths. Hurricane Katrina, the 16th storm of 2005, hit the gulf coast states of Louisiana, Mississippi, and Alabama as a category 4 hurricane on August 29th. Early estimates of the financial impact of Katrina reached 150 to 200 billion dollars. At least 972 individuals from Louisiana alone died due to Katrina with the total count of Katrina-related deaths around 1400 as of late September, 2005. Early estimates are that between 140,000 and 160,000 homes in New Orleans need to be leveled and 350,000 vehicles have been destroyed as 80% of the city was under water at some time during Katrina.

There is considerable discussion that both the frequency and the strength of the 2005 storm season results from human-induced global warming. While most experts will not point to a single weather event and blame it on global warming, global warming has the potential to make hurricanes more frequent and intense by warming the pools of water that form and nourish them. The Atlantic Multidecadal Oscillation (AMO) is credited with being the engine that drives hurricane cycles in the Atlantic. Experts note that the AMO was relatively cool from 1970 to 1994 (with relatively few hurricanes occurring during this period) and has been warming since 1995. Since 1995, the number of storms and hurricanes has increased (just as it has done in previous warm AMO cycles). This suggests that global warming may amplify the fundamental signal that the AMO creates.

tropical Pacific cyclonic generating region extends farther east during El Niño events resulting in an increased threat of cyclones for the more eastern islands. Cyclone development usually occurs west of the dateline both north and south of the equator. After developing, the cyclones are pushed west by the trade winds. After moving west, they are pushed poleward and ultimately eastward, threatening islands well off the equator such as Guam, the Republic of the Marshall Islands, and the Hawaiian Islands.

With climate change and subsequent warming, the warm water region that is normally confined to the western equatorial Pacific will likely move eastward into regions that only have warm waters during El Niño events. The projected result from this eastward movement of warm water is a gradual increase in the frequency of tropical cyclones for islands in the central and east-central Pacific on either side of the equator. Far western Pacific storm frequencies may not decrease as they would presently during El Niño events as sea-surface temperatures there will also be increasing, even if at a slower rate. Due to the projected increase in western-Pacific sea-surface temperature, the storm frequency could increase slightly.

Large scale mid-latitudinal storms are a function of the frequency and intensity of cyclonic activity. These storms cause large changes in sea-level pressure on short time scales and so seasonal differences in sea-level pressure can be used to indicate storminess. Figure 24 shows the projected changes in the ratio of sea-level pressure for the two periods 2006-2036 and 2070-2100) compared to a baseline period of 1990-2020. The model projects increased storminess from 2006-2036 in a region extending north and east of the Hawaiian Islands to the area north of the Federated States of Micronesia and east of the Commonwealth of the Northern Mariana Islands. For that same region in 2070-2100, the storminess is
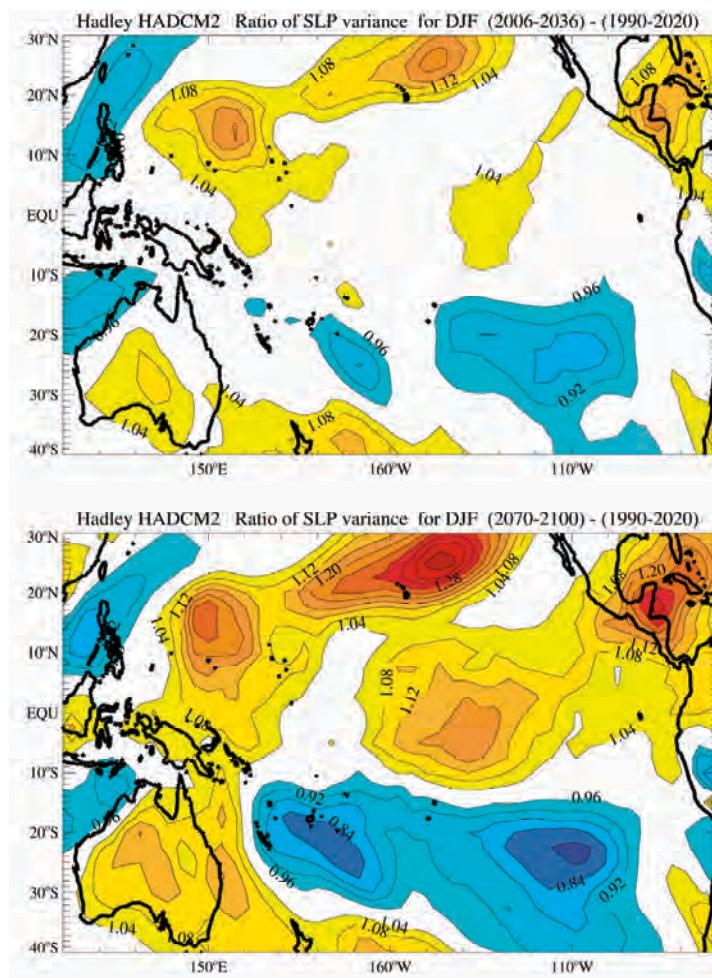
Figure 24. The ratio of SLP variance for DJF for the period 2006-2036 compared to 1990-2020 and the period 2070-2100 compared to 1990-2020. Higher ratios (>1) indicate more storminess in the future periods. (Shea et al., 2001).

53

amplified and also enlarged to encompass the entire Hawaiian Islands as well as most of the Federated States of Micronesia and Republic of the Marshall Islands. The equatorial region between 100° W and the dateline is also expected to experience more storminess from 2070-2100. Between 10° and 30° S in the southern hemisphere, storminess is projected to decrease for regions between 170° E and 90° W. This region includes Fiji and the French Polynesian Islands.

E. Sea Level

While global sea level rise is of concern to all coastal areas, this is especially the case for low lying Pacific Island nations. Some entire Pacific nations and archipelagos have maximum elevations of only a few meters above sea level making them especially vulnerable to sea level rise. For these atolls (see Box 5), a relatively small sea level rise could affect a large fraction of the island surface area. Sea level rise can result in loss of low-lying coastal agriculture areas, ecosystems, and human settlements via erosion and inundation. Sea level rise can also impact fresh water supplies for islands, which may already be under stress from lack of rainfall due to climate change and further exacerbated by increasing population. Elevated sea level conditions could also amplify the damaging effects of tropical cyclones and their associated storm surges.

Sea level rise and climate change can accelerate beach erosion and also have impacts on natural structures – e.g., mangroves and coral reefs – that serve to protect shorelines. While it is uncertain what the impacts of sea level rise would be on mangroves, the potential loss of coral reefs due to sea-surface temperatures rising above the coral's preferred temperature could jeopardize the natural protection from storm surge, wave activity, and long-term sea level rise afforded by a reef framework. Other factors associated with global change, such as elevated atmospheric carbon dioxide levels, could also reduce the growth rate of corals. Increased atmospheric carbon dioxide concentrations would lead to increased dissolution of carbon dioxide into seawater, which in turn would decrease surface ocean pH (acidify the surface ocean). By lowering surface ocean pH, some investigators believe that the ability of corals to grow would be retarded and in some cases the coral skeletons would become weak and more susceptible to wave and current damage. Reducing coral growth rates would further aggravate the effects of elevated sea-surface temperatures on the ability of coral reefs to keep up with sea level rise and subsequently protect shorelines from storm surge and wave action.

Box 5: Coral Reefs and Atoll Formation

Corals are anthozoans, organisms within the phylum Cnidaria. Anthozoans comprise more than 6,000 species and in addition to corals include sea fans, sea pansies, and sea anemones. Stony corals (schleractinians) make up the largest order of anthozoans. Stony corals and coralline algae are primarily responsible for providing the foundation and structure for coral reefs. Schleractinians are colonial organisms composed of individuals called polyps. Most corals contain symbiotic algae called zooxanthellae. The corals provide a protective environment and the compounds necessary for the algae to photosynthesize. The algae in return produce organic products – glucose, glycerol, and amino acids – that the coral use as building blocks in manufacturing proteins, fats, and carbohydrates. In addition, these algae produce organic products that are used by the coral to produce calcium carbonate. Massive reef structures are formed when each coral polyp secretes a skeleton of the mineral aragonite, which is calcium carbonate ($CaCO_3$). Coral reefs can grow from 0.5 to 2 centimeters (0.2 to 0.8 inches) per year under normal conditions and up to 4.5 centimeters (1.8 inches) per year under more favorable conditions (high light exposure, consistent temperature, moderate wave action). Reef building corals are restricted in their geographical distribution due to the environmental conditions needed by the coral polyps. In general, major reef building requires temperatures between 18 to 29° C, salinity between 32 to 42 parts per thousand, and the water must be clear enough for a high degree of light penetration. A concert of these favorable conditions is usually geographically restricted to tropical and subtropical waters between 30° S and 30° N.

Coral reefs begin to form after coral larvae attach to submerged edges of islands or continents. As the corals grow and expand the reef begins to take on one of three characteristic structures – fringing, barrier, or atoll. Fringing reefs are the most common type of coral reef and project seaward from the shoreline forming borders along the shoreline and surrounding islands. Barrier reefs also border shorelines, but at a much greater distance from the shoreline compared to fringing reefs (i.e., Australia's Great Barrier Reef). Barrier reefs are separated from their adjacent land mass by a lagoon of open water that can be deep. If a fringing reef forms around a volcanic island that subsides completely below sea level as the fringing reef continues to grow toward the surface then an atoll forms. Atolls are usually oval or circular with a central lagoon (Figure 5.1).

Figure 5.1. Stages of atoll formation
(http://earthobservatory.nasa.gov/Study/Maldives/maldives2.html)

Guinotte et al. (2003) studied the impact that the rise in future atmospheric carbon dioxide levels until 2069 will have on the aragonite saturation state (see Box 6) of seawater in the Pacific Ocean basin. Aragonite ($CaCO_3$), made of calcium (Ca) and carbonate ions (CO_3), is the mineral which coral polyps precipitate to form their skeleton and thus reef structure. The saturation state of the ocean water with respect to aragonite indicates whether aragonite will precipitate or will dissolve. Among other things, the aragonite saturation state is a

---

Box 6: Aragonite Saturation State of Seawater

The precipitation and dissolution of aragonite in seawater can be described by the chemical reaction:

$$Ca^{2+} + CO_3^{2-} \longleftrightarrow CaCO_3 \qquad\qquad (1)$$
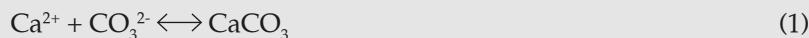
where Ca^{2+} is the dissolved concentration of calcium ions in seawater, CO_3^{2-} is the dissolved concentration of carbonate ions in seawater, and $CaCO_3$ is aragonite. Note that the arrow ($\longleftrightarrow$) denotes that the reaction can go both forward, left to right, or backward, right to left. The equation as read left to right is for the aragonite precipitation reaction and read right to left is for the aragonite dissolution reaction.

The saturation state of seawater with respect to aragonite can be defined as the product of the concentrations of dissolved calcium and carbonate ions in seawater divided by their product at equilibrium:

$$([Ca^{2+}] \times [CO_3^{2-}]) / [CaCO_3] = \Omega \qquad\qquad (2)$$

where dissolved calcium $[Ca^{2+}]$ is the seawater concentration of dissolved calcium ions, $[CO_3^{2-}]$ is the seawater concentration of carbonate ions, $[CaCO_3]$ is the solubility of aragonite in seawater, and Ω is the calculated saturation state.

When $\Omega = 1$, the seawater is exactly in equilibrium or saturation with respect to aragonite. In other words, the aragonite does not dissolve or precipitate. In relation to equation (1), equilibrium means that the forward precipitation reaction, left to right, and the backward dissolution reaction, right to left, are equal in their rate so there is no net precipitation or dissolution. When $\Omega > 1$, the seawater is said to be supersaturated with respect to aragonite. In this case, aragonite will precipitate or follow the left to right chemical reaction of equation (1). When $\Omega < 1$, the seawater is said to be undersaturated with respect to aragonite, which results in the aragonite mineral dissolving or following the right to left chemical reaction of equation (1).

When carbon dioxide is added to surface seawater from the atmosphere, the acidity of the surface seawater increases. If the surface acidity increases, then there is relatively less carbonate ion (CO_3^{2-}) in seawater, and thus the value of Ω decreases and so does the saturation state of seawater with respect to aragonite.
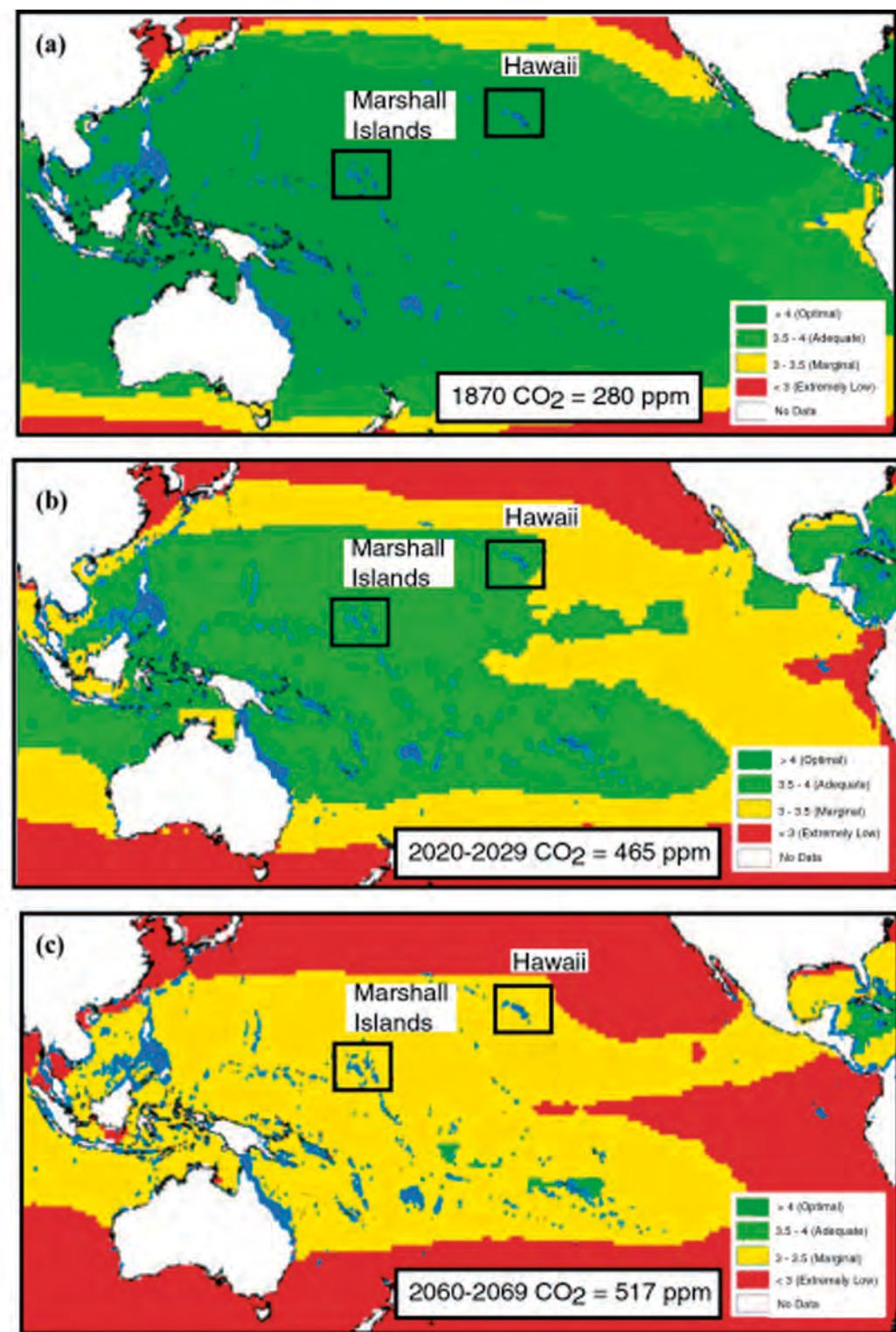
Figure 25. Pacific Basin aragonite saturation state: (a) Calculated preindustrial (1870) values;
Atmospheric carbon dioxide = 280 parts per million; (b) Projected values for 2020-2029;
Atmospheric carbon dioxide = 465 parts per million; (c) Projected values for 2060-2069;
Atmospheric carbon dioxide = 517 parts per million. (After Guinotte et al., 2003).

function of the amount of dissolved carbon dioxide in the water and the temperature of the water. Figure 25 shows the impacts of future projected atmospheric carbon dioxide levels on aragonite saturation state in the Pacific Ocean basin (Guinotte et al., 2003). Generally speaking, from present day to 2069, the area of optimal and adequate saturation states contracts from high to low latitudes and from the ocean basin margins toward the center of the basin. By the year 2069, there is almost a complete absence of adequate areas of aragonite saturation state in the Pacific Basin. The reefs of Hawai'i produce an estimated total annual economic benefit of $363 million dollars that future changes in surface ocean aragonite saturation state could negatively impact (Cesar et al., 2002).

The worldwide eustatic sea level change shown in Figure 26 represents thermal expansion of ocean surface waters and alpine and valley glacial melt. However, the change does not take into account ice sheet melt because of the uncertainty of the net effect of climate change on Antarctic and Greenland ice sheets. Sea level rise can vary from location to location due to differences in local heating and thermal expansion. The projection of future sea level rise is heavily dependent upon which future emission scenario is used to drive the climate change model. Using the entire range of emission scenarios, the Intergovernmental Panel on Climate Change
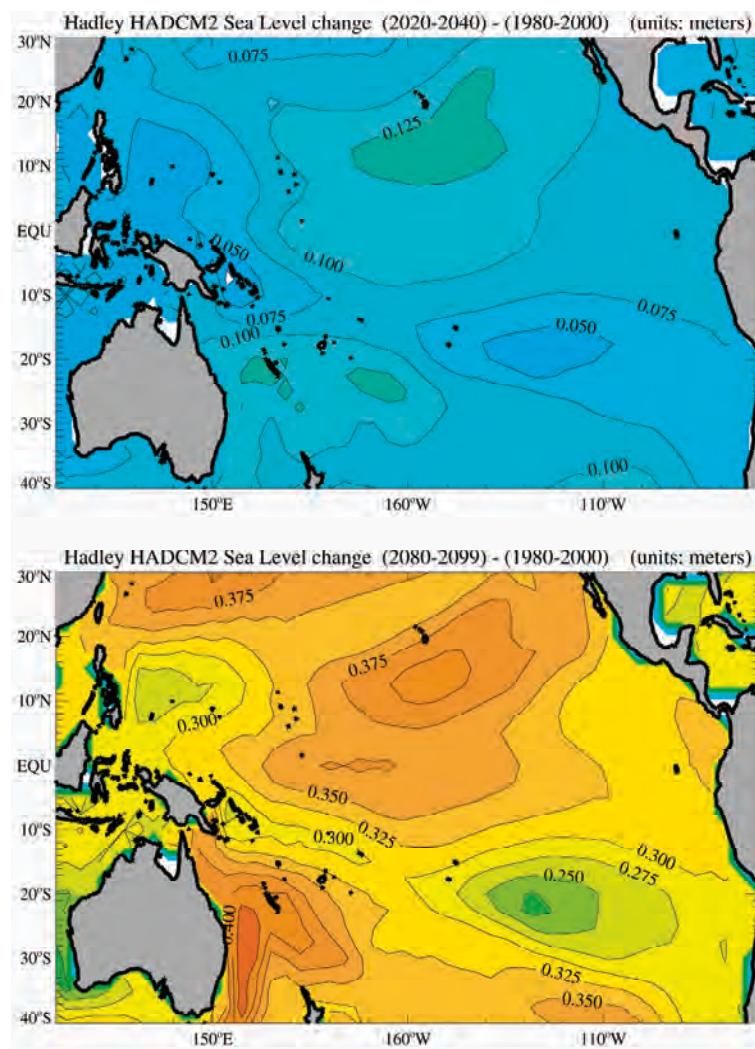
Figure 26. Sea level rise for the period 2020-2040 minus 1980-2000 and the period 2080-2099 minus 1980-2000. (Shea et al., 2001).

58

Special Report on Emission Scenarios projected a sea level rise of between 9 and 88 centimeters (3.5 and 34.7 inches) by the completion of the 21st century (Church et al., 2001). Table 2 provides some historical context for sea level trends at some Pacific islands. Finally, it should be noted that the islands of Hawai'i are being vertically displaced over very long time scales.

Table 2: Mean Sea Level Trends at Selected Pacific Island Stations (in centimeters)

Location	Rate of Change	Record Duration	Total Change
Hawai'i			
Honolulu	1.5 +/- 0.2 cm/decade	1905-1999	11.10 +/- 1.84 cm
Hilo	3.4 +/- 0.5 cm/decade	1927-1999	24.48 +/- 3.60 cm
Nāwiliwili	1.5 +/- 0.4 cm/decade	1954-2000	6.90 +/- 1.84 cm
Kahului	2.1 +/- 0.5 cm/decade	1950-1999	10.29 +/- 2.45 cm
Moku o Lo'e	1.0 +/- 0.5 cm/decade	1957-1999	4.20 +/- 2.10 cm
Guam	0.0 +/- 0.6 cm/decade	1948-1999	0.00 +/- 3.06 cm
American Samoa			
Pago Pago	1.6 +/- 0.6 cm/decade	1948-1999	8.16 +/- 3.06 cm
CNMI/Saipan	-0.1 +/- 2.2 cm/decade	1978-1999	-0.21 +/- 4.62 cm
Marshall Islands			
Majuro	2.5 +/- 1.0 cm/decade	1968-1999	7.75 +/- 3.10 cm
Kwajelein	0.9 +/- 0.4 cm/decade	1946-1999	4.77 +/- 3.10 cm
Wake	1.8 +/- 0.5 cm/decade	1950-1999	8.82 +/- 2.45 cm
Federated States of Micronesia			
Pohnpei	1.6 +/- 1.8 cm/decade	1974-1999	4.00 +/- 4.50 cm
Kapingamarangi	-1.6 +/- 2.3 cm/decade	1978-1999	-3.36 +/- 4.83 cm
Yap	-1.4 +/- 1.8 cm/decade	1969-1999	-4.21 +/- 5.40 cm
Republic of Palau			
Malakal	-0.4 +/- 1.8 cm/decade	1969-1999	-1.20 +/- 5.40 cm

The original data for this table provided by Mark Merrifield, University of Hawai'i (Merrifield, pers comm).

The plate the Hawaiian Islands ride on (called the Pacific Plate) moves up and down due to lithospheric (plate) flexure. This flexure is a result of the loading of the plate, or lithosphere, where the Island of Hawai'i (e.g., the Big Island) is located. The weight of the Island of Hawai'i, the largest of the Hawaiian Islands, bearing down on the underlying plate causes the plate to be pushed downward (Figure 27). In response, this distorts the surrounding plate resulting in the upward movement of the plate portion under O'ahu, which is approximately 400 kilometers (249 miles) from the Big Island. This upward plate motion during the past 125,000 years uplifting O'ahu has ranged between 0.02 to 0.06 millimeters (0.0008 to 0.002 inches) per year. The impact of even the upper limit of these uplift rates over the next 100 years would be at most 6 millimeters and therefore will not be a major factor with regard to near future climatically-driven sea level change.
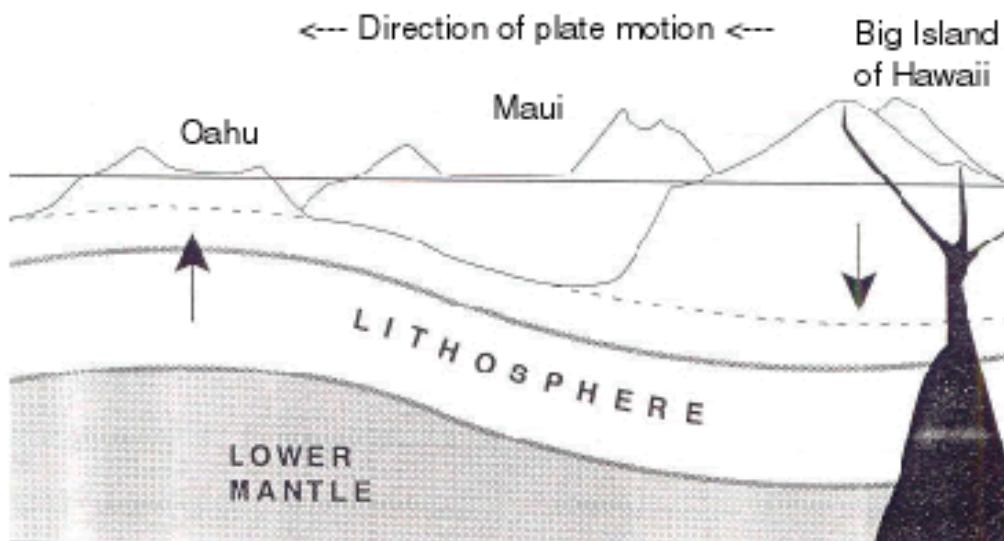
Figure 27. Lithospheric flexure under the massive volcanic accumulation that is the Big Island of Hawai'i causes compensatory arching at a radius of approximately 400 kilometers (248 miles) resulting in the uplift of the island of O'ahu. (After Grossman, 2001).

F. *Climate Change Projections from Multimodel Ensemble*

Annual mean surface temperature change for two emission scenarios (A2 and B2) at the end of the 21st century, 2071-2100 is shown in Figure 29. The primary difference between the two scenarios used in the Intergovernmental Panel on Climate Change model and the Hadley model is that the more recent *Special Report on Emission Scenarios* emission estimates for future sulfur emissions have been reduced, thereby producing less negative radiative forcing (cooling) from that source and giving rise to more warming from the

increase in greenhouse gases. The patterns of cooling caused by sulfate aerosols do not substantially affect the Pacific Ocean Basin region, except due to emissions from China, since those emissions are restricted mainly to industrial areas (Figure 28). The other difference between the A2 and B2 scenarios is that A2 generally has greater rates of increase in green-
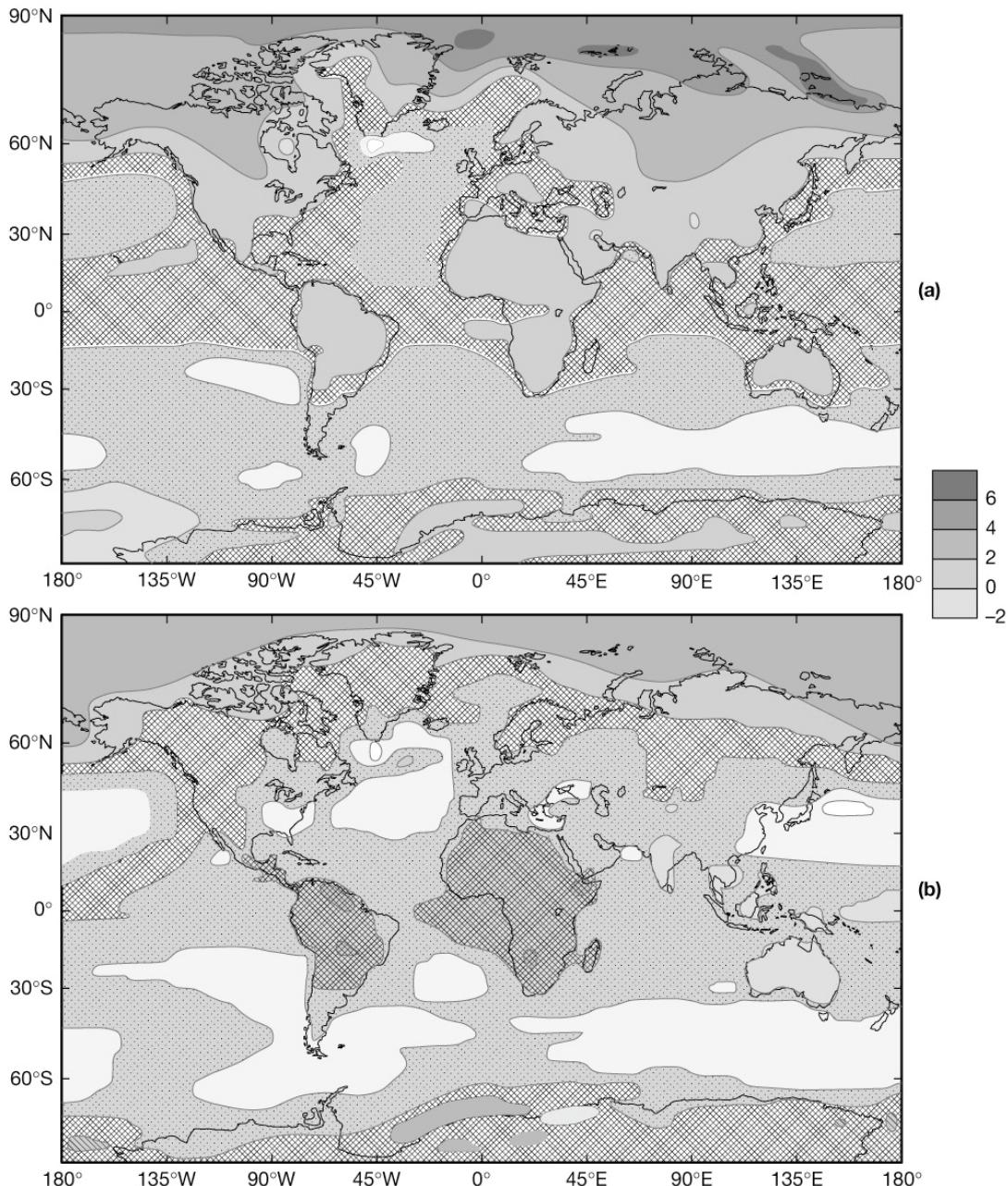
Figure 28. Model calculations of annual mean temperature changes in degrees Celsius from 1795 to 2050. In (a) only the effect of increasing greenhouse gases in the atmosphere on the temperature change is considered. In (b) the calculated temperature response is to both increasing greenhouse gases and aerosols in the atmosphere. (After Kattenberg et al., 1996).

61

house gases, and thus more positive radiative forcing (warming) than B2. Therefore, the climate changes in A2 are generally greater than in B2.

The multimodel results both show a general warming of the tropical Pacific in agreement with the Hadley model with greater warming east of the dateline relative to the Western Equatorial Pacific (compare Figure 29 with Figure 17). This response, similar to what occurs during an El Niño, is stronger in scenarios in the multimodel ensemble than in the Hadley model with surface temperature increases greater than 2° C (3.6° F) in B2 and 2.6° C (4.7° F) in A2 in the equatorial Pacific.
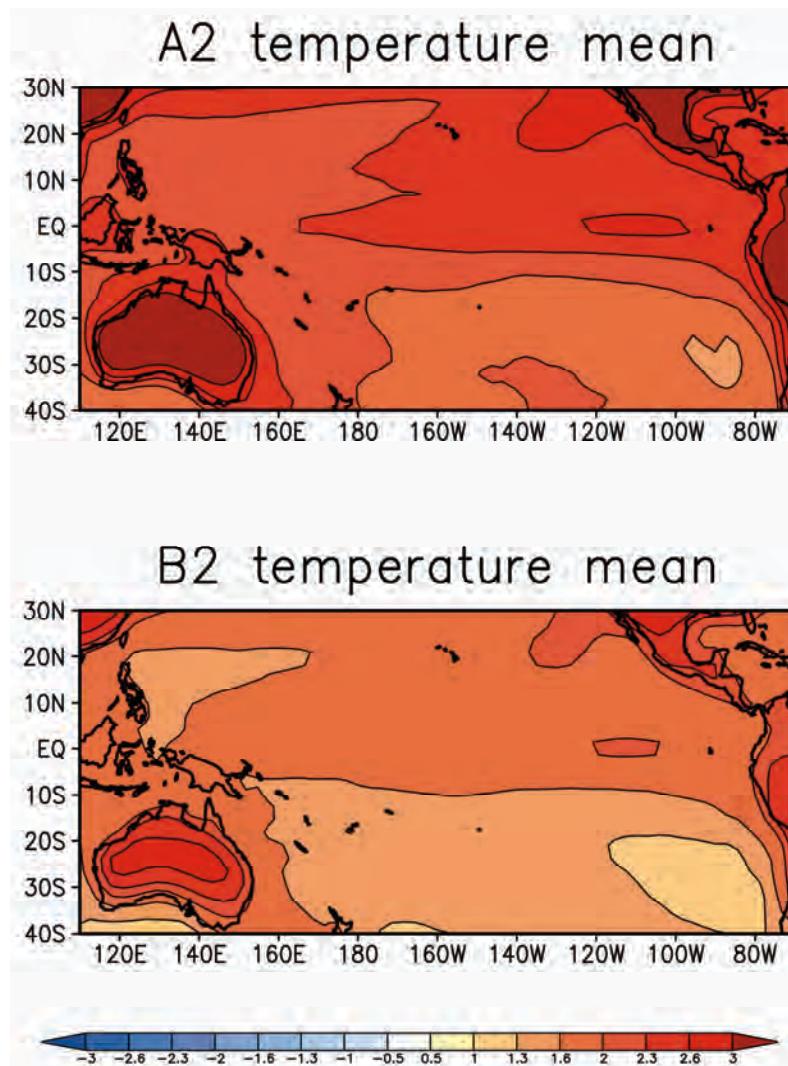
Figure 29. Mean surface air temperature change from the IPCC SRES A2 scenario, 2071-2100 minus 1961-1990, and mean surface air temperature change for SRES B2 scenario; units in ° C. (Shea et al., 2001).

The implications of the surface temperature changes seen in Figure 29 are reflected in the changes in annual mean precipitation seen in Figure 30. The mean "El Niño-like" surface temperature changes produce a similar El Niño-like change in precipitation with an eastward shift of anomalous precipitation. An increase approaching 100% in the equatorial Pacific near 160° W in A2 and greater than 50% east of the dateline in B2 is also evident in Figure 30. Since the surface temperature changes in the multimodel ensemble are more concentrated east of the dateline near the equator, areas in which precipitation increased more than 10% are confined mainly to the east of about 160° E and between about 5° N and 5° S in a region just north of the Marquesas Islands. The Hadley model precipitation changes extend more broadly in latitude and occur farther west. For both A2 and B2, areas of decreased precipitation in the multimodel ensemble are projected to occur around French Polynesia and westward to near Fiji and also near Hawai'i though those decreases are about 10% or less.
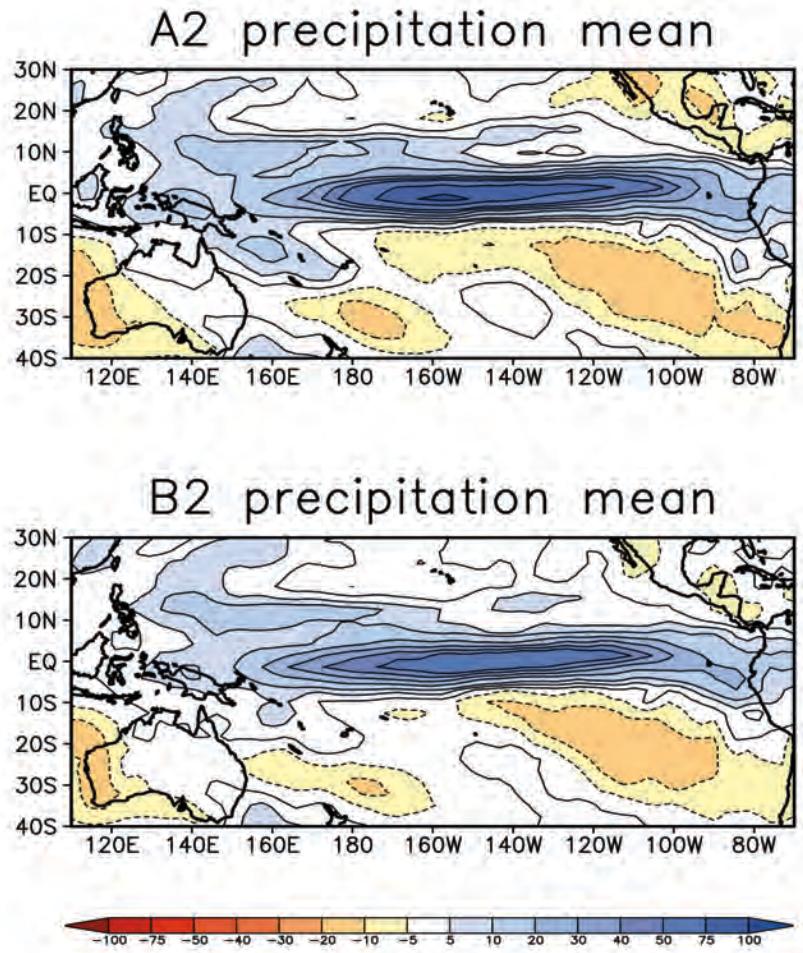
Figure 30. Mean percentage change in precipitation from the multimodel ensemble for the SRES A2 2071-2100 and mean percentage change in precipitation for SRES B2 scenario. Both scenarios are relative to mean air surface temperatures of 1961-1990. (Shea et al., 2001).

To provide an idea of model consistency and level of uncertainty, the range of model responses for surface temperature increase across the tropical Pacific is around 2 to 3° C (3.6 to 5.4° F) in A2 and 1.5 to 2° C (2.7 to 3.6° F) in B2 in Figure 31.
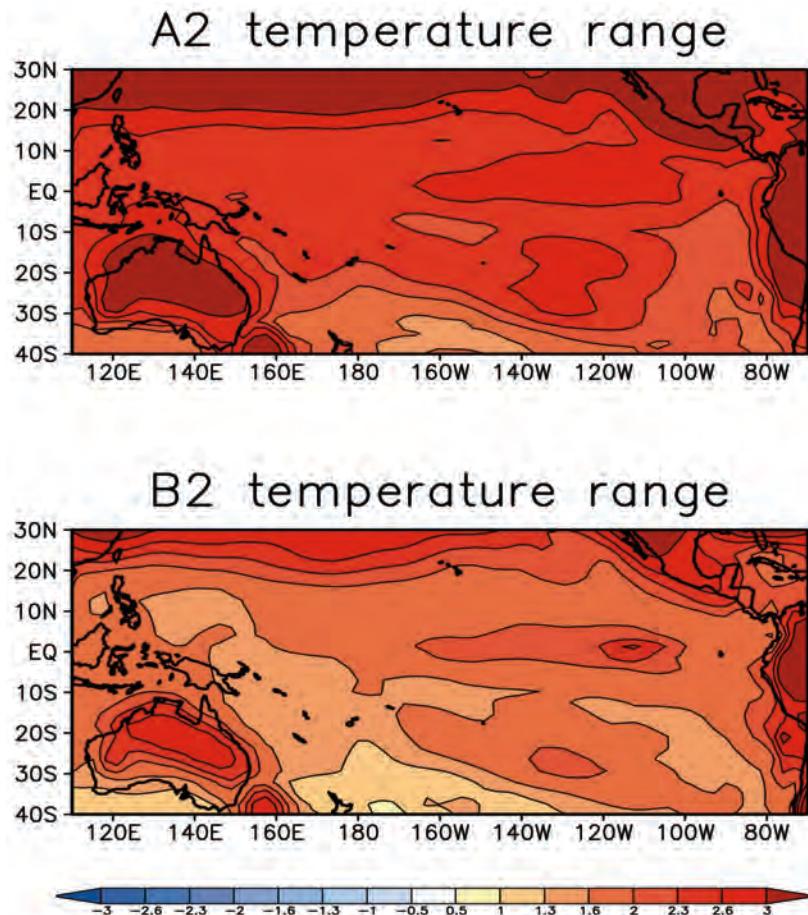
Figure 31. Range of surface air temperature change for the SRES A2 and B2 scenario. (Shea et al., 2001).

The range is less and thus the consistency among the nine models is generally greater in the equatorial tropics between 20° N and 20° S. As in the Hadley model, there is a relative maximum of warming projected to occur in a band extending through the Hawaiian Islands with a relative minimum in the Southeast Pacific south of about 15° S. As noted for the Hadley model, precipitation projections are much more uncertain than temperature projections. The range of precipitation changes for A2 and B2 exceed 200% in the Equatorial Pacific for both scenarios with smaller values to the north and south (Figure 32).
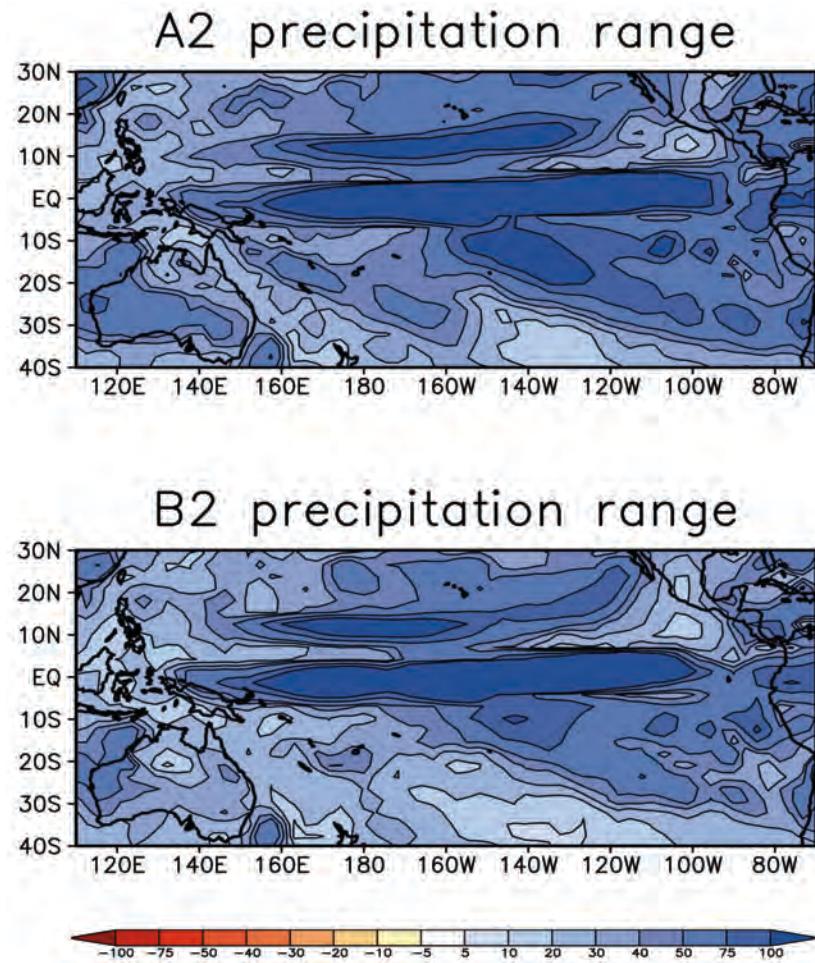
Figure 32. Range of percentage change in precipitation for the SRES A2 and B2 scenarios. (Shea et al., 2001).

G. *Summary of Model-Based Scenarios*

- A general warming trend in surface air temperature across the Pacific Basin
- A net regional enhancement in the hydrological cycle with (1) elevated precipitation in some regions and (2) some regions experiencing much drier conditions
- Uncertainty of how storm cycles will be impacted by temperature and hydrologic changes
- Potential changes in natural climate variability, which include potential prolonged El Niño conditions
- Increased ocean temperatures
- Changes in sea level driven by (1) long-term rise in sea level and (2) periodic changes associated with El Niño Southern Oscillation

65

V. Consequences of Predicted Climate Change in the Pacific Island Region: Focus on Oʻahu, State of Hawaiʻi and Majuro Atoll of the Republic of the Marshall Islands

The climate models previously reviewed predict short and long-term changes in sea-surface temperature, rainfall, the El Niño Southern Oscillation phenomenon and storm variability, and sea level for the Pacific Basin. These changes have implications for Pacific inhabitants and the entire world. Examples of impacts of past climate events include the recorded El Niño's of 1986-1987, 1991-1992, 1997-1998, and 2002-2003. The economic cost of the 1982-1983 El Niño at the time was estimated to be over 8 billion U.S. dollars.

The effects of the predicted modeled climate changes discussed in section *III. Overview of CGCM1 and HADCM2 Model-based Scenarios of Future Climate Conditions for the Pacific Basin* on the State of Hawaiʻi and the island of Majuro are discussed as two examples of how future climate change may impact Pacific Island inhabitants.

A. Pacific Basin Overview

All 58 million square miles of the Earth's land area would easily fit inside the Pacific Basin. There are roughly 30,000 islands in the Pacific Basin and the Pacific Ocean has served as a passageway interconnecting the island inhabitants. While there are cultural similarities and differences among the inhabitants of these small island states, one thing they certainly share is susceptibility to climate change and variability. For example, climate change and variability can impact the following Pacific island attributes to varying degrees: soil and coastal zone formation, hydrology, susceptibility to storm systems, and components of biogeography such as population density, species density, distribution, and biodiversity. The degree to which climate change and variability will impact Pacific islands depends upon a variety of factors such as the island's geology, area, height above sea level, extent of reef formation, and freshwater aquifer size.

The Pacific Islands are difficult to characterize geomorphically and include atolls, volcanic islands, continental islands, limestone islands, and mixtures of all these geomorphologies. Half of the Caroline Islands and 80% of the Marshall Islands are atolls. These atolls may only peak above sea level by a few feet making them extremely susceptible to changes in sea level and storm activity and their impacts on the water table of the atoll. At

the other extreme, volcanic islands such as the islands of Hawai'i can peak at over 3,962 meters (13,000 feet) above sea level. Islands are extremely affected by the interplay between their geology and climatological and oceanographic processes. Compared to other types of islands found in the Pacific, high volcanic islands like the Hawaiian islands tend to have larger surface areas, more groundwater, better soils for farming, and overall a more diverse resource base. Compared to high volcanic islands, low-lying atolls are prone to drought and erosion and have very limited natural resources. High Pacific islands generally can support the growth of tropical forests given their warm temperatures, moisture, and soils whereas atolls generally do not support dense vegetation due to soil composition and hydrological constraints. Oceanic islands tend to have lower levels of biodiversity and species found on them are more likely to be endemic. The lack of biodiversity makes island ecology extremely sensitive to climatological change. The Hawaiian Islands, although they comprise less than 0.002% of the total land area of the United States, are home to nearly 30% of the nation's endangered species.

B.   Hawai'i, the Island of O'ahu, and the Pearl Harbor Basin

The nearest continental land mass is over 3,864 kilometers (2400 miles) away making Hawai'i one of the world's most remote group of islands (Figure 16). Hawai'i's climate is also one of the most diverse on the planet. Of all the major 11 different biomes on Earth, only tundra is not found in Hawai'i. The surrounding tropical ocean supplies moisture to the air year round. This supply of moisture acts likes a thermostat and keeps seasonal temperature variations to a minimum. The warmest months are August through September and the coolest months are January through February. The islands are usually bathed in northeasterly trade winds due to a semi-permanent atmospheric high pressure cell that is situated northeast of the islands. The elevation of Hawai'i's mountains and ridges significantly influences the local weather and climate. In Hawai'i, rainfall amount and distribution closely follow the topographic contours of the islands. Rainfall is greatest at ridges and windward areas (northeast slope of ridges and mountains) and is least in leeward lowlands (see below orographic rainfall description). Mt. Wai'ale'ale on the island of Kaua'i is one of the wettest places on Earth receiving 1016 centimeters (400 inches) of rain per year. Elevated windward sides of the islands can receive more than 508 centimeters (200 inches) per year, and leeward areas can receive as little as 38 centimeters (15 inches) per year. The leeward areas have mostly dry warm months and receive most of their rainfall accumulation during the winter storms. The windward regions tend to show smaller seasonal variations because persistent trade wind showers govern their rainfall accumulation. El Niño conditions usu-

ally disrupt these patterns resulting in drought conditions for the entire state and more frequent hurricanes and tropical storms.

Described by Mark Twain as "the loveliest fleet of islands that lies anchored in any ocean", Hawai'i is comprised of 221 kilometers (137 miles) of islands encompassing a land area of 16,686 square kilometers (6,442.6 square miles). There are 8 major Hawaiian Islands: Kaua'i, O'ahu, Lāna'i, Moloka'i, Maui, Ni'ihau, Kaho'olawe, and Hawai'i (sometimes referred to as the "Big Island of Hawai'i"). The islands were discovered by Polynesian explorers between the 3rd and 7th century AD and later by the British captain James Cook in 1778. Hawai'i became the 50th state in the U.S. union in 1959. Honolulu, the capital city, is located on the island of O'ahu. The state resident population in 2000 was a little more than 1.2 million with 876,156 residing on the island of O'ahu and a yearly population growth at 0.9% (DBEDT, 2003a). The gross state product in 2000 was 39.1 billion U.S. dollars and the annual per capita income (in 1999) was $27,533 (DBEDT, 2003a). Age breakdown for Hawai'i in 2000 was: under 5 (6.5%); 5-19 (20.6%); 20-44 (36.8%); 45-64 (22.9%); 65+ (13.3%). The median age is 36.2 years old.
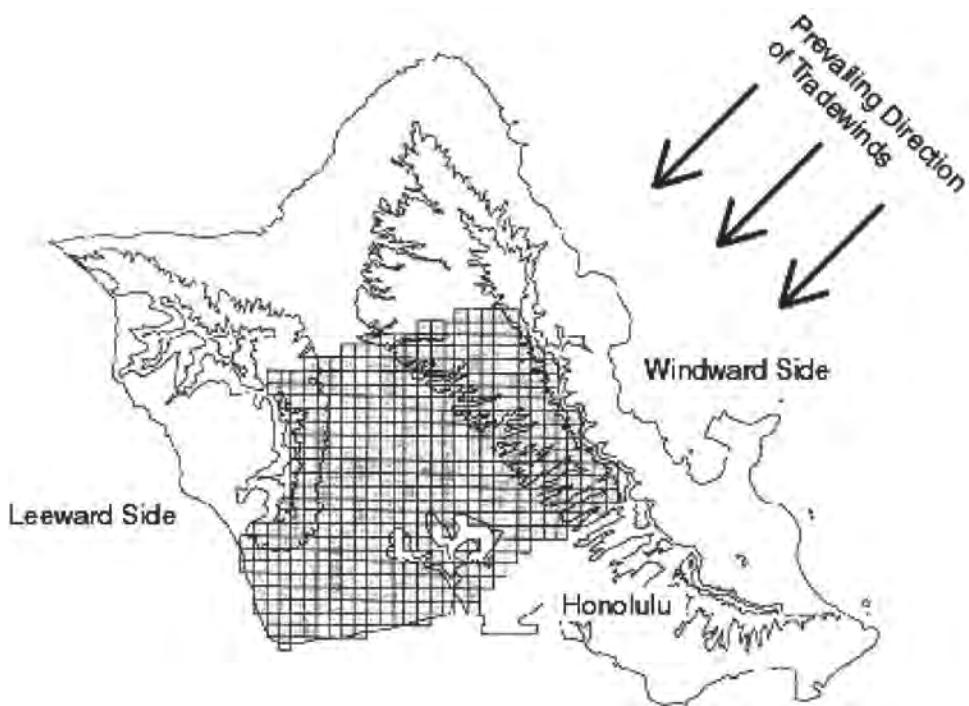
Figure 33. O'ahu Island and the Pearl Harbor basin study area (After Giambelluca et al., 1996). Subdivisions are 1 square kilometer grid cells.

Discussion of the implications of climate change on water resources in Hawai'i will focus on the island of O'ahu, specifically the Pearl Harbor basin that was investigated by Giambelluca et al. (1996; Figure 33). The basin and associated aquifer underlie part of Honolulu's intensively developed urban area. In addition, there are extensively irrigated former sugar-cane fields, irrigated and non-irrigated pineapple fields, and upland pastures and forests. The basin's climate is extremely varied with rainfall ranging from 500 to 6000 millimeters (19.7 to 236 inches) per year over a distance of only 25 kilometers (16 miles) (Figure 34). The maximum elevation of O'ahu is 1231 meters (4,040 feet) at Ka'ala peak.

Orographic processes are responsible for this wide range in rainfall (Figure 35). In addition, these orographic processes lead to wide spatial differences in cloudiness, solar radiation, and evaporation within the basin. The Pearl Harbor region is mainly depen-
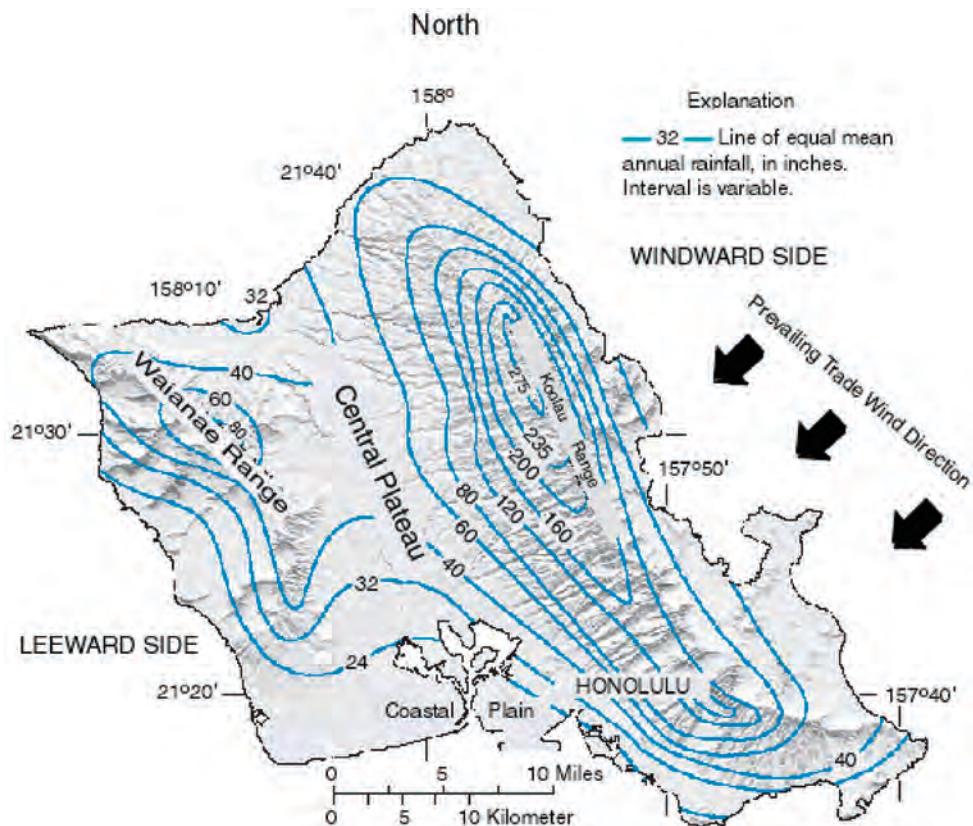
Figure 34. Median annual rainfall pattern of O'ahu, Hawai'i. Rainfall isopleths are in millimeters per year. (After Giambelluca et al., 1986).

69

dent upon underground sources for its water requirements. Groundwater supplies Oʻahu with 92% of its water use (Ridgley and Giambelluca, 1991). The development and use of the groundwater system have reached the point to where the sustainability of current and future water usage rates is in doubt.
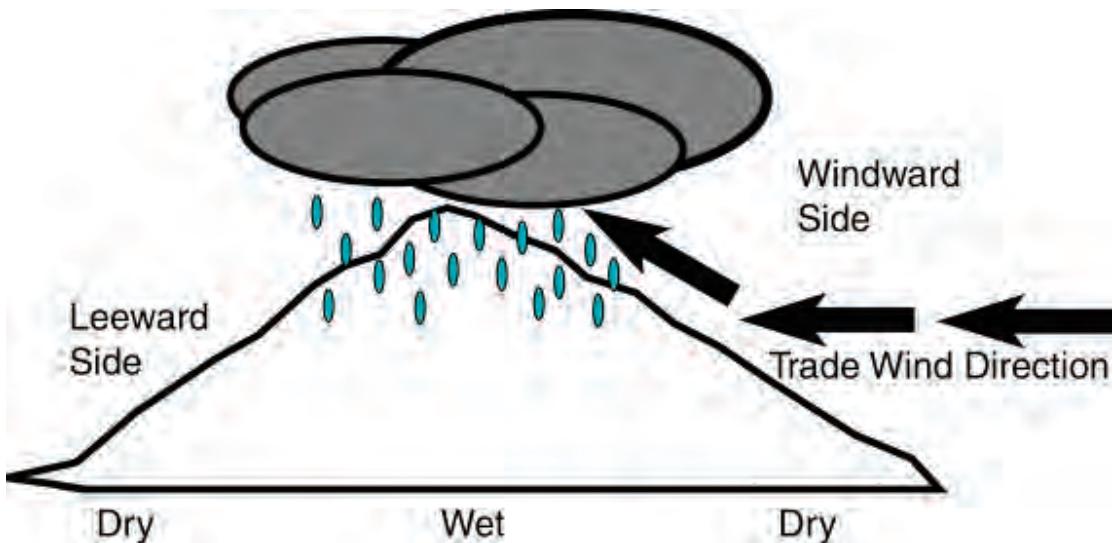
Figure 35. Orographic rainfall. As air is forced upward over the mountain, it cools, causing water vapor to condense and fall out as rain.

1. Temperature and Rainfall Projections: Implications for Climate and Water Resources in Hawaiʻi.

The temperature projections from the Hadley HADCM2 model show that the surface temperature in Hawaiʻi will increase for both short and long-lead simulations. Over the short-lead (2025-2034), sea surface temperatures (Figure 17) will increase between 0.5 to 1.3° C for December, January, and February and 2.0 to 3.0° C for the long-lead (2090-2099). For the months of June, July, and August, the short-lead temperature increase is between 1.0 to 1.6° C and the long-lead increase is from 2.3 to 3.3° C (Figure 17). The separate *Special Report on Emission Scenarios* A2 and B2 models (Figure 29) project increases in mean surface temperature of 2.3 to 2.6° C and 1.6 to 2.0° C, respectively, for 2071-2100. The differences between the two models and their projections primarily stem from the fact that A2 generally has greater increases of greenhouse gases and thus more positive radiative forcing (warming). However, all three models are in general agreement that the tropical Pacific will warm in the next century and that the warming will likely occur over the entire year and not just during the summer months.

The rainfall projections from the Hadley HADCM2 model show that rainfall in the vicinity of Hawai'i will increase for both short and long-lead simulations during the summer months. Over the short-lead (2025-2034), rainfall (Figure 18) will increase between 1.0 to 2.0 millimeters (0.04 to 0.08 inches) per day for June, July, and August and 3.0 to 4.0 millimeters (0.12 to 0.16 inches) per day for the same months over long-lead (2090-2099). The rainfall projections for December, January, and February for both short- and long-lead show that there will be no change in precipitation during the winter, although in the long-lead projections an area of reduced precipitation (0.5 millimeters or 0.020 inches per day) lies just the west of the islands (Figure 18). Except for an area southwest of the Hawaiian Islands in the *Special Report on Emission Scenarios* A2, the separate *Special Report on Emission Scenarios* A2 and B2 models project no change in the mean precipitation for the area around Hawaii from 2071-2100 (Figure 30).

Overall, the model projections suggest that Hawai'i will have elevated temperatures and precipitation (at least in the summer months of June, July, and August) in the near- (2025-2034) and long- (2090-2099) term. These projections are counter to some historic evidence that warmer periods in Hawai'i may not have had elevated precipitation, but instead experienced lower rainfall and increased evaporation which would lead to a decrease in the amount of available water. Lyon (1930) and Gavenda (1993), on the basis of soil distribution, concluded that higher rainfall was associated with colder, and not warmer, past climates. Additionally, studies of sediments and their distribution in Hawai'i suggest that higher trade wind velocities – therefore elevated orographic processes and rainfall – accompanied colder temperatures in the past (Molina Cruz, 1977; Chuey et al., 1987).

One problem with the larger regional (e.g., the Hadley HADCM2) or global climate models is that the relatively course spatial scale resolution of these models prohibits them from resolving finer scale processes that impact the hydrology of islands where orography is important, and thus the magnitude and spatial distribution of rainfall and evaporation. Using a hydrologic model, Giambelluca et al. (1996) project that a temperature rise of 3° C will result in a 10% increase in evaporation in the Pearl Harbor basin, and even if this change is accompanied by an increase of 10% in precipitation, there still may be a significant shortfall of water at the present water usage level. A 3° C temperature increase is within the range of the long-lead (Figure 17) sea surface temperature increase for both winter (December, January, and February) and summer (June, July, and August) months. There is a corresponding projected increase of 3.0 to 4.0 millimeters (0.12 to 0.16 inches) per day for the long-lead in precipitation for the summer months (Figure 18). Contrary to the Hadley HADCM2 model projections, the multimodel ensembles *Special Report on Emission Scenarios*

A2 and B2 both do not show increased annual mean precipitation from year 2071 to 2100 for Hawai'i (Figure 30). For the Pearl Harbor basin, a 10% increase in the yearly precipitation over the precipitation range of the basin (500 to 6000 millimeters or 19.7 to 236 inches per year) would correspond to an increase of 50 to 600 millimeters (2.0 to 24 inches additional rainfall per year. The summer long-lead rainfall projections of 3.0 to 4.0 millimeters (0.12 to 0.16 inches) per day (Figure 18) would correspond to an increase of rainfall by 274 to 365 millimeters (10.8 to 14.2 inches) for those 3 months during the long-lead (2090-2099). Note that this increase is only over 3 months and not the entire year. It is unclear whether there would be increased rainfall for the remaining 9 months, but for the long-lead winter month projections (December, January, February in Figure 18), there is no projected increase in precipitation. It is possible that the increased rainfall in the summer months (274 to 365 millimeters or 10.8 to 14.2 inches) over the long-lead will not balance the increased evaporation over the entire year caused by the elevated temperature (3° C) leading perhaps to non-sustainability in the water resource for the island of O'ahu.

2. El Niño Southern Oscillation and Storm Variability

Although historical evidence suggests that rainfall increases during cooler times, and thus decreases during warmer times, alteration of the El Niño Southern Oscillation and storm variability by climate change could offset the reduction in trade wind, orographic driven precipitation. The general future increase in sea surface temperatures along the equatorial Central and Eastern Pacific projected by the Hadley HADCM2 and Intergovernmental Panel on Climate Change *Special Report on Emission Scenarios* (Figure 17 and 20) suggests a greater tendency for El Niño-like conditions. It is uncertain whether future increases in ocean temperatures might change the character of the El Niño Southern Oscillation so that it appears more or less frequently. However, increased tropical and equatorial sea surface temperatures could lead to increased hurricane activity and the possibility of large-scale damage to property and resources. Hurricane Iniki made landfall on the island of Kaua'i, Hawai'i, in September 1992 causing 7 deaths, 1.8 billion dollars in damage, and $260 million in Federal Emergency Management Act disaster relief costs even though it landed on the 4th most populous island in the state (Island populations from largest to smallest: O'ahu → Big Island of Hawai'i → Maui → Kaua'i). Had Iniki made landfall on O'ahu, the cost and level of destruction would have been significantly greater not only to the island itself, but the entire state's economy.

The sea level pressure projections (Figure 24) for December, January, and February suggest that the level of storminess will increase around Hawai'i during the winter months.

This increased storminess and associated precipitation during the winter months (also when evaporation is lowest due to cooler temperatures) could offset the loss of water from increased evaporation due to higher average yearly temperatures predicted by the regional climate models. The issues brought up (see previous section *Hawai'i and the Pearl Harbor Basin (a) Temperature and rainfall*) with the inability of the relatively course regional scale precipitation models to resolve the smaller scale processes (e.g., orographic) that impact the hydrology of islands are also relevant to the impact of increased storminess and resultant rainfall to the islands of O'ahu.

3. Sea Level

The projected sea level rise from the Pacific Islands Regional Assessment Group report (Figure 26) for the Hawaiian Islands during the period 2020-2040 (relative to 1980-2000) is 10.0 to 12.5 centimeters (3.94 to 4.92 inches) and for the period 2080-2099 (relative to 1980-2000) is between 35.0 and 37.5 centimeters (13.8 to 14.8 inches). In 1985, the State of Hawai'i Coastal Zone Management Program and the Hawai'i Institute of Geophysics, in response to Senate Resolution 137 (see Appendix 1), compiled the report *Effects on Hawai'i of a worldwide rise in sea level induced by the "Greenhouse Effect"*. The impetus, in part, for Senate Resolution 137 was due to wide ranging and thus controversial estimates from various studies on the projected range (70 centimeters to 600 centimeters or 28 to 236 inches) of sea level rise for the next century (Revelle, 1983; Begley et al., 1981). The report's purpose was to determine the significance of the range of Environmental Protection Agency predictions for sea level rise by 2100 (Hoffman et al., 1983). These predictions were categorized as (a) lowest conceivable (0.57 meters or 1.9 feet), (c) lowest likely (1.5 meters or 4.8 feet), (c) highest likely (2.2 meters to 7.1 feet), and (d) highest conceivable (3.4 meters or 11.3 feet). It should be noted that presently most of projections of future sea level rise made in the 1980's, in light of more recent estimates, are considered overestimates, provided ice sheets do not melt.

The report scenarios focused on rise of sea level impacts to Honolulu's shoreline since this coastal city is both the state's major population center and the transportation hub that the state economy depends on. The "lowest conceivable" Environmental Protection Agency estimate of sea level rise (0.57 meters or 1.9 feet) for 2100 is greater than the Pacific Islands Regional Assessment Group report projected sea level rise for 2080-2099 (0.350 to 0.375 meters or 1.15 to 1.23 feet; Figure 26), so it is difficult to extrapolate the report's conclusions of this scenario to the Pacific Islands Regional Assessment Group projections. Figure 36 is a map of how a sea level rise of 0.57 meters (1.9 feet) would change Honolulu's pro-

jected shoreline and flood hazard zone compared to the contemporary shoreline and flood hazard zone. In this scenario, only parts of Sand Island are inundated by sea level rise. However, Honolulu International Airport's reef runway and greater areas of Waikīkī are both projected as flood hazard zones with this elevation in sea level.
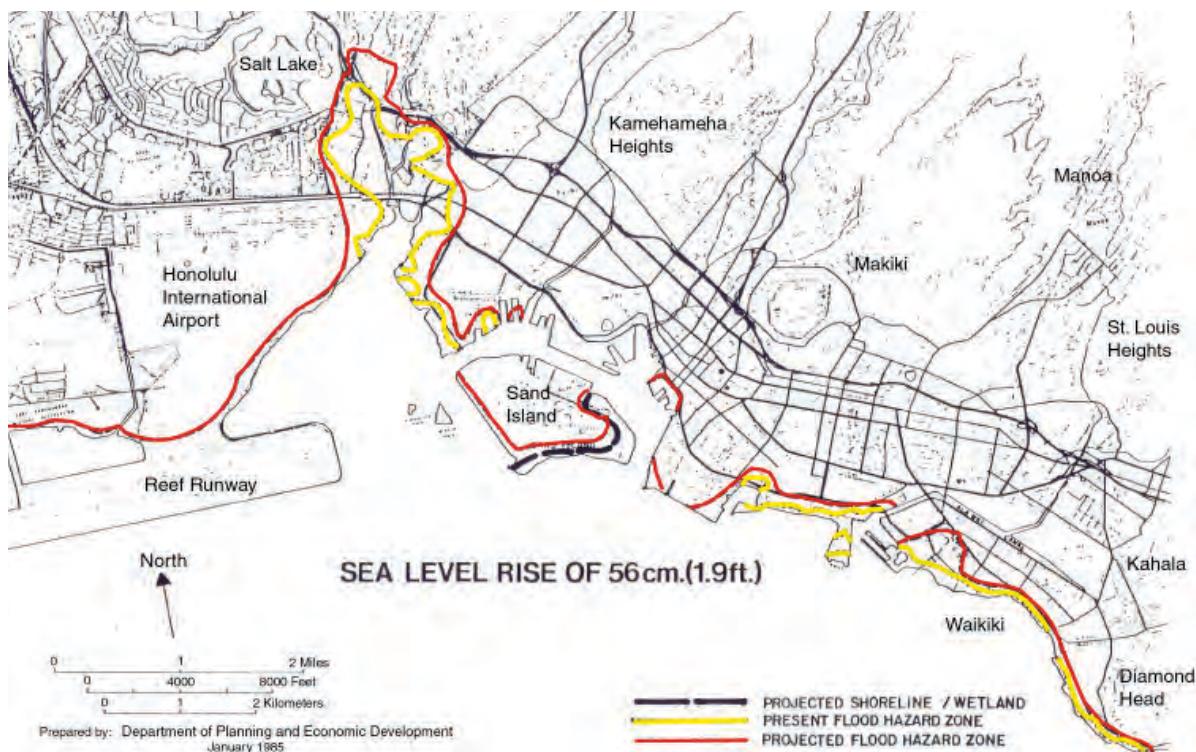
Figure 36. Projected impact to Honolulu shoreline of sea level rise of 56 centimeters (1.9 feet). (Hawai'i Coastal Zone Management Program, 1985).

In another Oahu study, Rodgers (1988) investigated the effects of a 1 meter (3.3 feet) sea level rise on shoreline migration and groundwater for the town of Kailua (population 43,780; DBEDT, 2003a) located on the eastern coast of O'ahu. The study anticipates that a 1 meter (3.3 feet) rise in sea level will not have a detrimental impact on Kailua's freshwater lens, although Kailua does not obtain drinking water from this source. Even if sea level rise would not be a detriment to local groundwater resources, it would cause the water table to rise and result in an increased opportunity for coastal flooding. O'ahu's freshwater lens rides on top of underlying, denser saltwater. As sea level rises, as it may around O'ahu and the globe (Figure 37; Rodgers, 1988), so will the level of the underlying saltwater bringing the freshwater lens, or height of the water table, closer to the land surface, thus promoting

flooding during heavy rain events (see below). Furthermore, tidal action can exacerbate the baseline rise in sea level over short time periods by elevating an already raised sea level due to global warming and climate change.
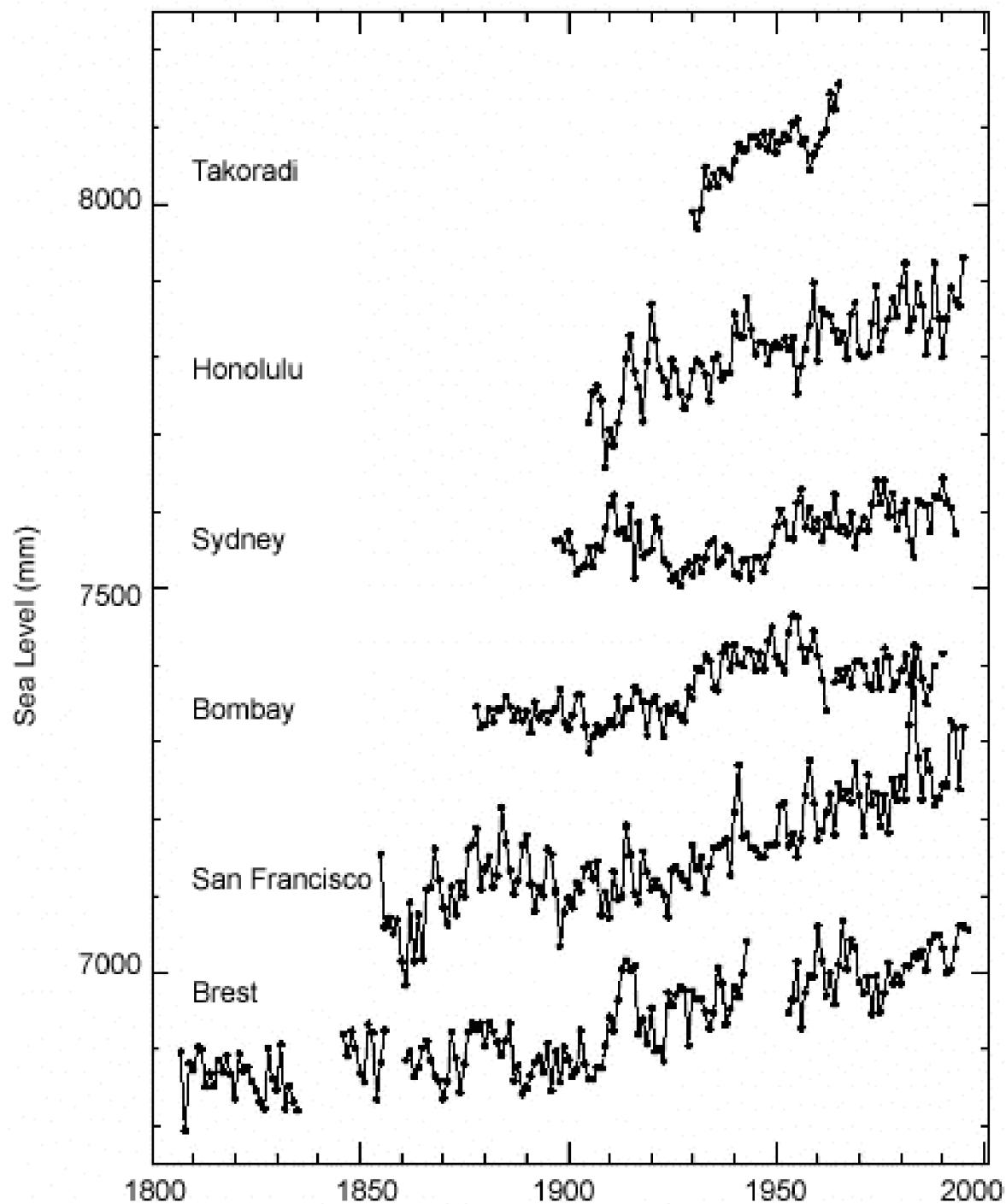
Figure 37. Sea level change measure by tide gauges. (National Ocean and Atmospheric Administration: http://gcmd.gsfc.nasa.gov/Resources/Learning/sealevel.html).

Some evidence of how sea level rise, sometimes in conjunction with high tide periods, can impact Oʻahu may have been provided between November, 2003 to March, 2004. During this interval of time, termed the "hoʻoilo" or wet season in Hawaiian, the Hawaiian Islands were repeatedly hit with heavy storm activity that was severe enough to spawn very rare occurrences of waterspouts and tornados. During this time, the island of Oʻahu and the remaining Hawaiian Islands received extensive intense rainfall (Table 3).

Table 3. Oahu rainfall station totals (in inches) from November 2003 through March 2004 for the Wilson Tunnel, Honolulu International Airport, and Aloha Tower (see Figure 38 for rainfall gauge locations). The percentage of the monthly rainfall total compared to the normal monthly rainfall is given in parentheses. Source: National Weather Service, Honolulu Forecast office.

Month	Wilson Tunnel	Honolulu Int. Airport	Aloha Tower[1]
Nov. 2003	19.67 (193%)	0.57 (25%)	1.60 (64%)
Dec. 2003	27.58 (251%)	4.81 (166%)	5.04 (136%)
Jan. 2004	19.78 (171%)	6.88 (255%)	7.98 (205%)
Feb. 2004	22.90 (260%)	9.47 (395%)	4.40 (183%)
Mar. 2004	19.02 (165%)	0.56 (29%)[2]	1.62 (54%)

[1] Aloha Tower is close to Mapunapuna; [2] by the end of March 2004, Honolulu International Airport had received within an inch of its yearly average of total rainfall.

Some examples of rainfall totals received were: (1) November 29th - 30th, 2003, Oʻahu received up to 29.1 centimeters (11.47 inches) in 24 hours (Wilson Tunnel, Oʻahu), (2) December 7th and 8th, parts of Oʻahu received over 28 centimeters (11 inches) of rain, (3) on February 27th, Oʻahu received almost 20 centimeters (8 inches) in a 24 hr period. These storms resulted in extensive flooding, especially in certain Honolulu industrial areas (e.g., Mapunapuna). The flooding was a function of a variety of factors such as saturated soil, clogged drainage, and high tide. Because the storm events lasted much longer than a day, the interval of their precipitation and resultant runoff occurred over enough time to encompass the daily high tide. The high tide (more than 0.6 meters or 2 feet at times; Table 4) imposed on the long-term sea level rise trend (Figure 37) resulted in the flooding of drainage to the ocean – i.e., runoff water can not drain to the ocean because the elevated sea level floods the drainage system. This backup due to elevated sea level increased the opportunity for flooding, especially given that the ground was already saturated.
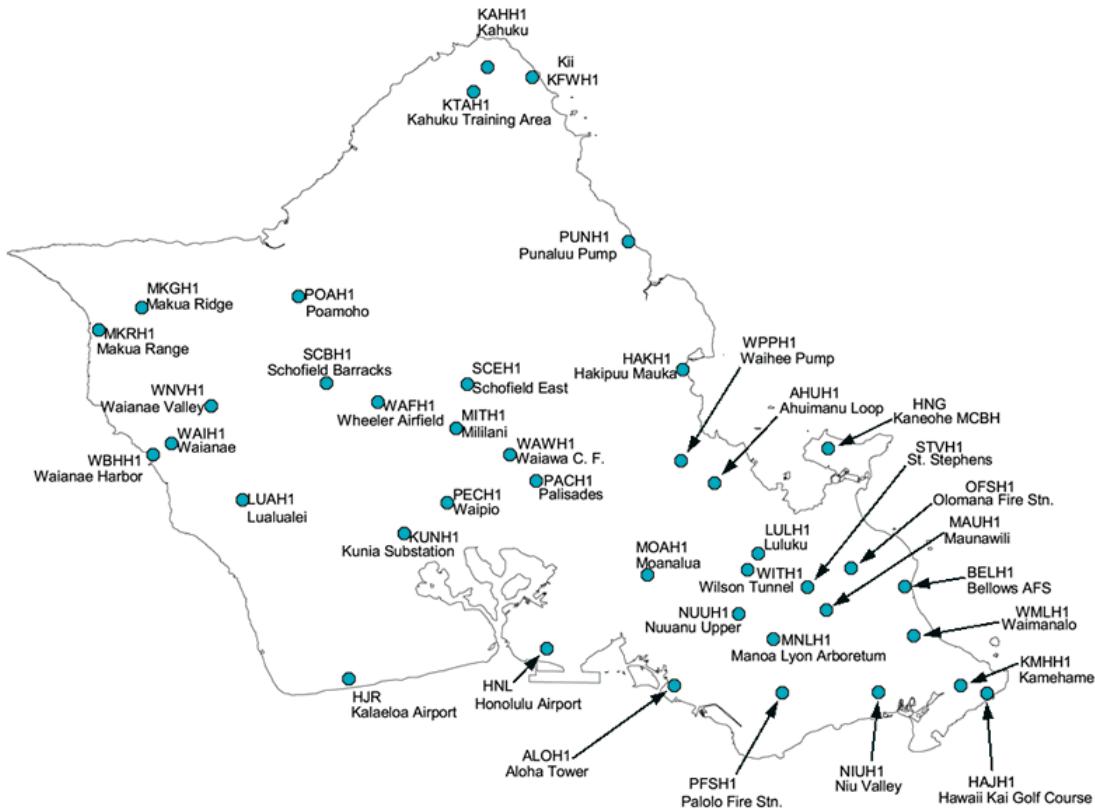
Figure 38. Rainfall gauge locations on Oʻahu (National Ocean and Atmospheric Administration:
http://www.prh.noaa.gov/hnl/graphics/oahu_rra.gif).

Table 4. Maximum high tide on major storm days for Honolulu (www.almanac.com)

Storm Date	Elevation (feet)
Nov. 29th –30th, 2003	2.08
Dec. 7th – 8th, 2003	2.18
Dec. 28th, 2003	1.92
Feb. 27th, 2004	1.56

4.   Implications of Climate Change for Hawaiʻi's Water Resources

How exactly climate change will impact Oʻahu's groundwater supply via alteration of precipitation and evaporation rates is difficult to assess. Giambelluca et al. (1996) noted that a temperature rise of 3° C would result in a 10% increase in evaporation in Oʻahu's Pearl Harbor basin. Even a concomitant precipitation rate increase of 10% would be too little to sustain the groundwater reservoir at present water usage levels. It is important to note

again that predicting how future climate change will impact island weather-related processes (e.g., orographic patterns) is currently difficult because the present climate models' spatial scale resolution is too course to model successfully how these weather-related processes will be impacted by climate change. However, it is likely that as population continues to grow on O'ahu, the groundwater supply will be taxed more and more, especially if climate change further exacerbates the problem.

The economic and social impacts of changing climate on the Hawaiian Islands are intimately tied to changes in rainfall and sea level. Given that the state's economy is heavily dependent upon the tourism industry (26%; DBEDT, 2003a), any damage to the reef runway, which is used for landing and takeoffs of long-range heavy jets, and Waikīkī could severely stress the state's economy. Waikīkī, one square mile of the total area of Honolulu, is associated with supporting 11% of the state's civilian jobs, 12% of the state and local tax revenues, and is responsible for $3.6 billion or 46% of statewide tourism's total contribution to the 2002 Gross State Product (DBEDT, 2003b).

Although the storms of late 2003 – early 2004 did not cause any significant damage to Waikiki, they did cause considerable damage elsewhere in Honolulu. Mapunapuna, an industrial section of Honolulu, was flooded several times during this period of time. Parts of Mapunapuna were under as much as several feet of water and mud resulting in significant damage to many businesses. During high tide, even without heavy rainfall, the ocean can back up onto streets in Mapunapuna through the drainage system. Sinking soil in the area has also put some areas below sea level further exacerbating the situation. Damage alone from the December 7th to 8th, 2003 storm induced by flooding in Mapunapuna was estimated at $20 million.

C. Majuro: The Republic of the Marshall Islands

The Republic of the Marshall Islands (RMI) consist of 34 atolls and islands and is situated about halfway between Australia and Hawai'i at roughly 9° N and 168° E (Figure 39). The islands consist of a series of mid-ocean reef platforms that rise up from ocean depths of more than 1524 meters (5,000 feet). The total land area of the islands is 181.3 square kilometers (70 square miles) and is approximately the size of Washington, DC. The islands and atolls enclose about 10,451 square kilometers (4,037 square miles) of lagoon area. The total population of the islands is 57,738 (CIA, 2004) with roughly 27,000 inhabitants on Majuro atoll. The population age distribution is as follows: 0-14 years (38.6%), 15-64 (58.4%),

65 (2.3%) (CIA, 2004). The median age is 19.3 years and the yearly population growth rate is 2.3% (CIA, 2004). Marshallese and English are the official languages.

Figure 39. Republic of the Marshall Islands. (Marshall Islands Visitors Authority: http://www.visitmarshallislands. com/marshallislands.htm)

The Republic of the Marshall Islands economy is to a certain extent driven by a yearly U.S. Government monetary contribution. The GDP is $115 million (2001 estimate). Agricultural production provides the primary form of subsistence and is concentrated on small farms with the most important crops being coconuts and breadfruit (CIA, 2004). The tourist industry employs less than 10% of the labor force (CIA, 2004). As of 1999, the unemployment rate was 30.9% (CIA, 2004). The islands have few natural resources and imports far exceed exports. The GDP growth has averaged 1% over the past decade. Fossil fuel provides 99% of the electricity and solar capture the remaining 1% (CIA, 2004). As of 2002, there were 4,400 telephone lines in use, 600 cellular phones, 5 internet service providers, and 1200 internet users (CIA, 2004).

Much like Hawai'i, the climate of the Republic of the Marshall Islands is tropical with northeasterly trade winds prevailing for most (about 80% of the time) of the year averaging 10 knots. Similar to Hawai'i, tropical storms and typhoons (i.e., hurricanes) are rare, but if they occur, they do so during the summer months and El Niño years. The trade winds can be frequently interrupted during the summer months by the movement of the Intertropical Convergence Zone across the area. Rainfall is heavy in the Republic of the Marshall Islands with the wettest months being October and November. The climate is very consistent with the difference in average temperatures between the warmest and coolest months

being only one degree centigrade. The average rainfall on Majuro Island, where the Republic of the Marshall Islands' capital is located, is 131 inches per year.

Majuro atoll is composed of a ring-shaped reef system enclosing a salt-water lagoon. The atoll is 40 kilometers (25 miles) in east to west length and 9.7 kilometers (6 miles) from north to south. The 64 low islets that make up Majuro atoll vary in width from 0.16 to 0.8 kilometers (0.1 to 0.5 miles). The total land area of Majuro is about 10.4 square kilometers (4 square miles) and the average elevation is 2.4 meters (8 feet). The Majuro lagoon occupies 323.6 square kilometers (125 square miles) and has an average depth of 46 meters (150 feet) with a maximum depth of 67 meters (220 feet).

The primary water supplies for Majuro atoll are the water catchment system at the airport, individual private catchments and groundwater wells, and the Laura area ground-water lens (SOPAC, 2001). The total storage of the airport catchment system is 87 million liters or 23 million gallons (SOPAC, 2001). The demand for water, which is increasing along with Marshall Island population growth, exceeds the capacity of the airport catchment system. Majuro's population has increased by 67% since 1980 (SOPAC, 2001). The catch-ment system is insufficient to meet the demands not only during periods of drought, but also during normal rainfall periods that can require water rationing. Droughts can cause severe water shortages requiring the population to ration their water use. The Laura area of Majuro atoll contains a sizeable lens of fresh water that can buffer water shortages during periods of drought. The volume of the Laura area freshwater lens is roughly estimated at 2.0 million cubic meters (2 billion cubic liters) or 7.58 million gallons (SOPAC, 2001). Unre-stricted water utilization levels for Majuro have been estimated to be 125 liters (33 gallons) per person per day (SOPAC, 1998). The recharge rate of the freshwater lens is 4400 cubic meters (4.4 million liters) per day (calculated from rainfall and evaporation rates; SOPAC, 2001). The optimum withdrawal rate of groundwater resources can only be part of the recharge rate. It is estimated that removal at the rate of 30% of the recharge rate will allow for the sustainability of the freshwater lens (Meinardi, 1991), so a safe yield amounts to about 1320 cubic meters or 1.3 million liters (350,000 gallons) per day. During a 6-month drought in 1992, the Laura lens was the only source of freshwater for all of Majuro's resi-dents underlining the importance of this resource (Barber, 1994).

1. Temperature and Rainfall

    The temperature projections from the Hadley HADCM2 model show that the surface temperature around Majuro will increase for both short and long-lead simulations. Over the short-lead (2025-2034), temperatures will increase between 1.0 to 1.3° C for December, January, and February and 2.3 to 3.0° C for the long-lead (2090-2099) (Figure 17). For the months of June, July, and August, the short-lead temperature increase is between 1.0 to 1.3° C and the long-lead increase is from 2.6 to 3.0° C (Figure 17). The separate Special Report on Emissions Scenarios A2 and B2 models (Figure 31) project increases in surface temperature of 2.0 to 2.3° C and 1.6 to 2.0° C, respectively, for 2071-2100. The differences between the two models and their projections primarily stem from the fact that A2 generally has greater increases of greenhouse gases and thus more positive radiative forcing (warming). However, all three models are in general agreement that the tropical Pacific will warm in the next century.

    The rainfall projections from the Hadley HADCM2 model show that rainfall in the area of Majuro will increase for both short and long-lead simulations during the summer months. In Figure 18, over the short-lead (2025-2034), rainfall will increase between 0.5 to 1.0 millimeters (0.02 to 0.04 inches) per day for June, July, and August and 2.0 to 3.0 millimeters (0.08 to 0.12 inches) per day for the same months over long-lead (2090-2099). The rainfall projections for December, January, and February for both short- and long-lead show an increase of 3.0 to 4.0 millimeters (0.12 to 0.16 inches) per year (Figure 18). The separate *Special Report on Emissions Scenarios* A2 and B2 models project a 5 to 20% increase in the precipitation for the area around the Marshall Islands from 2071-2100 (Figure 30).

2. El Niño Southern Oscillation and Storm Variability

    Severe storms with damaging winds are infrequent near Majuro atoll, although typhoons can occur in the vicinity of the atoll. In 1918, a major storm resulted in the loss of many lives when the population was only 1400. Wave action tends to be trade wind driven, although South and North Pacific swells and tropical storms and typhoons can also generate wave action. The trade wind waves are present throughout the year, but are highest from December to April. South and North Pacific swells are generated during the winter in their respective hemispheres. The wave heights for North Pacific swells 1.5 to 4.6 meters (5 to 15 feet) are generally higher than the South Pacific swells 0.6 to 1.8 meters (2 to 6 feet).

Tropical cyclone formation occurs near the Marshall Islands and so the islands are rarely exposed to full-strength typhoons. As the storms form and move west of the Marshall Islands they strengthen. No storm with typhoon strength has impacted Majuro Atoll for more than 30 years. From 1974 to 1988 only two tropical storms and no typhoons approached Majuro within 280 kilometers or 150 nautical miles (Holthus et al., 1992).

During the 1982-1983 El Niño Southern Oscillation event, due to the drought, Majuro's water reservoir held 22.7 million liters (6 million gallons) on January 1, 1983. By January 17th, 1983 the water reservoir had dropped to 18 million liters (4.8 million gallons). By May 1983 more than a year later, the storage had dwindled to 3 million liters (0.8 million gallons), which had to be reserved for hospital use (Republic of the Marshall Islands, 1999). During the 1997-1998 El Niño Southern Oscillation event, Majuro again experienced an extreme water deficit and was forced to ration water supplies. At the height of the 1997-1998 El Niño Southern Oscillation generated drought, municipal water on Majuro was only available for seven hours every fourteen days.

3.   Sea Level

The *Vulnerability Assessment to Accelerated Sea Level Rise* (Holthus et al., 1992) case study investigated the impacts of three different sea level rise scenarios on four different study areas at Majuro Atoll (see Figure 40 and Table 5).

Table 5. Majuro Study Area (adapted from Holthus et al., 1992).

Study Area Characteristics				
	Area 1	Area 2	Area 3	Area 4
Land area (miles^2/km^2)	0.8 / 2.1	1.2 / 3.1	0.4 / 1.0	0.2 / 0.5
Land length (miles/km)	4.7 / 7.6	2.3 / 3.7	5.0 / 8.1	2.6 / 4.2
Shoreline length (miles/km)	4.8 / 7.7	4.0 / 6.4	5.0 / 8.1	2.5 / 4.0
Landwidth (feet/m)				
- minimum	330 / 101	660 / 201	165 / 50.3	165 / 50.3
- maximum	1980 / 604	4290 / 1308	895 / 252	660 / 201
Reef flat area (miles^2/km^2)	0.8 / 2.1	1.2 / 3.1	0.5 / 1.3	0.7 / 1.8
Population	14,600	< 2,000	0	19
Habitation	Urban	Rural	Airport	Uninhabited

Study area 1: The Jaroj-Wulka-Telap area is the commercial and population center of Majuro Atoll. For Majuro Atoll, most of the facilities and the principal settlement are in this area. Of the total Majuro population of 19,600, about 14,600 of them live in this area. This area was chosen by the researchers to represent the urban atoll setting that is characterized by high human settlement, major infrastructure development, significant shoreline alteration, largely degraded land and reef resources, and the location of government, commerce, transportation, and telecommunication centers.

Study Area 2: The Laura area is the largest island of Majuro and it contains important groundwater resources. Although the Laura area is the largest island, it only has a population of around 2,000. This area was chosen as indicative of a rural atoll setting, which makes up a vast majority of Pacific atoll land areas. These areas generally lack significant infrastructure development and shoreline alteration, are sparsely populated, and subsequently have terrestrial and marine habitats that are not significantly altered.

Study area 3: A long and narrow area that consists of airport causeways connecting the area's islets. This area is representative of common and typical long and narrow land atoll areas.
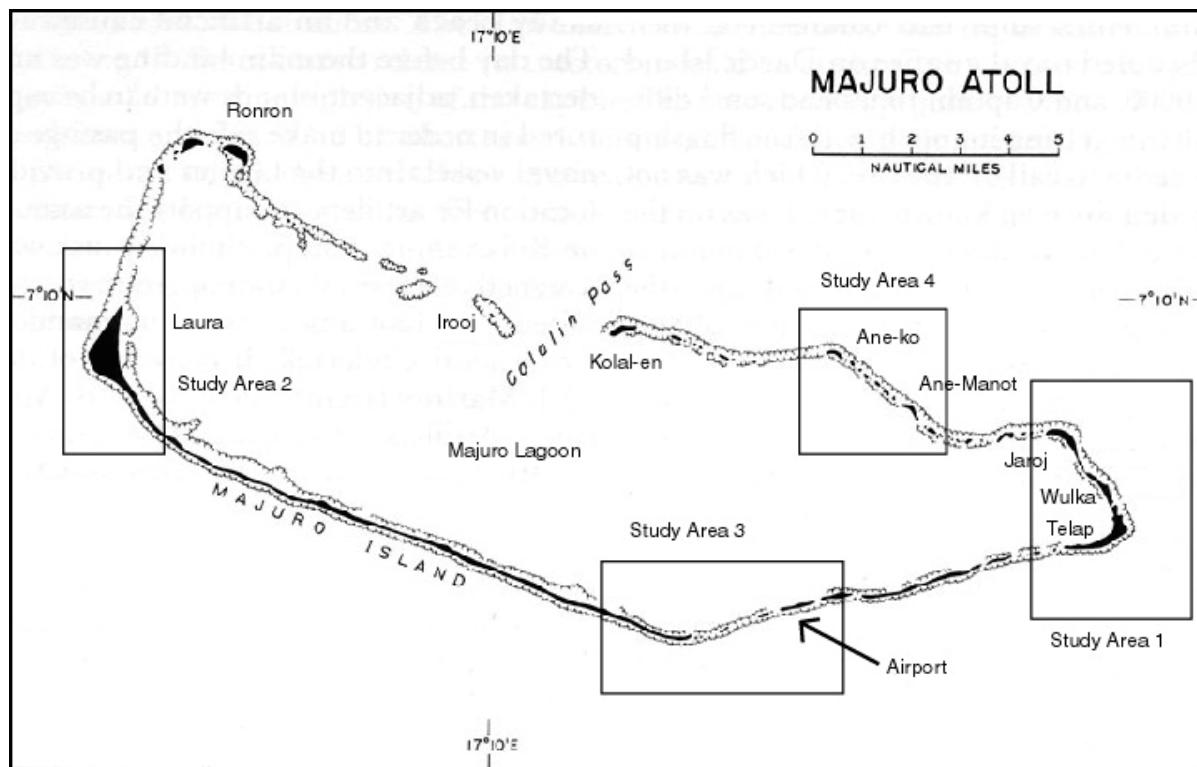
Figure 40. The four Majuro Atoll study areas. (After Holthus et al., 1992).

83

Study area 4: A chain of 10 small islets at the northeast end of Majuro Atoll. The islets are separated from each other by reef flat except during low tide. Study area 4 was chosen to represent portions of atolls that consist of a series of small islands that are not inhabited and also provide terrestrial and marine resources.

The three scenarios investigated were (1) no sea level rise, (2) 0.3 meters (1 foot) sea level rise and, (3) 1.0 meter sea level rise (3.3 feet). Based on historic wave data, three different wave conditions were analyzed to determine how vulnerable Majuro shorelines were to combined wave action and rising sea level. The three different conditions were (1) 2-year event representing annual conditions, (2) 50-year event representing probably extreme conditions, and (3) typhoon event representing worst-case conditions.

a.   Water Level Rise

To determine the inundation limits and wave run up limits of a storm, the water level rise has to be determined. The rise in water along a shoreline during storm events is a function of 3 components: (1) tide height, (2) storm surge (caused by the reduced atmospheric pressure of a storm and also the wind stress setup), and (3) wave setup. The wind stress setup is the increase in water level from still conditions due to the wind. The wave setup is the change in water level on the shore due to the effects of waves running up the shore and breaking. The water level rise is considered in tandem with a tide level that is 0.8 meter (2.6 feet) above mean sea level. The total water level rises for the four study areas are summarized in Table 6.

Table 6. Water level rise components in feet above mean sea level (adapted from Holthus et al., 1992).

		Study Area	Annual Extreme	50-Year Extreme	Typhoon Event
Ocean Side	ASLR0 = 0	1	4.9	6.0	8.3
		2	4.9	6.0	8.3
		3	4.9	6.0	8.3
		4	3.9	4.5	6.3
	ASLR1 = 1.0	1	5.7	7.0	9.3
		2	5.7	7.0	9.3
		3	5.7	7.0	9.3
		4	4.9	5.3	6.9
	ASLR2 = 3.3	1	7.8	9.0	11.3
		2	7.8	9.0	11.3
		3	7.8	9.0	11.3
		4	6.8	7.3	9.0
Lagoon Side	ASLR0 = 0	1	3.6	4.1	7.7
		2	3.6	4.1	7.7
		3	3.0	3.3	5.7
		4	2.9	3.0	4.9
	ASLR1 = 1.0	1	4.5	5.0	8.6
		2	4.6	5.1	8.6
		3	4.0	4.3	6.6
		4	3.9	4.0	5.7
	ASLR2 = 3.3	1	6.5	7.1	10.6
		2	6.7	7.2	10.8
		3	6.2	6.4	8.6
		4	6.2	6.3	7.9

ASLR is accelerated sea level rise scenarios given in feet of rise (i.e., ASLR1 = 1.0 is an accelerated sea level rise of 1.0 foot.

b.   *Majuro Atoll Physical Changes and Natural System Responses*

In the Holthus et al. (1992) case study, the Bruun erosion rule (Bruun, 1962) was used to estimate the amount of shoreline erosion that the three future sea level scenarios – i.e., 0 meter, 0.3 meters (1.0 foot), and 1.0 meter (3.3 feet) rise in sea level – would cause at Majuro Atoll. Shoreline retreat in response to sea level rise was estimated using a generalize shoreline slope of 1/10 on both the ocean and lagoon sides. Thus the additional shoreline retreat would be 3 meters (10 feet) for ASLR 1 and 10 meters (33 feet) for ASLR 2. Table 7 presents

estimates of shoreline retreat and dry land lost due to sea level rise and erosion for ASLR 1 and ASLR 2.

Table 7. Estimates of shoreline retreat and dry land lost (in feet) due to sea level rise and erosion (adapted from Holthus et al., 1992).

	Shore Elevation (feet)	Water Depth (feet)	Shoreline Retreat (feet)		Dry land lost (acres)		
			ASLR (1.0 ft)	ASLR (3.3 ft)	Present Dry Land (acres)	ASLR (1.0 ft)	ASLR (3.3 ft)
Study area 1					510	50	160
Ocean	8	2	40 – 80	130 – 260		35	110
Lagoon	6	28	20 – 30	70 – 110		15	
Study area 2					740	45	140
Ocean	10	2	50 – 130	170 – 420		35	110
Lagoon	6	28	20 – 50	70 – 150		10	30
Study area 3					230	15	50
Ocean	8	2	50	150		10	30
Lagoon	6	14	30	100		5	20
Study area 4					130	30	100
Ocean	8	2	80	250		20	75
Lagoon	6	14	40	130		10	25

The projected shoreline retreat with ASLR = 1 foot is between 12.2 to 40 meters (40 to 130 feet) on the ocean side and from 6.1 to 15.2 meters (20 to 50 feet) on the lagoon sides of the study areas. The projected shoreline retreat with ASLR = 1 meter (3.3 feet) is between 40 to 128 meters (130 to 420 feet) on the ocean side and from 21.3 to 45.7 meters (70 to 150 feet) on the lagoon side. The estimated loss of total land area from the four study sites with ASLR = 0.3 meters (1.0 foot) is 0.57 square kilometers (0.22 square miles or 140 acres). The estimated loss of total land area from the four study sites with ASLR = 1 meter (3.3 feet) is 1.8 square kilometers (0.70 square miles or 450 acres). The Pacific Islands Regional Assessment Group projection of sea level rise for short-lead period (2020-2040; Figure 26) for the area of the Marshall Islands is between 0.08 and 0.1 meters (0.25 to 0.33 feet). The projections of sea level rise for the long-lead period (2080-2099; Figure 26) are between 0.33 to 0.35 meters

(1.1 to 1.2 feet). It is important to remember that these projections include sea level rise due to thermal expansion of ocean water and glacial melt, but do not include ice-sheet melt because of the uncertainty of the net effect of climate change on the Antarctic and Greenland ice sheets.

Accelerated sea level rise can affect groundwater resources in at least two ways. The first effect is due to flooding by storm high tides. The flooding damage is not permanent, but it can damage the ground water resource for an extended period of time. The second effect is via the loss of land area from frequent tidal inundation of low-lying areas or by shoreline erosion.

Coral atolls like Majuro are more susceptible than volcanic islands like Oʻahu, Hawaiʻi to climate changes and sea level rise. Some reasons for this are the limited land area and low relief of atolls. The size of freshwater lenses in atolls are influenced by factors such as rates of recharge (i.e., precipitation), rates of discharge, and extent of tidal inundation. Precipitation triggers the formation of a freshwater lens. Recharge is necessary to maintain the lens otherwise the groundwater supply will diminish. Groundwater discharge is governed by local flow systems and water use. For most Pacific islanders, groundwater use is secondary to individual catchment systems for drinking and bathing. Rooftops and cisterns provide catchment and groundwater is primarily used for irrigation. Local geology, island shape, and island size also affect the groundwater lens. The local rock must be porous and permeable enough to permit recharge of the lens but also to prohibit salt water intrusion during tidal fluctuations.

Miller and Mackenzie (1988) estimated the effect of sea level rise on the fresh water resources of Majuro atoll investigating specifically study area 2 (Laura atoll), which is the predominant source of fresh groundwater for the surrounding area. The freshwater lens lies within several geologic formations (Figure 41a).

The upper sediment lithofacies (a unit of similar rock type) is comprised of well-sorted, unconsolidated coral fragments and is underlain by the upper limestone lithofacies. Both upper sections are underlain by the lower sediment facies, which is comprised of poorly sorted unlithified wackestone (muddy sandstone) (Anthony and Peterson, 1987). The development of the freshwater lens under Laura's surface has been substantially affected by Quaternary (Pleistocene and Holocene) sea level fluctuations with subsequent controls on limestone diagenesis. Figure 41a shows a cross section of the atoll's geology and ground-
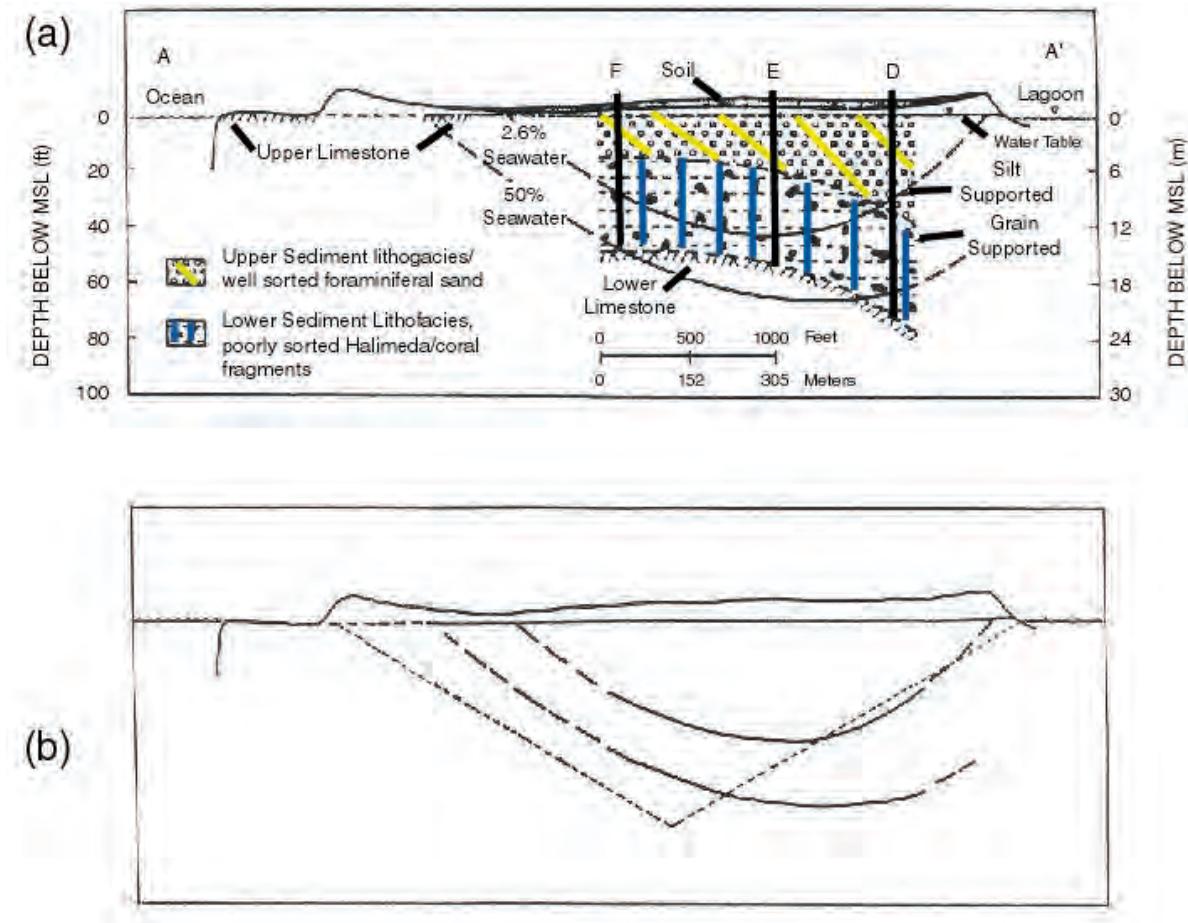
Figure 41. (a) Cross section of Laura atoll showing Ghyben-Hertzberg lens (After Anthony and Peterson, 1987) and (b) approximation used by Miller and Mackenzie (1988).

water lens. The local geology causes the lens to be asymmetrical, but Miller and Mackenzie (1988) used a symmetric lens [delineated in Figure 41(b)] for their study along with a projected rise in sea level of 1 m. The loss of land area from inundation is estimated by assuming that the atoll dunes will migrate to preserve the near shore profile as predicted by the Bruun rule (Bruun, 1962). If sea-level were to rise one meter (3.3 feet), the shoreline would recede 150 meters (493 feet) inland on each coast, which would result in a loss of more than 25% of the atoll's surface area. If this were to occur, and keeping all geologic parameters constant, 373,000 cubic meters (99 million gallons) of fresh water would be lost from the lens depth, which is approximately 50% of the freshwater lens volume. Holthus et al. (1992), using the methods employed by Miller and Mackenzie (1988), calculated that for an ASLR = 0.3 meters (1 foot) that the Laura area fresh water lens would decrease in volume by 10%.

4. Implications of Climate Change for Majuro's Water Resources

Population pressure on water resources will exacerbate water resource problems related to climate change and sea level rise. With climate change there may be more rainfall and thus more catchment water, but sea level rise will both decrease surface area and also intrude into the freshwater lens, which will in turn make land unusable for agriculture. In addition, against the background of elevated sea level, high tides and storm activity can result in both a loss of habitable, cultivatable land and a reduction in the amount of available fresh water. Accelerated sea level rise may affect the loss of groundwater resources in two ways: (1) increased frequency of flooding due to storm high tides and (2) island area loss via either frequent tidal inundation of low-lying areas or by erosional loss of shoreline.

One means to reduce the probability of accelerated sea level rise combined with storm high tides negatively impacting groundwater and other resources (e.g., land for living and cultivating crops, airport area, infrastructure) is to employ protection measures. Holthus et al. (1992) investigated the cost of building shoreline protection for study areas 1 and 3 based on costs to build similar shoreline structures constructed on Kwajalein Atoll (Republic of the Marshall Islands). Table 8 gives cost estimates for shore protection of study areas 1 and 3 for a sea level rise = 0.3 meter (1 foot), which is in line with the 2080-2099 projection in Figure 26.

Table 8. Cost estimates (in millions of U.S. dollars) for shore protection of study areas 1 and 3 under scenarios of (a) ASLR = 1 foot and a typhoon event and (b) ASLR = 1 foot and the 50-year event (modified from Holthus et al., 1992). Cost estimates include both construction costs and 25-year life cycle maintenance costs. Study area 1 is Jaroj-Wulka-Telap area and study area 3 is where the airport is located.

(a) ASLR = 1 foot and the Typhoon[1] event

Area	Shoreline length (ft)	Type and cost (in millions $US) of structure materials	
		Armor Stone	Tribar
Study area 1	58,000	105	100
Study area 3	18,000	22	25
Total costs		127	125

(b) ASLR = 1 foot and the 50-year[1] event

| Area | Shoreline length (ft) | Type and cost (in millions $US) of structure materials | |
		Armor Stone	Tribar
Study area 1	58,000	46	52
Study area 3	18,000	6	8
Total costs		54	60

[1] see Table 5 for sea level elevations at specific study areas during these events

At the time of the study, to protect study area 1 and study area 3 (i.e., airport) from a sea level rise = 0.3 meters (1 foot) and a 50-year event will cost between 54-60 million U.S. dollars. The cost to protect areas 1 and 3 against a sea level rise = 0.3 meters (1 foot) and a typhoon event is 125-127 million U.S. dollars. The projected gross national product for 2022 is close to 200 million U.S. dollars, so the island nation would need to spend 25%-63% of its 2022 gross national product to protect only study areas 1 and 3 from a sea level rise = 0.3 meters (1 foot), and a 50-year and typhoon event, respectively. The costs for protecting these areas would have to be spread out over many years due to the limited economic capability of the Marshallese economy.

The sea level rise would also result in added costs to the Marshall Islands due to the reduction in freshwater resources from salinization of the Laura atoll freshwater lens. This freshwater resource has in the past been the only viable source of freshwater for Majuro (e.g., during the 6-month drought in 1992). Continued rise in sea level will reduce the volume of the lens suitable for human use and requires either rationing, especially during droughts and/or continued population growth, or development of other methods to provide freshwater – e.g., desalinization plants, tankers delivering freshwater, etc. Additionally, El Niño events, which cause droughts in the Majuro area, may increase in frequency with the climate change predicted by the Pacific Islands Regional Assessment Group models. Assuming consumption of 33 gallons per person per day, a desalinization plant would cost Majuro households (assuming 7 people per household) $US380 to $US583 per year (SOPAC, 1998). The average yearly salary of a Marshallese citizen is roughly $US2,000.

VI. Conclusions

Future global climate change and the resultant impacts to water resources are very serious problems for Pacific Island nations. For small island-atoll nations like Majuro or large volcanic islands like the Hawaiian Islands and O'ahu, water is a most precious natural resource. Due to the recorded trends in atmospheric concentrations of carbon dioxide, methane, nitrous oxide, chlorofluorocarbons, hydrofluorocarbons, aerosols, etc. and the future projections and consequences of climate change obtained from climate models (e.g., Intergovernmental Panel on Climate Change, Pacific Islands Regional Assessment Group, etc.) the world community, through the United Nations, has produced and ratified legally binding agreements such as the 1997 Kyoto Protocol that require signatory nations to reduce their emissions of greenhouse gases.

Majuro and O'ahu, Hawai'i represent two different types of Pacific islands. Majuro of the Republic of the Marshall Islands is a small low-lying atoll two to three meters above sea level. The impact of projected sea level rise on Majuro's water resources is potentially severe. The low-lying atoll lacks the groundwater resources for its freshwater needs and relies primarily on rainwater catchment systems for freshwater supply. The groundwater reservoir does provide a freshwater source for times when rainfall is low and thus rainfall catchment is reduced. Rising sea level, exacerbated by storm activities, all due to climate change, will reduce Majuro's volume of fresh groundwater. In addition to climate change, rising population will place additional pressures on the groundwater resource. To build shoreline protection measures for Majuro is costly to protect its groundwater and land area resource from rising sea level and storm events. Desalinization is another measure that could be implemented to support, at least in part, Majuro's present and future freshwater needs; albeit at considerable cost.

Compared to the low-lying atoll Majuro, the island of O'ahu is a relatively large volcanic island with a peak elevation of over 1200 meters (3,936 feet) and a much larger groundwater resource. This groundwater resource already supplies O'ahu with 92% of freshwater use. The development and use of the groundwater system have reached the point where the sustainability of current and future water usage rates is in doubt. Even if future climate change were to lead to increased precipitation for O'ahu, the elevated temperature, via its influence on evaporation rate, could result in a reduction in groundwater recharge rates and thus a decrease in the groundwater reservoir size. Add to this the increased groundwater usage due to island population growth and also the background

future rise in sea level and Oʻahu's groundwater resource could be significantly taxed. The future rise in sea level could also threaten the economy of Oʻahu and Hawaiʻi by negatively impacting vital areas (e.g., airport runway and Waikīkī) in close proximity to shorelines. The rise in sea level can also result in the flow of salt water from the ocean to land via the storm drainage system, which during storm events can result in flood damage to areas such as the Mapunapuna industrial district.

Much of the research that is the impetus and basis for the Kyoto Protocol is derived from the Intergovernmental Panel on Climate Change reports (IPCC, 1990; 1996; 2001). A summary of the key concerns for small island states from the 2001 Intergovernmental Panel on Climate Change report (IPCC, 2001b) is:

- The adaptive capability of the human systems is generally low for small island states and their vulnerability is high; small island states are likely to be among the countries most seriously impacted by climate change.

- The projected sea level rise of 5 millimeters (0.2 inches) per year for the next 100 years will cause enhanced coastal erosion, loss of land and property, dislocation of people, increase risk from storm surges, reduced resilience of coastal ecosystems, saltwater intrusion into freshwater resources, and high resource costs to respond to and adapt to these changes.

- Islands with very limited water supplies are highly vulnerable to the impacts of climate change on the water balance.

- Coral reefs would be negatively affected by bleaching and by reduced calcification rates due to higher carbon dioxide level and ocean acidification; mangrove, sea grass bed, and other coastal ecosystems and their associated biodiversity would be adversely affect by rising temperatures and accelerated sea-level rise.

- Declines in coastal ecosystems would negatively impact reef fish and threaten reef fisheries, those who earn their livelihoods from reef fisheries, and those who rely on the fisheries as a significant food source.

- Limited arable land and soil salinization makes agriculture of small island states, both for domestic food production and cash crop exports, highly vulnerable to climate change.

- Tourism, an important source of income and foreign exchange for many islands, would face severe disruption from climate change and sea-level rise.

92

The Kyoto Protocol was entered into force on February 16, 2005. Triggered by Russia's ratification, the Protocol became legally binding for its then 128 Parties on February 16, 2005. As Joke Waller-Hunter, Executive Secretary of the Climate Change Secretariat, stated, "A period of uncertainty has closed. Climate change is ready to take its place again at the top of the global agenda." The Protocol's enforcement meant that the signatory industrialized countries must reduce their combined emissions of six major greenhouse gases during the first-year period, 2008-2012, to below 1990 levels. For example, the European Union must cut its combined emissions by eight percent while Japan must cut its emissions by six percent.

As of early 2005, there were only four industrialized countries that had not yet ratified the Kyoto Protocol: Australia, Liechtenstein, Monaco, and the United States. Both Australia and the United States have indicated they will not do so and together they account for over one third, in 2005, of the greenhouse gas emissions by the industrialized world. It remains to be seen though whether the global community minus the United States and Australia, even by forging ahead with climate protection commitments, can blunt future global climate change and its negative impacts, especially for small island nations, due to human forcings. Also, it is unknown, what, if any, impact the United States' policy of technological mitigation of greenhouse gas emissions will have on future global climate change.

One final note: The Munich Re group, one of the world's largest re-insurance companies that has been monitoring the cost of natural disasters since 1960, determined that the cost of natural disasters worldwide in 2003 was $US60 billion and that by the year 2050 could exceed $US300 billion based on projected climate change (Munich Re, 2004). By 2050, the losses linked with climate change for low lying island states such as the Marshall Islands could exceed 10% of their national wealth or gross domestic product (UNEP, 2001). However, the Munich Re group report does not estimate the costs for preventing losses associated with future climate change.

VII. References

Anthony, S.S. and Peterson, F.L. 1987. Carbonate Geochemistry and Hydrogeology Relationships: Laura, Majuro Atoll. Marshall Islands. Water Resources Research Center Technical Report No. 172. 77pp.

Barber, B. 1994. Rural and urban water supply and sanitation review. Republic of the Marshall Islands Environmental Protection Agency. United Nations Development Programme.

Begley, S., Dallas, R., and Givens, R. 1981. Is Antarctica Shrinking? Newsweek, October 5, 1981, p. 72-74.

Bruun, P. 1962. Sea-level rise as a cause of shore erosion. Journal of the Waterways and Harbor Division. 88(WW1). p. 117-130.

Central Intelligence Agency, 2004. World Factbook.

Cesar, H., P. van Beukering, P., Pintz, S., Dierking, J. 2002. Economic Valuation of the Coral Reefs of Hawaii. Final report to the National Oceanic and Atmospheric Administration Coastal Ocean program. Cesar Environmental Economics Consulting. Arnhem, The Netherlands.

Church, J.A., Gregory, J.M., Huybrechts, P., Kuhn, M., Lambeck, K., Nhuan, M.T., Qin, D., and Woodworth, P.L. 2001. Changes in Sea Level in Climate Change 2001: The Scientific Basis. Contribution of Working Group I to the Third Assessment Report of the Intergovernmental Panel on Climate Change (Houghton, J.T., Ding, Y., Griggs, D.J., Noguer, M., van der Linden, P., Dai, X., Maskell, K., Johnson, C.I. editors). Cambridge University Press. Cambridge, U.K.

Chuey, J., Rea, D. and Pisias, N. 1987. Late Pleistocene paleoclimatology of the Central Equatorial Pacific: a quantitative record of Eolian and Carbonate deposition. Quaternary Research. 28. pp. 323-339.

Covey, C. 1984. The earth's orbit and the ice ages. Scientific American. v. 250. p. 58-66.

Department of Business, Economic Development, and Tourism, Hawaii. 2003a. 2002 The State of Hawaii Data Book: A Statistical Abstract. State of Hawaii. 889pp.

Department of Business, Economic Development, and Tourism, Hawaii. 2003b. The economic contribution of Waikiki. Electronic reports. 9pp.

Dignon, J. and Hameed, S. 1989. Global emissions of nitrogen and sulfur oxides from 1860 to 1980. Journal of the Air and Waste Management Association. v. 39. p. 180-186.

Friis-Christensen, E., and Lassen, K. 1991. Length of the solar cycle, an indicator of solar activity closely associated with climate. Science. v. 254. p. 698-700.

Gavenda, R.T. 1993. Hawaiian Quaternary Paleoenvironments. A review of geological, pedological and botanical evidence. Pacific Science. 46. p. 295-307.

Giambelluca, T.W., Nullet, M.A., and Schroeder, T.A. 1986. Rainfall atlas of Hawaii. Honolulu: Hawaii Department of land and Natural Resources. Report R76.

Giambelluca, T.W., Ridgley, M.A. and Nullet, M.A. 1996. Water balance, climate change and land-use planning in the Pearl Harbor Basin, Hawaii. Water Resources Development. 12(4). p. 515-530.

Grossman, E.E. 2001. Holocene sea level history and reef development in Hawaii and the central Pacific ocean. Doctoral Thesis. Department of Geology and Geophysics. University of Hawaii at Manoa. 257pp.

Guinotte, J.M, Buddemeier, R.W., and Kleypas, J.A. 2003. Future coral reef habitat marginality: temporal and spatial effects of climate change in the Pacific basin. Coral Reefs. 22. p. 551-558.

Hameed, S. and Dignon, J. 1992. Global emissions of nitrogen and sulfur oxides in fossil fuel combustion 1970-1986. Journal of Air and Waste Management Association. v. 42. p. 159-163.

Hawaii Coastal Zone Management Program, 1985. Effects on Hawaii of a Worldwide Risde in Sea Level Induced by the "Greenhouse Effect": A report in Response to Senate Resolution 137 (1984). Department of Planning and Economic Development. 10pp.

Hoffman, J.S., Keyes, D., and Titus, J.G. 1983. Projecting Future Sea Level Rise: Methodology, Estimates to the Year 2100, and Research Needs. United States Environmental Protection Agency. 2nd edition (revised).

Holthus, P, Crawford, M., Makroro, C. and Sullivan, S. 1992. Vulnerability assessment for accelerated sea level rise. Case Study: Majuro Atoll, Republic of the Marshall Islands. SPREP Reports and Studies Series no. 60. 107pp.

Intergovernmental Panel on Climate Change, 1990. Scientific Assessment of Climate change – Report of Working Group I. Houghton, J.T., Jenkins, G.J., and Ephraums, J.J. (Eds). Cambridge University Press. 365pp.

Intergovernmental Panel on Climate Change, 1996. Climate Change 1995: The science of climate change. Working Group 1. Houghton, J.T., Meira Filho, L.G., Callender, B.A., Harris, N., Kattenberg, A., and Maskell, K. (Eds). Cambridge University Press. 572pp.

Intergovernmental Panel on Climate Change, 2001. Climate Change 2001: The Scientific Basis. Working Group 1. Houghton, J. T., Ding, Y., Griggs, D.J., Noguer, M., van der Linden, P. J. and Xiaosu, D. (Eds.). Cambridge University Press. 881pp.

Intergovernmental Panel on Climate Change, 2001b. Climate Change 2001: Impacts, Adaptation, and Vulnerability. Working Group II. McCarthy, J.J., Canziani, O.F., Leary, N.A., Dokken, D.J., and Kasey, S.W. (Eds.). Cambridge University Press. 1032pp.

Kattenberg, A., Giorgi, F., Grassl, H., Meehl, G.A., Mitchell, J.F.B., Stouffer, R.J., Tokioka, T., Weaver, A.J., and Wigley, T.M.L., 1996. Climate models – projections for future climate change. In Climate Change 1995: The Science of Climate Change. J.T. Houghton, L.G. Meira Filho, B.A. Callander, N. Harris, A. Kattenberg, and K. Maskell (eds.). Cambridge University Press. Cambridge. Pp. 285-357.

Laws, E.D. 1992. El Nino and the Peruvian anchovy fishery. Global Change Instruction Program Module 104. University Corporation for Atmospheric Research. Boulder, CO.

Lyon, H.L. 1930. The flora of Moanalua 100,000 years ago. Abstract. In: Proceedings, Hawaiian Academy of Science. Fifth Annual Meeting, Bernice P. Bishop Museum Special Publication. 16. p. 6-7.

Mackenzie, F.T. 1995. Climatically important biogenic gases and feedbacks on global climatic change. *In* Biotic Feedbacks in the Global Climatic System. Will the warming feed the warming? G.M. Woodwell and F.T. Mackenzie (eds.) Oxford University Press, New York. pp. 22-46.

Mackenzie, F.T. 1999. Global Biogeochemical Cycles and the Physical Climate System. Global Change Instruction Program. University Corporation for Atmospheric Research. Boulder, Co. 69pp.

Mackenzie, F.T., Lerman, A., and Ver, L.M. 2001. Recent Past and Future of the Global Carbon Cycle. *in* Geological Perspectives of Global Climate Change (Gerhard, L.C., Harrison, W.E., and Hanson, B.M. eds.). p. 51-82.

Mackenzie, F.T. 2003. Our changing planet. 3rd edition. Prentice Hall. New Jersey. 580pp.

Meinardi, C.R. 1991. A Groundwater Primer. IRC Technical Paper Series. Nr 21. The Hague.

Miller, D.L.R. and Mackenzie, F.T. 1988. Implications of climate change and associated sea-level rise for atolls. Proceedings of the 6th International Coral Reef Symposium, Australia. Vol 3. p. 519-522.

Molina-Cruz, A. 1977. The relation of the Southern Trade Winds to upwelling processes during the last 75,000 years. Quarternary Research. 8. pp. 324-338.

Munich Re, 2004. Topics Geo. Annual review: Natural Catastrophes 2003. Munich, Munich Re. 56pp.

Open University, The. 1989. Ocean Circulation. Pergamon Press. Oxford, England. 238pp.

United Nations Environmental Programme, 2001. Disasters. Insuring against catastrophes: *In* Our Planet. vol. 11. No. 3. 31pp.

Republic of the Marshall Islands, 1999. October 19 – 23 Workshop on ENSO impacts on water resources in the Pacific. Nadi, Fiji.

Revelle, R. 1983. Probably future changes in sea level resulting from increased atmospheric carbon dioxide, in Changing Climate. Carbon dioxide assessment committee. Washington, D.C.: National Academy Press, pp. 433-447.

Ridgley, M.A. and Giambelluca, T.W. 1991. Drought, groundwater management and land use planning: the case of central Oahu, Hawaii. Applied Geography. 11. p. 289-307.

Rodgers, D.L. 1988. Possible effects of sea level rise on Kailua, Oahu and implications for Pacific atolls. Masters Thesis. Department of Geology and Geophysics. University of Hawaii at Manoa. 100pp.

Ropelewski, C.F. 1992. Predicting El Niño events. Nature. v. 356. p. 476.

Sabine, C.L., Feely, R.A., Gruber, N., Key, R.M., Lee, K., Bullister, J.L., Wanninkhof, R., Wong, C.S., Wallace, D.W.R, Tilbrook, B., Millero, F.J., Peng, T.H., Kozyr, A., Ono, T., and Rios, A.F. 2004. The oceanic sink for anthropogenic CO_2. Nature. v. 305. p. 367-371.

Shea, E.L., Dolcemascolo, G., Anderson, C.L., Barnston, A., Guard, C.P., Hamnett, M.P., Kubota, S.T., Lewis, N., Loschnigg, J., and Meehl, G. 2001. *Preparing for a changing climate. The potential consequences of climate variability and change*. A report of the Pacific Islands Regional Assessment Group. East-West Center. 102pp.

Smil, V. 1997. Cycles of Life: Civilization and the Biosphere. Scientific American Library. W.H. Freeman and Co. New York.

South Pacific Applied Geoscience Commission, 1998. Water supply for Majuro, Republic of Marshall Islands. A Technical Appraisal for Feasible Options. Technical Report 258. 45pp.

South Pacific Applied Geoscience Commission, 2001. Water Resources Assessment. Laura, Majuro, Marshall Islands. Technical Report 342. 20pp.

Streete, J. 1991. The Sun-Earth System. University Corporation for Atmospheric Research. Global Change Instructional Program. Module 102. Boulder, CO.

United States Global Change Research Program. 2001. *Climate Change Impacts on the United States - Foundation Report: The Potential Consequences of Climate Variability and Change*. Cambridge Press. 618pp.

VIII. Appendix A – Senate Resolution 137, 1984

ORIGINAL

(To be made one and seven copies)

THE SENATE

TWELFTH........... LEGISLATURE, 19 ..84

STATE OF HAWAII

S.R. NO. 137

SENATE RESOLUTION

REQUESTING A STUDY OF THE WORLDWIDE GREENHOUSE EFFECT ON HAWAII'S COASTAL DEVELOPMENTS.

WHEREAS, the "greenhouse effect", the continued burning of fossil fuels worldwide and the resultant buildup of carbon dioxide in the earth's atmosphere which retains more heat in the atmosphere, has long been of concern to scientists; and

WHEREAS, most scientific estimates concur that an average global warming of 2 to 3 degrees Celsius will accompany an atmospheric doubling of the current levels of carbon dioxide and this could occur as early as 2010; and

WHEREAS, scientists also predict that the warming in the northern polar areas may be as high as 6 to 10 degrees Celsius; and

WHEREAS, a temperature change of such magnitude in such a short time period will dramatically affect rainfall patterns, temperature, growing seasons, winds, storm frequencies, ocean currents, and rates of photosynthesis which will have major implications not only for world agriculture and ocean resources, but may also result in a general rise in global sea levels from 15 to 25 feet; and

WHEREAS, while there is much disagreement on the potential for and extent of a general rise in sea levels, any significant rise in sea levels would affect much of the State of Hawaii and the long-range implications of this phenomenon must be studied in order to avoid adverse impacts to the greatest degree possible; now, therefore,

BE IT RESOLVED by the Senate of the Twelfth Legislature of the State of Hawaii, Regular Session of 1984, that the Department of Planning and Economic Development Coastal Zone Management Program and the Hawaii Institute of Geophysics conduct a study on the possible effects of the greenhouse effect on Hawaii's sea levels, the implications for coastal developments, and recommended alternatives for action to minimize the adverse effects on Hawaii's population; and

ORIGINAL

THE SENATE

TWELFTH........... LEGISLATURE, 19 ...84

STATE OF HAWAII

S.R. NO. 137

SENATE RESOLUTION

REQUESTING A STUDY OF THE WORLDWIDE GREENHOUSE EFFECT ON HAWAII'S COASTAL DEVELOPMENTS.

WHEREAS, the "greenhouse effect", the continued burning of fossil fuels worldwide and the resultant buildup of carbon dioxide in the earth's atmosphere which retains more heat in the atmosphere, has long been of concern to scientists; and

WHEREAS, most scientific estimates concur that an average global warming of 2 to 3 degrees Celsius will accompany an atmospheric doubling of the current levels of carbon dioxide and this could occur as early as 2010; and

WHEREAS, scientists also predict that the warming in the northern polar areas may be as high as 6 to 10 degrees Celsius; and

WHEREAS, a temperature change of such magnitude in such a short time period will dramatically affect rainfall patterns, temperature, growing seasons, winds, storm frequencies, ocean currents, and rates of photosynthesis which will have major implications not only for world agriculture and ocean resources, but may also result in a general rise in global sea levels from 15 to 25 feet; and

WHEREAS, while there is much disagreement on the potential for and extent of a general rise in sea levels, any significant rise in sea levels would affect much of the State of Hawaii and the long-range implications of this phenomenon must be studied in order to avoid adverse impacts to the greatest degree possible; now, therefore,

BE IT RESOLVED by the Senate of the Twelfth Legislature of the State of Hawaii, Regular Session of 1984, that the Department of Planning and Economic Development Coastal Zone Management Program and the Hawaii Institute of Geophysics conduct a study on the possible effects of the greenhouse effect on Hawaii's sea levels, the implications for coastal developments, and recommended alternatives for action to minimize the adverse effects on Hawaii's population; and

Author Biographies

Fred T. Mackenzie and Michael W. Guidry

Dr. Fred T. Mackenzie is currently a professor of Oceanography and Geology and Geophysics in the School of Ocean and Earth Science and Technology at the University of Hawai'i. He received his B.S. degree in geology and physics at Upsala College and his M.S. and Ph.D. degrees in geology and geochemistry from Lehigh University. His current research projects include: modeling of the Earth surface system through geologic time; biogeochemical cycling of carbon, nitrogen and phosphorus and CO_2 exchange in the coastal zone; effects of rising CO_2 and temperature on coral/carbonate ecosystems; kinetics and thermodynamics of mineral-solution reactions; and implications of global warming for concepts of sustainability for Pacific island nations and Hawai'i. Mackenzie's background includes teaching and research experience at various universities and research groups, including Shell Oil Company, the Bermuda Biological Station for Research (where he served as staff geochemist and assistant director and helped maintain operations at Hydrostation S), West Indies Laboratory of Fairleigh Dickinson University, Harvard University, John Hopkins University, Northwestern University (where he served as chair of the Department of Geological Sciences for seven years), the Universite Libre de Bruxelles, and the Stareso Marine Laboratory (Corsica).

Mackenzie is the author and co-author of more than 250 scholarly publications including five books with multiple editions and nine edited volumes in ocean, Earth and environmental science, and biogeochemistry. His latest books are: *Our Changing Planet, 3rd edition*, which is an introductory text in Earth system science and global environmental change, and Carbon in the Geobiosphere-Earth's Outer Shell to be published in 2006. He and his research colleagues and students have presented about 150 research papers for which there are abstracts at national and international meetings. He has supervised the Ph.D. dissertations of 30 graduate students and the M.S. theses of 10 students during his career. He is currently directing the research programs of two graduate students and three post-doctoral researchers.

Mackenzie is a Fellow of the Mineralogical Society of America, the Geological Society of America, the Geochemical Society and the European Union of Geochemistry, the American Association for the Advancement of Science, and a Life Trustee of the Bermuda Biological Station for Research. He has served on innumerable national and international committees, including those for NSF, NASA, NOAA, DOE, and EPA. He has received a number of research and teaching awards during his career, including the Francqui International Medal of Science from the Universite Libre de Bruxelles, a Wissenscahftskolleg Fellowship from the Advanced Studies Institute in Berlin, Citation for Outstanding Accomplishments in the field of Atmospheric Chemistry from The Electrochemical Society, the M. W. Haas Medal from the Department of Geology at the University of Kansas, the first Michael T. Halbouty Chair and Medal from Texas A&M University, the 2003 Distinguished Research Scientist Award from the Hawai'i Academy of Science, the 1995 Hawai'i Scientist of the Year Award from Achievement Rewards for College Scientists, the 2005 Francis J. Pettijohn Medal Award for Excellence in Sedimentology from the Society for Sedimentary Geology, the 2006 Claire C. Patterson Medal Award in Environmental Geochemistry of the Geochemical Society, the current William Deering Visiting Chair in the Department of Geological Sciences from Northwestern University, the Regents' Medal for Excellence in Teaching from the University of Hawai'i, the Regents Medal for Excellence in Research from the University of Hawai'i, Presidential Citations for Excellence in Teaching from the University of Hawai'i and Northwestern University, and the 2003 Undergraduate Teaching Award from the Department of Oceanography, University of Hawai'i.

Dr. Michael W. Guidry is currently a research scientist in the School of Ocean and Earth Science and Technology at the University of Hawai'i. His current research projects include: modeling of the Earth surface system through geologic time; kinetics and thermodynamics of mineral-solution reactions; and creating interactive web-deliverable science curriculum for graduate, undergraduate, and K-12 education.